Hydrodynamic and Nuclear Experiments (U)

Study Leaders:
R. J. Hemley
D. I. Meiron

Contributors:

H. Abarbanel

M. Adams

L. Bildsten

P. Dimotakis

S. Drell

D. Eardley

N. Fortson

R. Garwin

R. Jeanloz

J. Katz

R. Schwitters

November 2011

JSR-11-340

JSI-2011-027 Copy C/6

Department of Energy Declassification Review

1st Review Date:	Determination: [Circle Number(s)]
Authority: ☐ DC ☐	1. Classification Retained
Name: S. F_____	2. Classification Changed To:____
	3. Contains No DOE Classified Info
2nd Review Date:	4. Coordinate With:____
Authority:____ DD	5. Classification Cancelled
Name:____	6. Classified Info Bracketed
	7. Other (Specify)

JASON
The MITRE Corporation
7515 Colshire Drive
McLean, Virginia 22102-7508
(703) 983-6997

NNSA.T.000057540
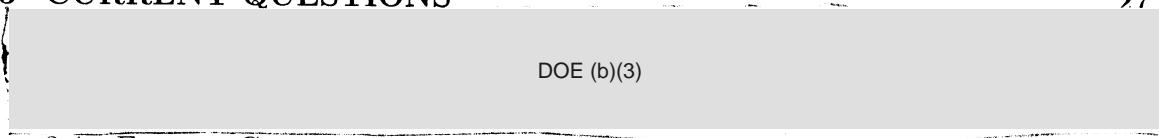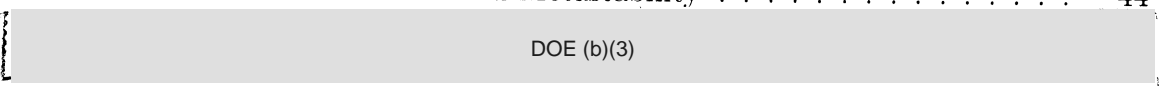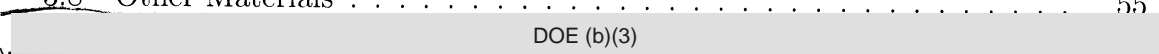
REPORT DOCUMENTATION PAGE		Form Approved OMB No. 0704-0188

1. REPORT DATE (DD-MM-YYYY) December 5, 2011	2. REPORT TYPE Technical	3. DATES COVERED (From - To)

4. TITLE AND SUBTITLE

Hydrodynamic and Nuclear Experiments (U)

5a. CONTRACT NUMBER

5b. GRANT NUMBER

5c. PROGRAM ELEMENT NUMBER

6. AUTHOR(S)

M. Adams, R. Schwitters, et al.

5d. PROJECT NUMBER
13109022

5e. TASK NUMBER
PS

5f. WORK UNIT NUMBER

7. PERFORMING ORGANIZATION NAME(S) AND ADDRESS(ES)

The MITRE Corporation
JASON Program Office
7515 Colshire Drive
McLean, Virginia 22102

8. PERFORMING ORGANIZATION REPORT NUMBER

JSR-11-340

9. SPONSORING / MONITORING AGENCY NAME(S) AND ADDRESS(ES)

U.S Department of Energy
1000 Independence Ave, SW
Washington D.C, 20585

10. SPONSOR/MONITOR'S ACRONYM(S)

11. SPONSOR/MONITOR'S REPORT NUMBER(S)

12. DISTRIBUTION / AVAILABILITY STATEMENT

Distribution authorized to US Government agencies only; Special Authority ODNI SEC S-08; Reason: 1.4(g); 27 January 2011. Other requests for this document shall be referred to DNI.

13. SUPPLEMENTARY NOTES

14. ABSTRACT

JASON was asked by the National Nuclear Security Administration (NNSA) to examine the current plans from the NNSA laboratories for hydrodynamic and subcritical experiments and to make recommendations for future efforts. The NNSA recently established the Office of Nuclear Experiments to coordinate a single long-term program of hydrodynamic experiments using surrogate materials and subcritical experiments using plutonium. The goal of this program is to develop improved understanding of the underlying physics of the materials and components in nuclear weapons in support of recent efforts such as the National Boost Initiative. JASON reviewed ongoing activities and plans for these experiments at the NNSA laboratories. The following summarizes the principal findings and recommendations of the report.

15. SUBJECT TERMS

16. SECURITY CLASSIFICATION OF:			17. LIMITATION OF ABSTRACT	18. NUMBER OF PAGES	19a. NAME OF RESPONSIBLE PERSON Dr. Robert Hanrahan
a. REPORT SECRET/ RD	b. ABSTRACT SECRET/RD	c. THIS PAGE SECRET/RD	UL		19b. TELEPHONE NUMBER (include area code) 202-496-5156

Standard Form 298 (Rev. 8-98)
Prescribed by ANSI Std. Z39.18

Contents

DOE (b)(3)

DOE (b)(3)

DOE (b)(3)

1 EXECUTIVE SUMMARY

JASON was asked by the National Nuclear Security Administration (NNSA) to examine the current plans from the NNSA laboratories for hydrodynamic and subcritical experiments and to make recommendations for future efforts. The NNSA recently established the Office of Nuclear Experiments to coordinate a single long-term program of hydrodynamic experiments using surrogate materials and subcritical experiments using plutonium. The goal of this program is to develop improved understanding of the underlying physics of the materials and components in nuclear weapons in support of recent efforts such as the National Boost Initiative. JASON reviewed ongoing activities and plans for these experiments at the NNSA laboratories. The following summarizes the principal findings and recommendations of the report.

1.1 Overview

Modern stewardship of the US nuclear-weapon stockpile uses a science-based understanding both of weapons performance and of the behavior over time of the weapons and their components in the stockpile. This relies on the calibration of codes based on data available from the more than 1000 nuclear-explosion tests that were performed until the early 1990s. It was recognized from the outset of the Stockpile Stewardship Program (SSP), and in fact since the Manhattan Project, that experiments beyond those of nuclear-explosion tests were needed. Important advances and successes in the first two decades of the SSP include certification of a primary using a new manufacturing process, assessments of pit lifetimes, weapons life-extension programs, and the development of advanced simulation codes. But there are new challenges such as those arising from continued aging of the stockpile, the potential for new technical requirements (including surety), and the ongoing need to educate and train the next generation of scientists and engineers having responsibility for nuclear weapons.

Meeting these challenges requires a continued effort to improve understanding of weapons performance for assessing the stockpile based on the quantification of margins and uncertainties (QMU). In conjunction with theory and simulation, a broad range of experiments supply relevant scientific and engineering data. Two kinds of data are obtained from such experiments, materials properties (particularly those of plutonium) and implosion characteristics for weapons-related geometries and materials in integrated systems. The requisite tools span a broad range of scales and costs, from bench-top instrumentation to large and complex facilities. This experimental program is executed at a variety of sites throughout the DOE complex. This effort is also informed by the large archival database provided by previous nuclear-explosion tests.

The program of hydrodynamic and nuclear experiments has several technical as well as programmatic objectives, and comprises a broad range of fundamental, focused, and integral experiments. Fundamental experiments include measurements of fundamental properties of materials, that is, intrinsic or atomic-level properties such as structures, phases, equations of state and other thermodynamic properties. Focused experiments include studies of non-equilibrium properties, as well as the behavior of real materials, and, in particular, weapons materials, with their defects, impurities, and microstructure; these can involve high-explosive-driven hydrodynamic experiments on plutonium in subcritical assemblies or on plutonium surrogates. Finally, integral experiments are conducted to assess the coupling of combinations of materials and may examine several operative phenomena simultaneously; they include large-scale hydrodynamic experiments as well as subcritical plutonium experiments, in weapons-relevant geometries.

The present study is motivated in part by a request to assess a program for a new series of integral experiments. These are subcritical implosion experiments on subscale primaries diagnosed via radiography or internal diagnostics compared with equivalent experiments on surrogate materials at full and subscale. The program is underway, and a plutonium subscale experiment is scheduled for execution in 2012.

We distinguish between the scientific, engineering, manufacturing, and programmatic value of the subscale plutonium experiments to the Stockpile Stewardship Program. This study assessed the scientific value of these experiments. We define scientific value here to mean the potential of these experiments to advance our understanding of weapons performance. This is to be contrasted with the engineering value, which concerns advances regarding the engineering and production of components of the experiments (e.g., the design and fabrication of smaller pits with improved tolerances), and the programmatic value, such as the need to exercise the processes of the nuclear weapons complex or to maintain an ongoing authorization basis for experiments with plutonium. On the other hand, we do comment on the role of the subscale experiment program in driving the development of new diagnostics, enhancing the responsiveness of the laboratories to new experimental challenges, and the potential benefits of the planned experiments for professional development. Finally, we do not specifically review the subscale experiments to be conducted in 2011-2012; rather, summaries of plans and progress on those experiments that were provided to us served as a basis for our assessment of future efforts in the experimental program.

The following are the principal findings and recommendations of the study; supporting material and more specific findings and recommendations are provided in subsequent chapters.

1.2 Findings

1. JASON finds that the scientific base of the Stockpile Stewardship Program remains strong, and continues to provide a mechanism for maintaining a reliable, safe and secure nuclear deterrent. The program must remain prepared to adapt to new challenges that may arise in the future as a result of technical surprise or policy changes. A robust, responsive and prioritized experimental effort is essential for Stockpile Stewardship.

2. Fundamental and focused experiments are designed specifically to measure key material and dynamic properties that determine early time primary performance and set up the initial conditions for boost. Important issues in this regime are the determination of the equation of state, phase diagram, strength and ejecta properties of plutonium at high pressures and temperatures. Fundamental and focused experiments offer the best near-term approach to obtaining the data essential for planning and interpreting integral subcritical, including subscale, experiments as well as validating theory and simulation. They will also help attract, develop and retain scientific and technical expertise.

3. Subscale plutonium experiments are integral validation exercises, and enable assessments of the ability to predict the integrated dynamic response of materials during the implosion of a primary. Such experiments, which also address issues of surrogacy and scaling, can be a component of the long-term plan for hydrodynamic and nuclear experiments for Stockpile Stewardship. However, as currently planned and with proposed diagnostics the near-term subscale experiments by themselves, cannot be used to determine material properties to the accuracy required to distinguish between competing materials models. These experiments will also not provide the accuracy needed to determine implosion features that are key to understanding the boost process and quantifying weapon performance. Future subscale and other subcritical experiments will benefit from improvements in existing radiographic facilities and recent developments in internal diagnostics.

4. The NNSA laboratories have not adequately prioritized and executed experiments that are needed to provide information crucial for understanding primary performance, including boost. The 2007 Dynamic Plutonium Experiments program plan provides an appropriate framework for obtaining the requisite data, but the plan is several years behind schedule and must be updated with better plans for implementation as well as for sustaining necessary facilities.

1.3 Recommendations

1. Prior to undertaking future plutonium subscale experiments or investing in associated facilities, the scientific value of those experiments should be established. Initial priorities should emphasize fundamental and focused experiments that address outstanding scientific issues in understanding implosion physics essential for determining initial conditions for boost. Such an approach will provide data essential for planning and interpreting integral, including subscale, experiments and the associated diagnostics.

2. NNSA and the nuclear weapons laboratories should revisit and update the 2007 plan for the Dynamic Plutonium Experiments program plan, evaluate and prioritize focused, fundamental, and integral (including subscale) experiments, and put planned experiments on a realistic schedule with appropriate funding. Integration of the programs in the three laboratories should be stressed, and the full range of experimental facilities needs should be prioritized.

3. The laboratories, together with NNSA, should strengthen foundational science in support of the weapons program. The coordination of science initiatives among the laboratories should be re-examined in partnership with NNSA in the context of modern national security needs. A strengthened science base will enable the weapons program to adapt to new challenges that may arise in the future, whether due to technical surprise or policy changes. The program should also enhance professional development and interactions with the broader research community to the extent possible.

1.4 Response to Study Charge Questions

The following are responses to specific questions posed in the charge.

1. **What fundamental static and dynamic materials properties data need to be acquired?**

   The data that need to be acquired are the equation of state, strength, kinetics, and phase transitions of plutonium at high pressures and temperatures. These data are key to understanding the boost process in primaries. Related data should be obtained for selected other materials, including plutonium surrogates, for purposes of annual assessments, life extension programs, and resolution of potential significant finding investigations (SFIs). QMU techniques will determine the necessary quantity, quality, and diversity of measurements required.

2. **What experiments would best inform the understanding of hydrodynamic phenomena important to Stockpile Stewardship?**

   Fundamental and focused experiments are the best near-term approach to improving the understanding of hydrodynamic phenomena relevant to Stockpile Stewardship. As indicated above, such experiments are designed specifically to measure key material and dynamic properties relevant to determining the initial conditions for boost. Priority should be given to experiments that measure or constrain the equation of state of plutonium at high pressures and temperatures as well as the locations of static and dynamic phase boundaries (particularly behavior at the melt line). The next priority should be experiments that can validate strength models, followed by those which characterize the formation and evolution of ejecta, spall, and damage in plutonium. Similar experiments should be conducted on plutonium surrogates.

3. **How should NNSA utilize subcritical experiments, including subscale configurations, to best address the overall goals of Stockpile Stewardship?**

Subcritical focused experiments can be used to address several important issues such as the formation and evolution of ejecta as well as the characterization of mix. Such experiments are useful for isolating, diagnosing and studying various dynamic effects that are operative in primary implosions. Again, the interpretation of the results of these experiments will rely critically on data from focused and fundamental experiments. Subscale experiments should be used as validation tests of the overall level of understanding obtained from fundamental and focused experiments and as tests of the use of scaling and surrogacy to make inferences about primary implosion phenomena at full scale.

4. **Is the balance among large, mid-sized and small-scale experiments appropriate?**

There are too few fundamental and focused experiments with plutonium, but a quantitative assessment of the balance remains to be done. In general, the balance among small, medium and large scale experiments should be determined by assessing the needs for key data. The 2007 Dynamic Plutonium Experiments plan provides a useful starting point, but it needs better implementation, and a corresponding integration plan for facilities that is properly prioritized and sustainable.

5. **How should the hydrodynamic experimental program (including DARHT, CFF, pRad, U1a, and other facilities) be augmented? Are there areas of the experimental program where increased investments are warranted?**

The program should be augmented through investment in fundamental and focused experiments on the plutonium properties described above, and through the creation of an integrated sustainable plan for facilities and experiments. Increased investments are warranted for pulsed-power facilities and for new diagnostics for measuring dynamic materials behavior, including pyrometry, imaging, spectroscopy, and diffraction. In addition, should a program of scaled experiments be pursued at U1a it will be necessary to upgrade the existing

radiographic facilities so that they can be used to provide images of the quality required to make meaningful comparisons with the results of simulations.

6. **What other opportunities might be provided by the experimental program to address the need for professional development?**

Professional development would be enhanced with the development of coherent programs of analysis and experiments that define specific goals, their importance and systematic steps for achieving them, leading to peer-review publication of results. Management should develop incentives to promote weapon scientist skills, and to encourage scientists across the laboratories with expertise in different fields (*i.e.*, outside of the weapons program) to support work related to the weapons program in addition to their other research activities.

2 INTRODUCTION AND OVERVIEW

2.1 Background

The moratorium on underground nuclear explosive tests led to the creation of the Stockpile Stewardship Program to maintain this country's nuclear deterrent. This program is based upon the extensive data obtained from underground tests (UGTs) combined with modeling and simulation and surveillance of the enduring stockpile. A component of the stockpile stewardship is a broad experimental program designed to provide validation of the models and codes, examine components of the weapons systems, provide knowledge needed for life extension programs (LEPs) and develop new fundamental knowledge related to weapons behavior.

This experimental program consists of a broad range of instrumentation, techniques, and facilities on many different scales – from experiments that examine component materials to those that assess performance of the integrated system (short of a yield-producing nuclear explosion). The support of this effort in stockpile stewardship has resulted in significant advances in understanding weapons performance, and it continues to evolve from over the past two decades. As we move further from the age of UGTs, there have been calls for new classes of experiments. New techniques have been developed, and new knowledge gained. Moreover, the national security requirements have evolved, with a focus, for example, on weapons surety and aging, and away from the threats envisaged during the Cold War. The balance of effort in the experimental program has been of concern to the NNSA, and, in response, an Office of Nuclear Experiments was recently created by NNSA to coordinate and support this overall experimental program.

2.2 Study Charge

The following is the study charge to JASON from NNSA:

"Hydrodynamic experiments have been important in the development and evaluation of nuclear weapons since the Manhattan Project. Since the end of nuclear explosive testing, hydrodynamic and subcritical experiments have assumed a special role as the only experiments conducted using nuclear weapons-related assemblies driven with high explosives. As such, these experiments provide unique integrated tests of codes and designs. The importance of these experiments led to the construction of DARHT, the development of U1a as the site for underground subcritical experiments, and the continued investment in other firing sites and smaller scale dynamic plutonium capabilities by NNSA. While these tools were being developed, the rate of actual hydrodynamic and subcritical experiments has been relatively low."

"The goal of the newly-formed Office of Nuclear Experiments in NNSA is to coordinate a single long-term program of hydrodynamic experiments using surrogate materials, and subcritical experiments using plutonium aimed at developing a better understanding of the underlying physics of the materials and components in nuclear weapons. This effort will be coordinated with the boost initiative which JASON reported on in 2008[1]. JASON will be asked to look at the current plans from the NNSA labs for hydrodynamic and subcritical experiments and to make recommendations for future efforts using available experimental facilities and platforms. In particular, the JASONs are asked to consider the following questions:

1. What fundamental static and dynamic materials properties data need to be acquired?

2. What experiments would best inform the understanding of hydrodynamic phenomena important to stockpile stewardship?

3. How should NNSA utilize subcritical experiments, including subscale

---

[1]This refers to the JASON study of boost undertaken in 2008 [1]

configurations, to best address the overall goals of the stockpile stewardship program?

4. Is the balance of effort among large, mid-sized, and small-scale experiments appropriate?

5. How should the hydrodynamic experimental program (including DARHT, CFF, pRad, U1a, and other facilities) be augmented to address critical scientific issues in stockpile stewardship? Are there areas of the experimental program where increased investments are warranted?

6. What other opportunities might be provided by the experimental program to address the need for training and professional development of scientists and engineers for stockpile stewardship?"

This study provides an assessment of the hydrodynamic and nuclear experiment program of NNSA carried out by the three nuclear weapons laboratories, Los Alamos National Laboratory (LANL), Lawrence Livermore National Laboratory (LLNL), and Sandia National Laboratory (SNL), as well as associated facilities used by those laboratories at the National Nuclear Security Site (NNSS, formerly the Nevada Test Site), and other supporting facilities. The study addresses technical issues of the program, but provides no cost-benefit analyses. We focus on scientific needs as opposed to programmatic considerations. An example of a programmatic consideration is the use of the proposed subscale experiments to exercise engineering and manufacturing components of the NNSA complex or to ensure that there continues to be an authorization basis for plutonium experiments at the U1a site. This study also does not include any assessment of enhancements in engineering and manufacturing capability that could result from the implementation of a specific experimental program. It should also be noted that the Atomic Weapons Establishment (AWE) of the United Kingdom also has a program of subscale experiments that are a component of the UK weapons certification process. The NNSA laboratories do collaborate with AWE on these experiments, but this study provides no assessment of this collaboration nor of the AWE subscale experiment program.

To provide some technical background on the relevant issues, we describe briefly in Section 2.3 the early time performance of a primary. The physical characteristics of primary implosion set the requirements for measurements to be made through the experimental program to be discussed in this report[2]. We will categorize the types of experiments that are necessary to obtain the requisite physical measurements as fundamental, focused, and integral experiments and discuss the relative roles of such experiments. In Section 3 we discuss some of the important science issues associated with understanding early time primary performance. Section 4 discusses some aspects of the overall experimental program, including integral, focused and fundamental experiments. In Section 5 we describe the proposed subscale experiments, which is followed by a discussion of some aspects of the specific diagnostics to be used in these experiments in Section 6. In Section 7 we discuss an overall strategic plan for the experimental program with an emphasis on maintaining expertise and strengthening foundational science for the weapons program. Some additional topics regarding the quantification of uncertainty are covered in an Appendix. In Section A we discuss several approaches to uncertainty quantification. In Section B we discuss some more formal aspects of how Bayesian Inference can be used to compare experiment with theory.

2.3   Early-time Primary Performance

The experimental program discussed in this report is most relevant to the early time performance of the primary of a nuclear weapon. DOE (b)(3)

DOE (b)(3)

---

[2]We have examined here only the early-time aspects of primary performance as this is the regime that is explored in hydrodynamic, subcritical, and the newly proposed subscale experiments. Additional experiments are carried out in support of radiation-dominated processes like secondary ignition on high energy density facilities such as NIF but we do not cover these aspects in this study.
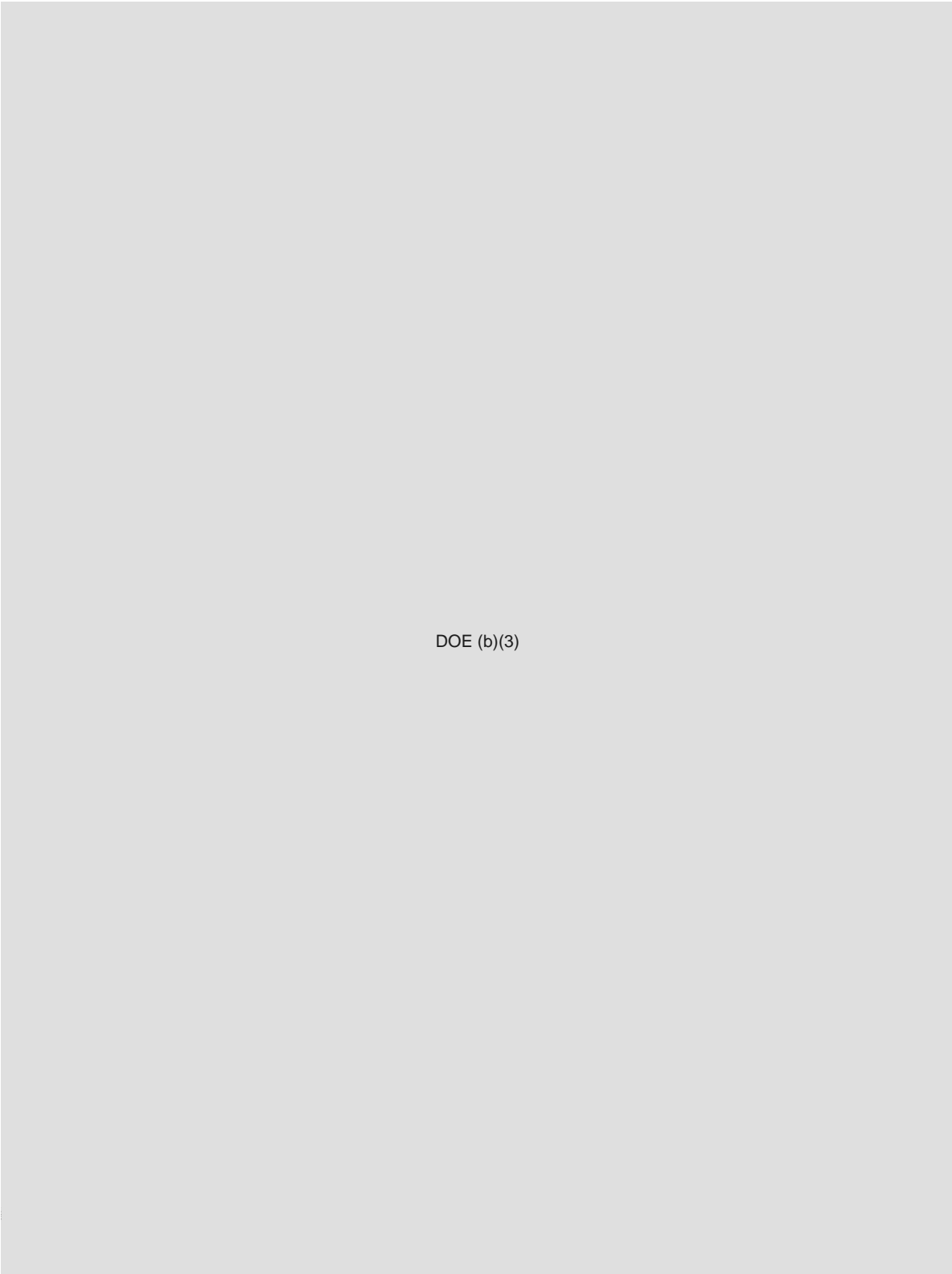
DOE (b)(3)

The process described above is shown graphically in Figure 1.
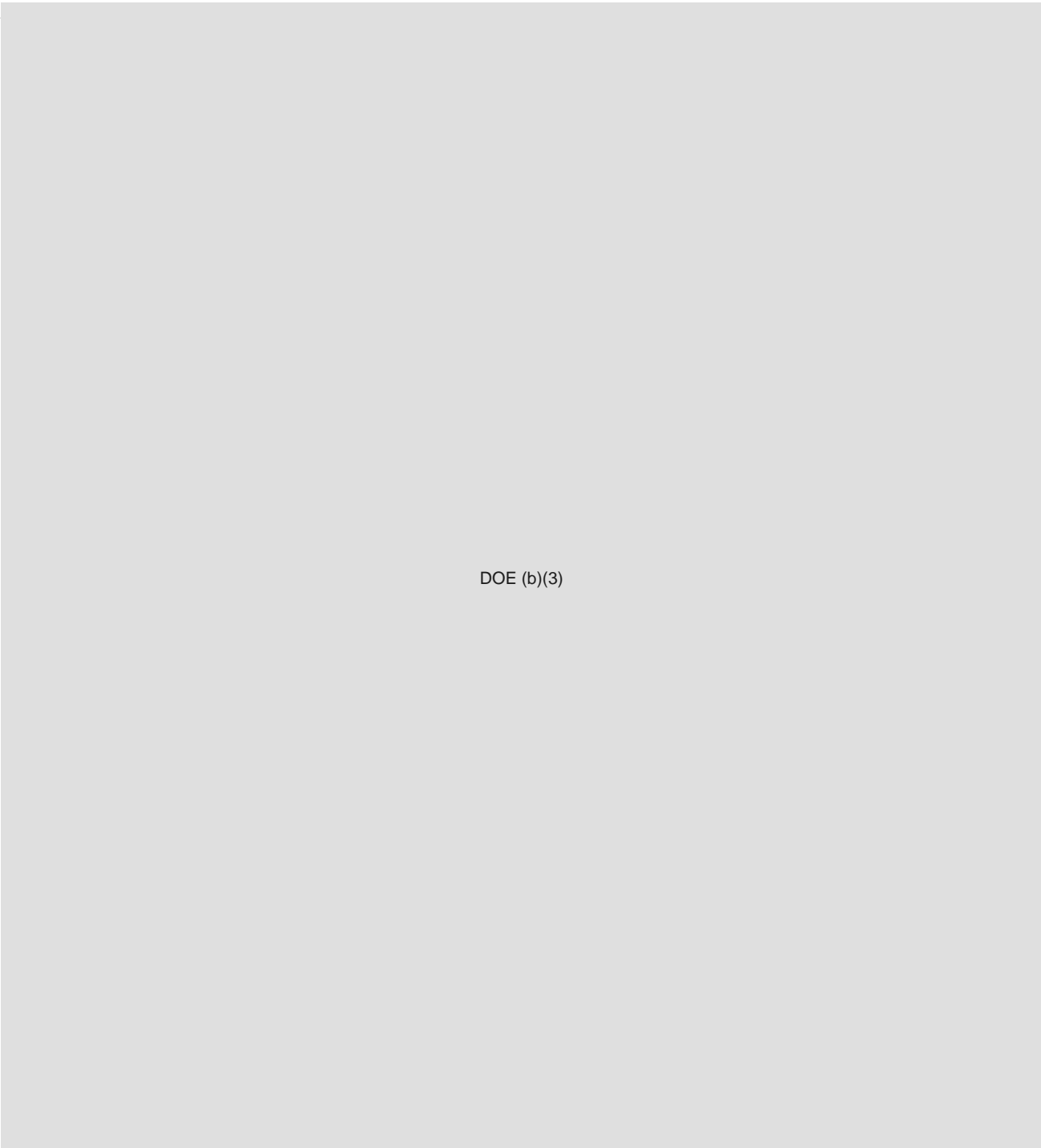
DOE (b)(3)

Of central importance to the energy output of the primary is the rate of neutron production due to fission. This is often characterized by plotting the logarithmic
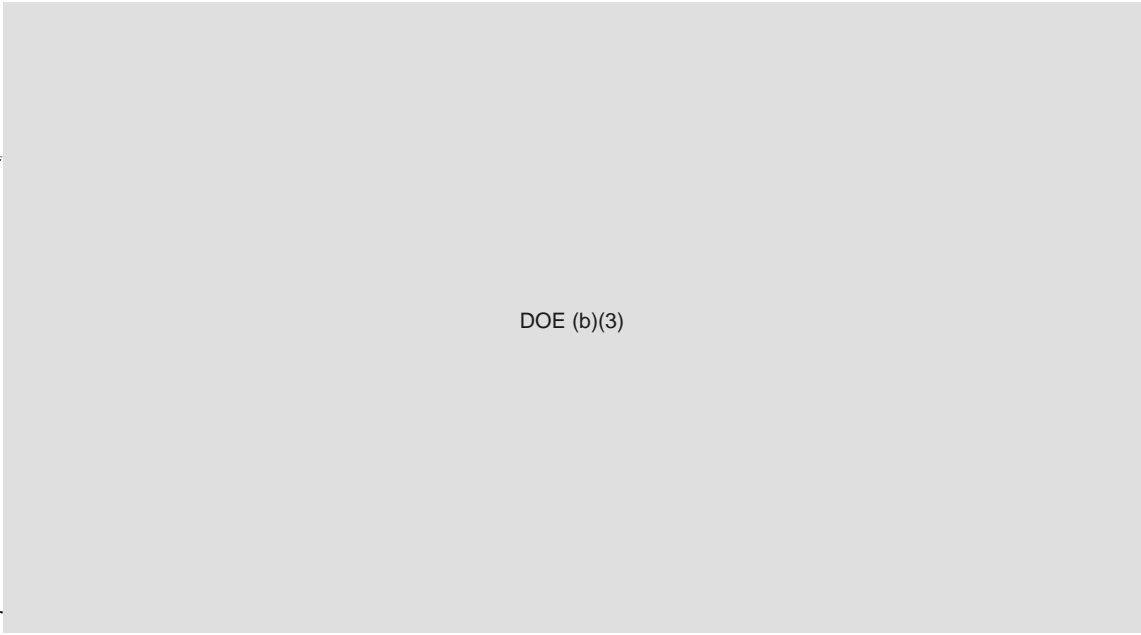
DOE (b)(3)

DOE b(3)

derivative with respect to time of the neutron population $n(t)$ and is denoted by

$$\alpha(t) = \frac{1}{n}\frac{dn}{dt}.$$

This reactivity or "α curve" is a key indicator of primary performance.
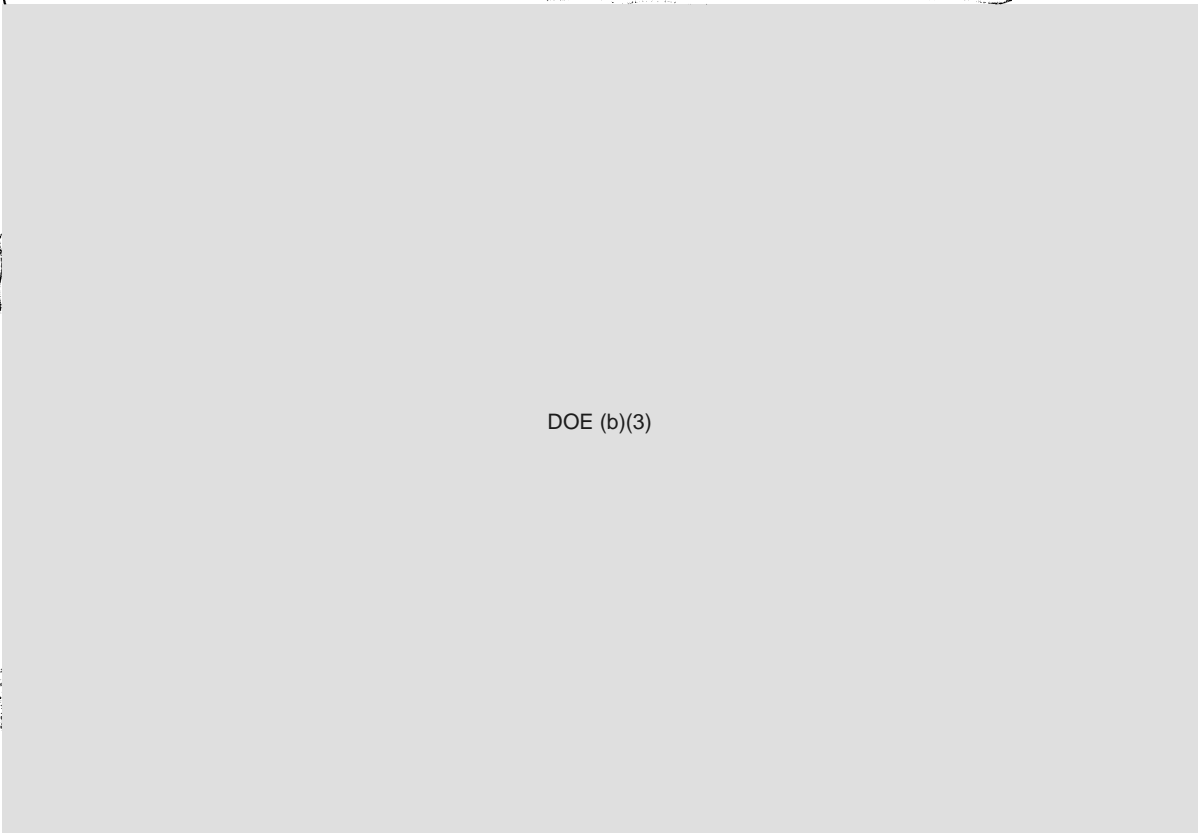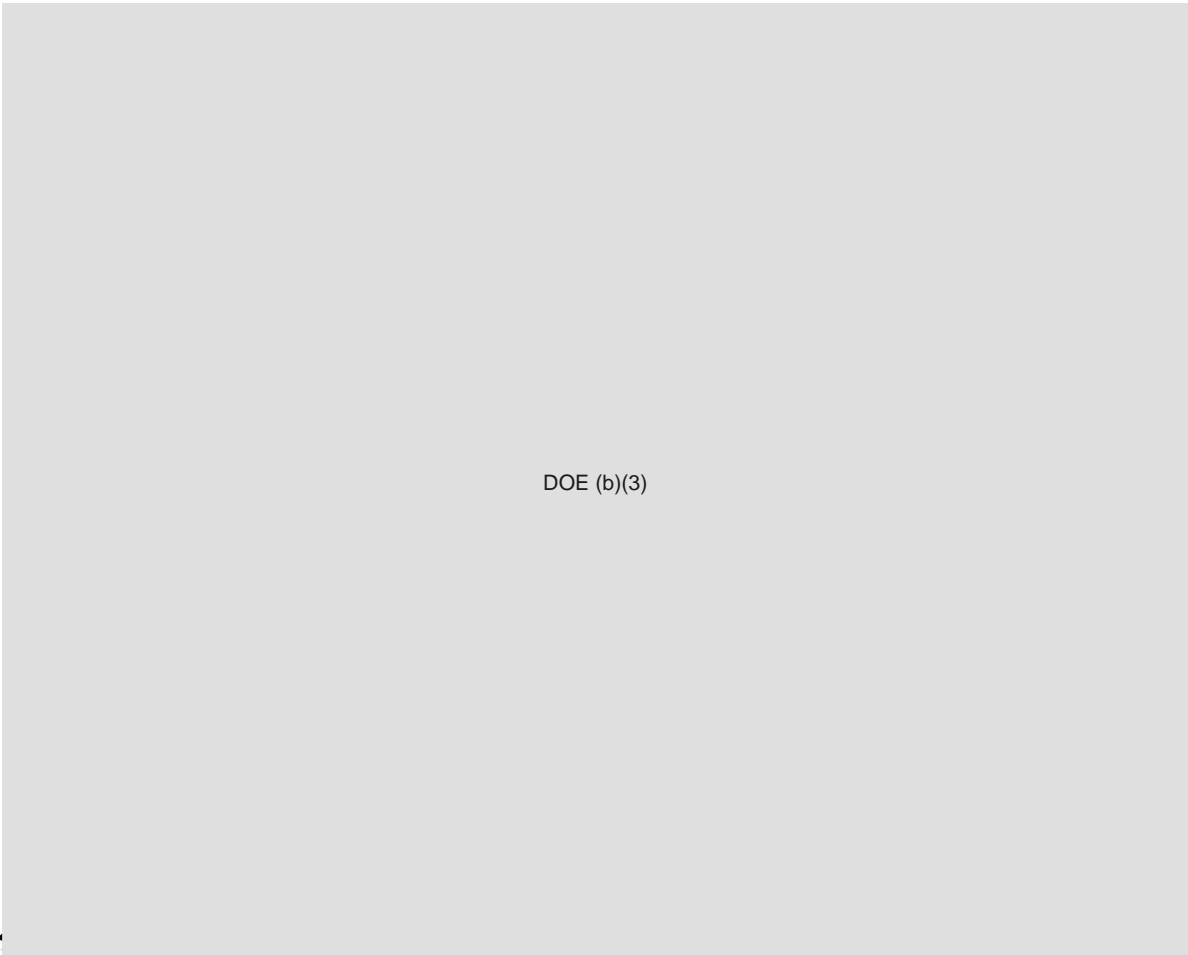
DOE (b)(3)

DOE b(3)

DOE (b)(3)

DOE (b)(3)

DOE (b)(3)

2.4 Categories of Experiments

Hydrodynamic and nuclear experiments have been central to our understanding of the early time primary performance of a nuclear weapon. We distinguish two kinds of data that are obtained from these types of experiments. The first are those directed at material (including chemical) properties. Of central importance are data associated with plutonium, and its pressure-temperature-density (P-T-ρ EOS), its phase diagram (including melt line), transformation kinetics, and chemical reaction dynamics. The list extends to surrogates for plutonium, tampers, gases, and other materials. Information on materials behavior can be obtained from theoretical calculations that have been validated at P-T-strain rate conditions that differ from those of direct relevance to primary performance and thus require additional experimental validation.

The second are those concerned with implosion dynamics and related hydrodynamic phenomena. Information on these phenomena requires time dependent measurements on bulk materials in weapons-related geometries as well as integrated systems with multiple components and materials. They include the subscale experiments to be described in Section 5. A variety of tools are used within this experimental program to obtain these data ranging from bench-top instrumentation to large and complex platforms that span a broad range of scales and costs. They include diagnostics as well as facilities that will be described. The list includes the underground nuclear tests that are no longer performed, but which have provided a large archival database for analysis.

We categorize the various experiments as fundamental, focused, and integral:

Fundamental experiments - Fundamental experiments are those that address physics and chemistry questions, typically of pristine materials.

Focused experiments - Focused experiments are defined here as those that examine the properties of real materials, including defects, microscopic and mesoscopic structure, and texture. As such, these experiments constrain non-equilibrium properties. The samples include Pu coupons to assembly components, and focused experiments therefore include some subcritical experiments.

Integral experiments - Integral experiments include larger scale subcritical experiments that involve assemblies and weapons-related geometries. They involve multiple assembled components to full assemblies. They range from hydrodynamic experiments that test engineering designs to science-driven experiments that address questions of the performance of integrated components. The proposed subscale experiments are in this category.

While this taxonomy is not perfect, it provides a useful organizing principle that we apply to the following discussion.

Table 2: Overview of the experimental facilities throughout the NNSA complex (continued on following page).

Science Capabilities	Location	Type of Capability	Description	# Experiments per Quarter			
				FY11Q1	FY11Q2	FY11Q3	FY11Q4
Dual Axis Radiographic Hydrodynamic Test (DARHT) facility	LANL	Integrated, non-nuclear weapons experiments	DARHT captures high resolution images of moving, non-nuclear weapon assemblies. Experiments are used to obtain information critical to certifying weapons performance in the absence of underground testing. DARHT captures images from two views and at multiple times.	0	0		
Contained Firing Facility (CFF)	LLNL	Integrated, non-nuclear weapons experiments	CFF capabilities include high resolution imaging and high fidelity velocity measurements of moving, non-nuclear weapon assemblies. Experiments are used to obtain information critical to certifying weapons performance in the absence of underground testing. A single image and many velocity measurements are captured per experiment. CFF has a substantially larger field of view than DARHT.	2	2		
National Ignition Facility (NIF)	LLNL	Focused experiments: Radiation, plasmas and materials	NIF provides a platform to investigate fundamental properties of material, plasma, radiation, fusion ignition, and thermonuclear burn at temperatures and pressures relevant to those obtained in a nuclear weapon. In the absence of underground testing, these conditions are not possible on any other experimental platform.	64	80		
Z-Machine	SNL	Focused experiments: Radiation, plasmas and materials (including plutonium)	The Z Machine provides a platform to investigate fundamental properties of material, plasma, and radiation, and effects of radiation on electronics. Relatively large samples and plasmas may be studied as well as certain advanced certification concepts in parameter regimes of interest.	11 (1)	34 (1)		
Omega	UR-LLE	Focused experiments: Radiation, plasmas and materials	Omega provides a platform to investigate fundamental properties of HED material properties, plasmas, inertial confinement fusion, and radiation as well as for the development of targets, diagnostics and experimental platforms for the NIF. Omega is uniquely accessible to universities through the National Laser User's Facility. Targets are millimeters in diameter.	303	487		

2.5 Overview of Experimental Facilities

Hydrodynamic and nuclear experiments are conducted at a broad range of facilities across the NNSA complex. In Tables 2 and 3 we list the major facilities as well as the number of experiments performed using Pu. M. Hockaday [4] provided a useful overview of facilities and capabilities and we review these briefly here.

The following are some of tools, facilities, and platforms used for fundamental and focused experiments each includes a range of diagnostics, some of which are discussed in detail in later sectinos:

Table 3: Overview of the experimental facilities within the NNSA complex (continued from previous page).

Science Capabilities	Location	Type of Capability	Description	# Experiments per Quarter			
				FY11Q1	FY11Q2	FY11Q3	FY11Q4
High Explosive Application Facility (HEAF)	LLNL	Focused experiments: Explosives, Materials	HEAF provides a platform to investigate fundamental properties and reactions of chemical explosives, as well as gas guns to study materials. Experiments are focused on continually improving the safety of our stockpile.	205	217		
The Joint Actinide Shock Physics Experimental Research (JASPER) Facility	NNSS	Focused experiments: Metals (including plutonium)	JASPER provides a platform to investigate the properties of metals, including plutonium, at high shock pressures, temperatures and strain rates. JASPER, LBPG, and TA-55 each cover unique areas of material phase space with some overlap.	0	0		
Large Bore Powder Gun (LBPG)	NNSS	Focused experiments: Metals (including plutonium)	LBPG provides a platform to investigate the properties of metals, including plutonium, at high shock pressures, temperatures and strain rates, but with a larger target (size of experiment) than JASPER. JASPER, LBPG, and TA-55 each cover unique areas of material phase space with some overlap. (Note: still in development).	0	0		
Los Alamos Neutron Science Center (LANSCE)	LANL	Focused experiments: Metals	LANSCE is a linear accelerator that uses neutrons to study fundamental material properties.	14	0		
Proton Radiography (pRad)	LANL	Focused experiments: Materials	pRad is a beam line and proton optics capability that uses protons to study fundamental material properties. pRad uses the LANSCE accelerator to produce protons for radiography of static and dynamic materials.	12	0		
Big Explosives Experimental Facility (BEEF)	NNSS	Integrated, non-nuclear weapons experiments	BEEF is an experimental facility that allows the study and investigation of materials as they are merged together by high-explosive detonations.	1	1		
TA-55	LANL	Focused experiments: Metals (including plutonium)	TA-55 provides several platforms to investigate the properties of metals, including plutonium, at high shock pressures, temperatures and strain rates. The TA-55 gas gun is located in a Category II nuclear facility, but is limited to Category III quantities.	9 (6)	20 (20)		
U1a Facility	NNSS	Subcritical experiments	Provides capability for subcritical physics experiments providing material and system response data.	1 (1)	1 (1)		

Diamond Anvil Cells - Diamond anvil cells (DACs)are used to explore the static properties of Pu. In addition they are used to explore the static phase diagram. Some of these experiments are performed at DOE Office of Science facilities such as the Advanced Photon Source (APS) among other facilities.

TA-55 40 mm Gas/Powder Gun - This is a gas gun encased in a large glove box. It is capable of exploring pressures up to 300 kbar in Pu. At present a VISAR diagnostic is used to measure dynamic response of Pu targets.

JASPER - JASPER is the Joint Actinide Shock Physics Research Facility located at the Nevada Nuclear Security Site (NNSS). It is a two stage gas gun able to explore pressures up to several Megabar. Using graded impactors it can also explore off-Hugoniot states of the EOS.

Large Bore Powder Gun - This a gun facility that has a 40' barrel and a 3.5" bore. While it cannot explore very high pressures (it is limited to several hundred kilobars), the large bore allows the use of larger samples and provides measurement times of up to several microseconds, allowing improved off-Hugoniot measurements. The gun is currently being prepared for installation at NNSS.

HEAF - The High Explosive Applications Facility at LLNL is used for investigations of high explosive performance as well as for development of new HE formulations.

Z Machine - The Z machine at SNL is a pulsed power facility. It can be used to accelerate flyer plates upwards of 30 km/s and provide quasi isentropic compressions on samples up to several megabar. Using a special containment system, measurements on Pu have been made up to 1 Mbar with future capability targeting 3.5 Mbar.

NIF - The National Ignition Facility utilizes laser drive to compress samples using shock or quasi-isentropic compression, potentially to in excess of 100 Mbar. Currently, samples have been ramp compressed to 50 Mbar. It can also be used to explore high strain rates (up to 10^7/s). It has not yet been qualified to handle Pu, but has provided important data on surrogates such as Ta.

Phoenix - Phoenix is an explosively driven pulsed power platform designed to isentropically compress Pu samples up to pressures of 30 Mbar. Because larger sample sizes can be used, it is intended to explore longer time scales for dynamic response compared to Z. Phoenix is still in the testing stage, and a decision to begin an experiments on Pu will be made in FY12.

Omega - The Omega laser facility is located at the Laboratory for Laser Energetics at the University of Rochester. It is used to perform high energy density experiments but at lower pressures than NIF. There is no authorization to work with Pu at this facility.

Hydrodynamic experiments (so-called "hydros") utilize the following facilities.

DARHT - DARHT is a dual axis radiographic hydrodynamic test facility located at LANL. Using two electron beam accelerators, it provides orthogonal views of a hydrodynamic experiment like the implosion of a surrogate primary enclosed in a vessel using 18-20 MeV X-rays. The second axis provides up to 4 pulses so that epochal views are possible. DARHT is currently the premier radiographic facility within the weapons complex. Unfortunately, there is no authorization at present to use it for Pu experiments.

CFF - CFF is the Contained Firing Facility located at LLNL. Because of its large footprint and the large field of view of its radiographic facilities (FXR), CFF can be used for a variety of applications like nuclear counter terrorism and to explore surety concepts. Pu experiments are not performed at CFF.

pRad - The pRad facility is located at the Los Alamos Neutron Science facility (LANSCE). It uses accelerated protons to image implosions. It provides epochal views (up to 41 frames) and can in principle image through areal densities of up to 50 g/cm^2. While experiments with special nuclear materials can be performed at LANSCE the amount of material is limited to less than 11 g of Pu driven by 30 g or less of HE.

For subcritical experiments and the new subscale experiments, the following facilities are involved

U1a - U1a is an experimental complex located at the NNSS. It provides a capability to perform subcritical Pu experiments underground with a suite of diagnostics. It is also the location for the new proposed subscale experiments.

BEEF - The Big Explosive Experimental Facility (BEEF) is located at U1a and performs experiments with HE pushing metal using larger quantities of HE than can safely be used at CFF, DARHT or HEAF.

Cygnus - Cygnus is the X-ray facility used "down-hole" at the U1a site. It is a dual axis facility able to capture radiographs at two views spaced sixty degrees

apart. The dose capability of Cygnus is considerably less than DARHT (4 - 4.5 R at 1 m versus that of DARHT at 600 R at 1 m) as is the end-point energy (2.25 MeV vs. 20 MeV). The spot size is comparable to that of DARHT, about 1.1 mm.

Tables 2 and 3 also list the number of experiments performed with plutonium in the first and second quarters of FY11. As many of the facilities listed above have no authorization to perform experiments with Pu, it is not surprising that there are not many experiments listed. However, several of the facilities (notably Z, JASPER, pRad, and U1a) are authorized to work with Pu yet the number of experiments is quite low. We note again that while DARHT is ideally suited to image implosions with Pu, the authorization to perform these experiments at LANL is in incomplete.

2.6 Dynamic Plutonium Experiments Program

In 2007 the three nuclear weapons laboratories (LANL, LLNL, and SNL) finalized the plans for a ten year initiative to determine key properties of Pu relevant to the creation of initial conditions for boost in a primary [5]. DOE (b)(3)

DOE (b)(3)

DOE b(3)
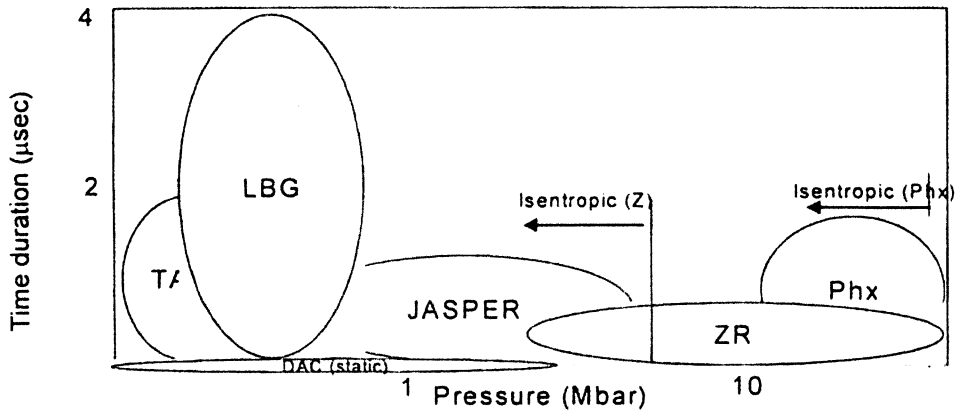
Figure 4: The pressure and time regimes to be explored in the experiments described in the Dynamic Plutonium Experiments (DPE) program plan.

DOE (b)(3)

The DPE program was organized around four technical elements:

1. EOS of Pu

2. constitutive properties

3. complex hydrodynamics

4. experimental capabilities.

A survey of existing or future experimental facilities was performed and a matching of capability to required data was established. The program is notable in that it was organized with a tri-lab perspective and with a focus on the P-T trajectories that are accessed in a primary implosion. Shown in Figure 4 are the regions and time durations accessed by the various experimental facilities.

DOE (b)(3)

24

More recently, it has been demonstrated that lasers such as NIF may also be useful in such investigations.

Several issues have arisen which have led to delays in the execution of the DPE program. A higher degree of nuclear regulatory oversight was imposed on the JASPER facility which required the temporary closure of the facility. Safety issues arose with the use of the Large Bore Powder Gun at LANL and, as a result, this facility will be reconstructed at U1a. Finally, the Phoenix experiments have encountered technical issues associated with the robust delivery of current to the armature that provides the compression. In total, these issues resulted in a three year delay in some of key experiments and this has contributed to the relatively low rate of experiments in Pu over the past few years.

DOE (b)(3)

DOE (b)(3)

2.7 Assessing Priorities for Future Experiments

The sections above provide an overview of the physical states encountered in a primary and also describe the significant investment made by NNSA to address these questions. An important question that arises is how to set the relative priorities for the type of data that are required.

DOE (b)(3)

DOE (b)(3)

DOE (b)(3)

In setting these priorities, it is also important to understand what accuracy is required for the various materials properties to be measured.

DOE (b)(3)

This also indicates why the DPE approach has merit: initial priorities were assessed in the DPE plan based on the best experimental results available with the goal of either validating or refuting these priorities.

Once such priorities are in hand, it is then possible to consider the types of experiments which will best provide the required data. In the next chapter, we attempt to provide some estimates of the importance of the phenomena described above. Our investigations are very cursory, but provide some guidance as to the relative accuracies required. We then follow this discussion with some experimental approaches which show promise in obtaining the required data. Note that the 2007 plan for the DPE program plan described above provided a very good start on addressing these issues. However, for a variety of reasons it has proven to be difficult to complete this work.

3 CURRENT QUESTIONS

In this section, we consider some of the physical phenomena discussed in the previous chapter and attempt to provide some measure of their relative importance to primary performance.

DOE (b)(3)

DOE (b)(3)

DOE (b)(3) What emerges from this discussion, and will be amplified in the next chapter, is the important role of fundamental and focused experiments as the best near term approach to clarifying the issues.

DOE (b)(3)

DOE (b)(3)
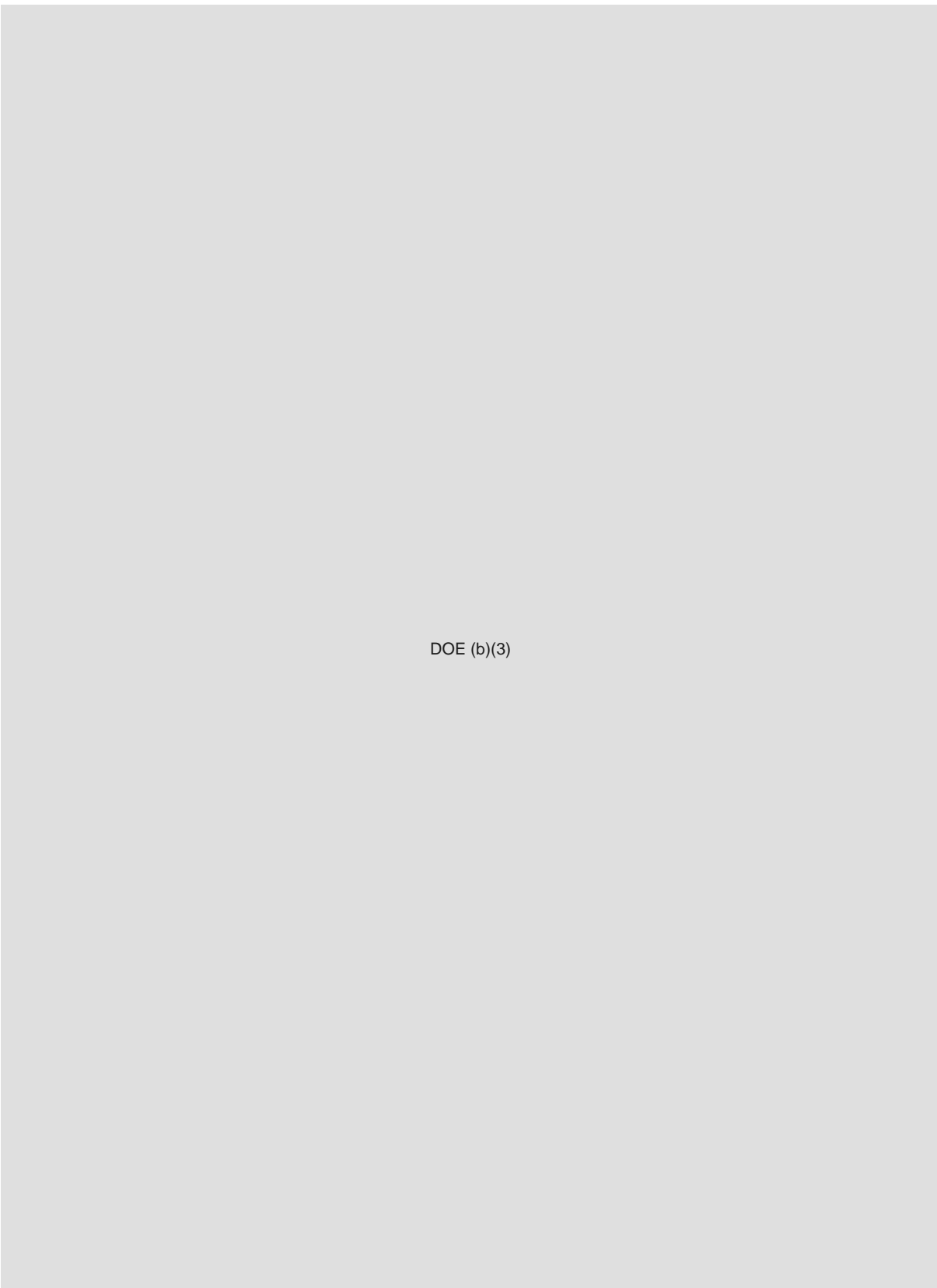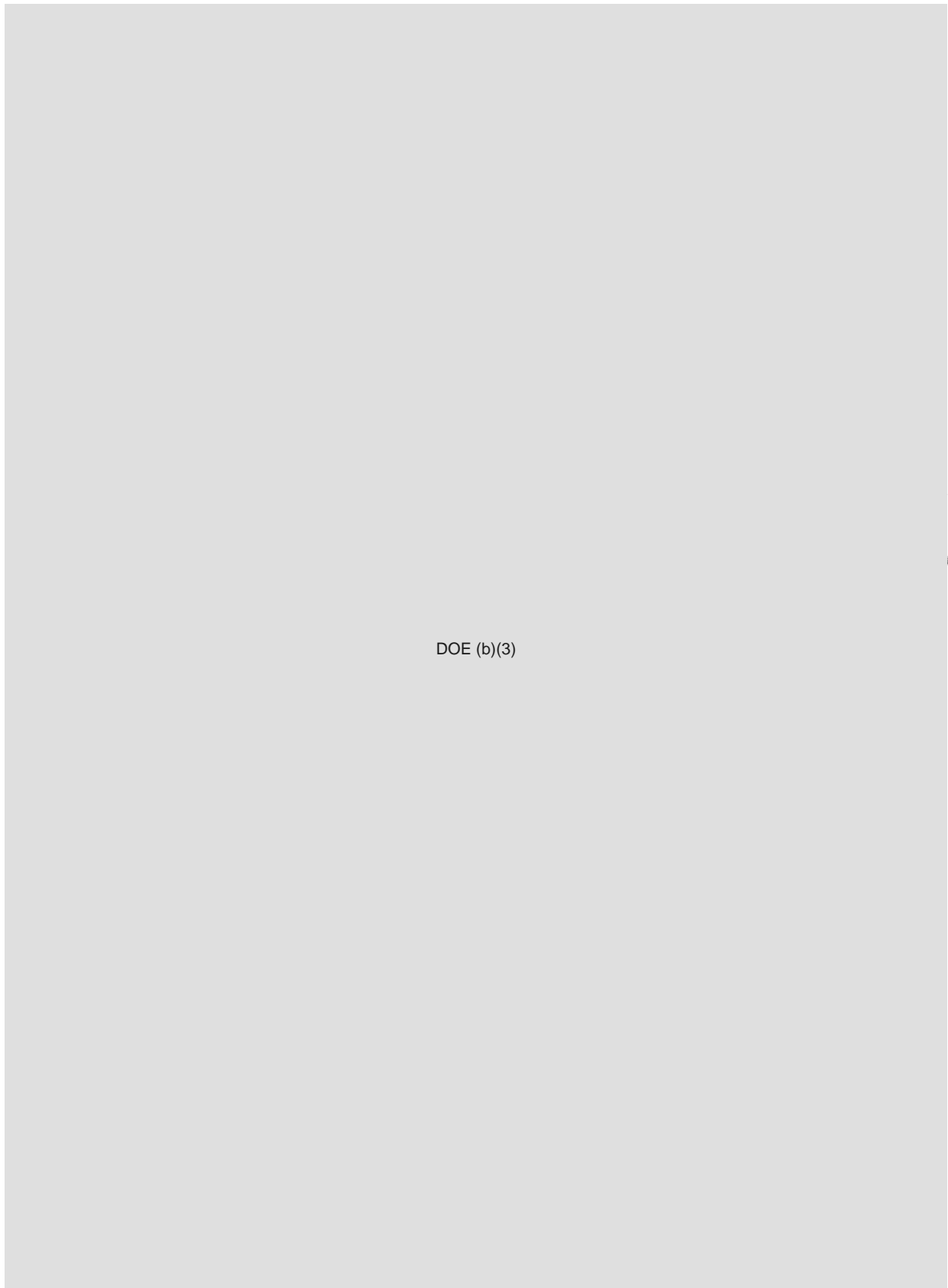
DOE (b)(3)

DOE
b(3)

DOE (b)(3)

DOE (b)(3)

DOE
b(3)
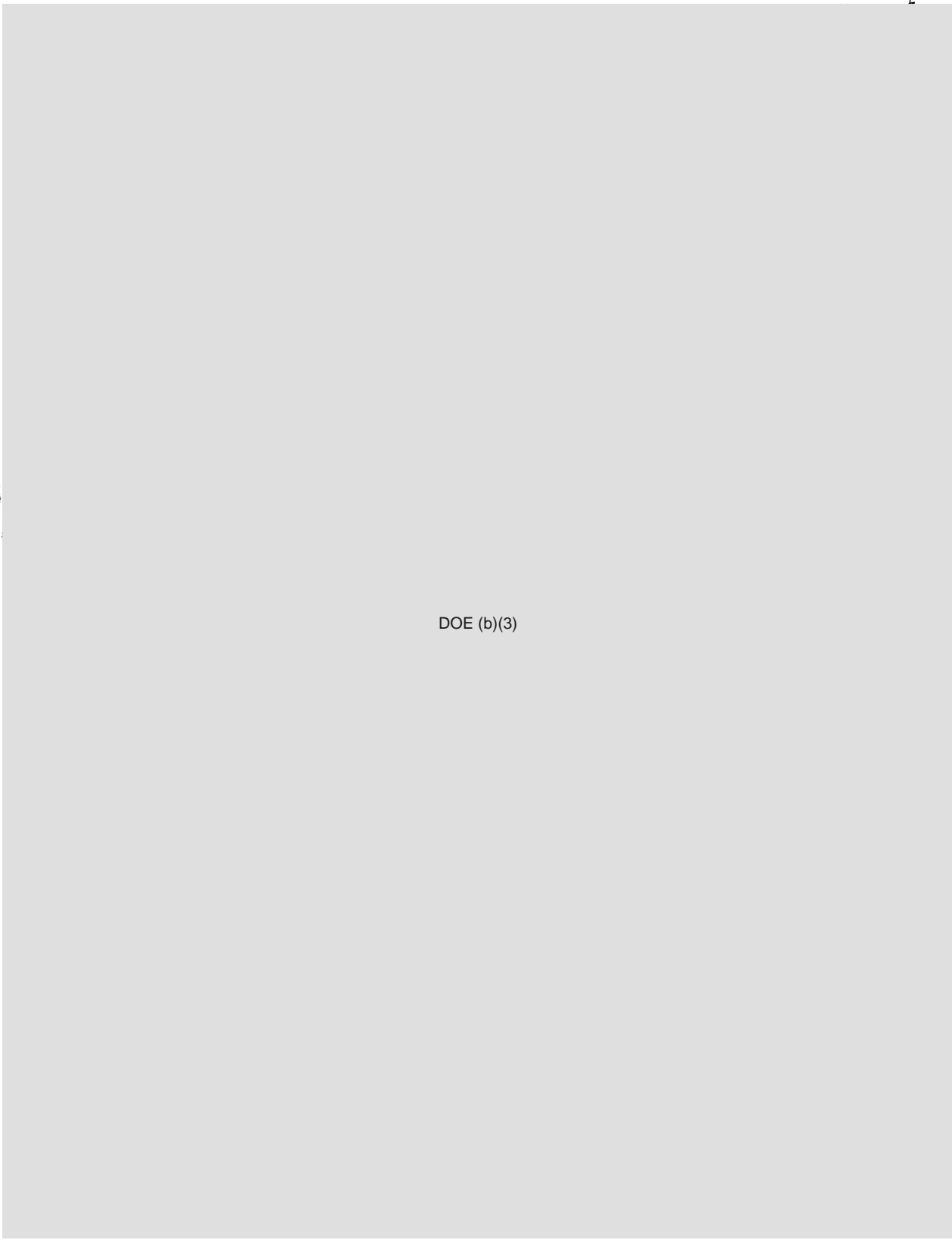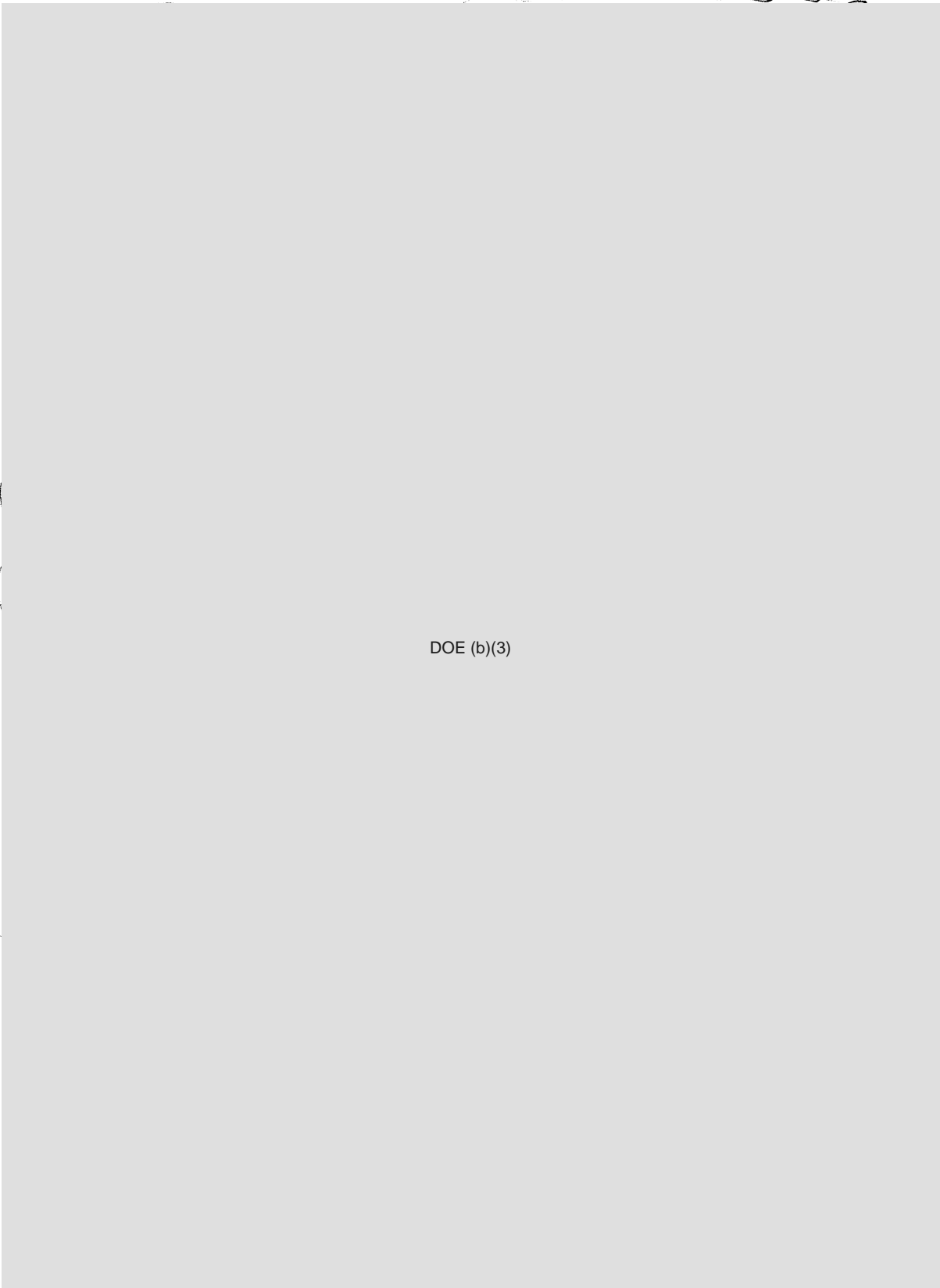
DOE (b)(3)
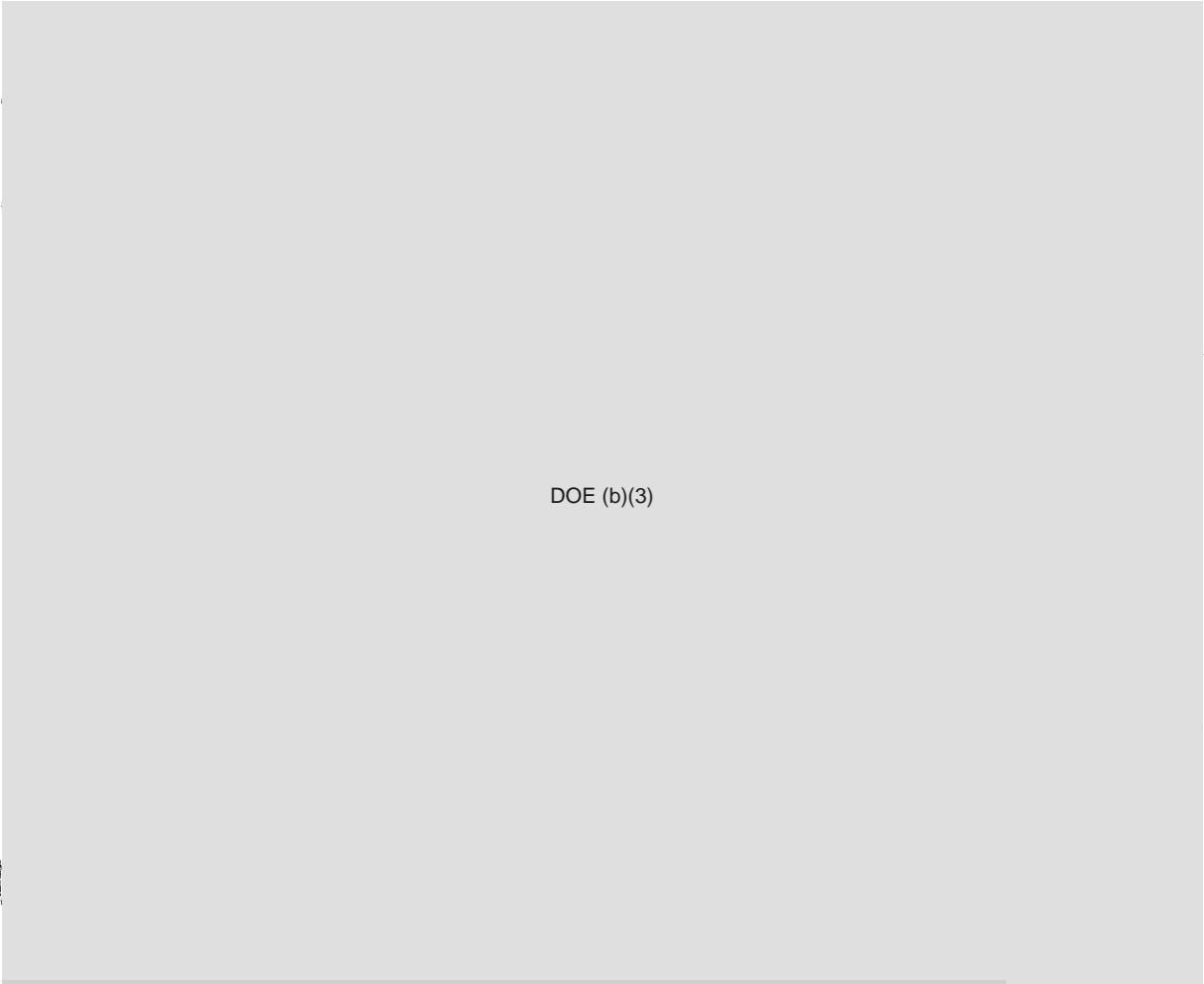
DOE (b)(3)

DOE (b)(3)

DOE (b)(3)

DOE (b)(3)

DOE (b)(3)   These may
be used to reveal related physical phenomena, as described in the next section, but
quantitative information requires studies of Pu itself.
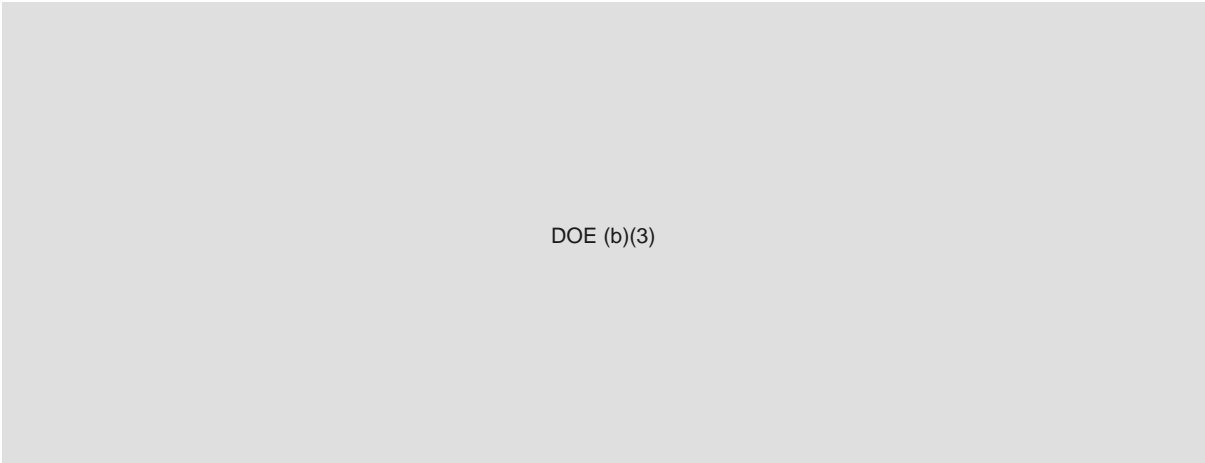
DOE (b)(3)
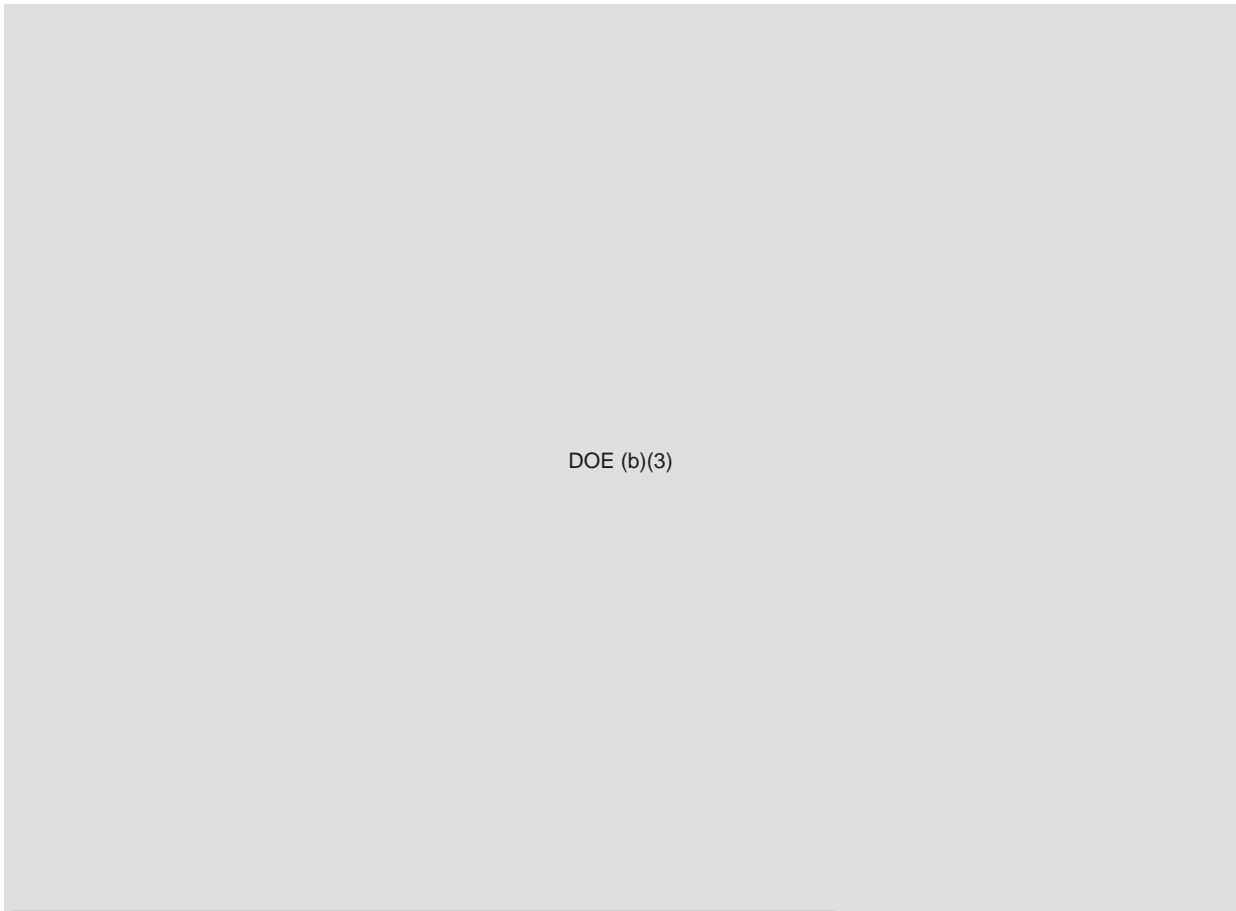
DOE (b)(3)

DOE (b)(3)
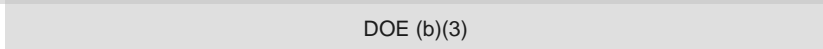
DOE (b)(3)

The quality of the data compared to what could be obtained now (*e.g.*, on third generation synchrotron sources) is revealed by examination of results obtained at that facility on Fe compared with what has been measured more recently on that element [10].

DOE (b)(3)

DOE (b)(3)
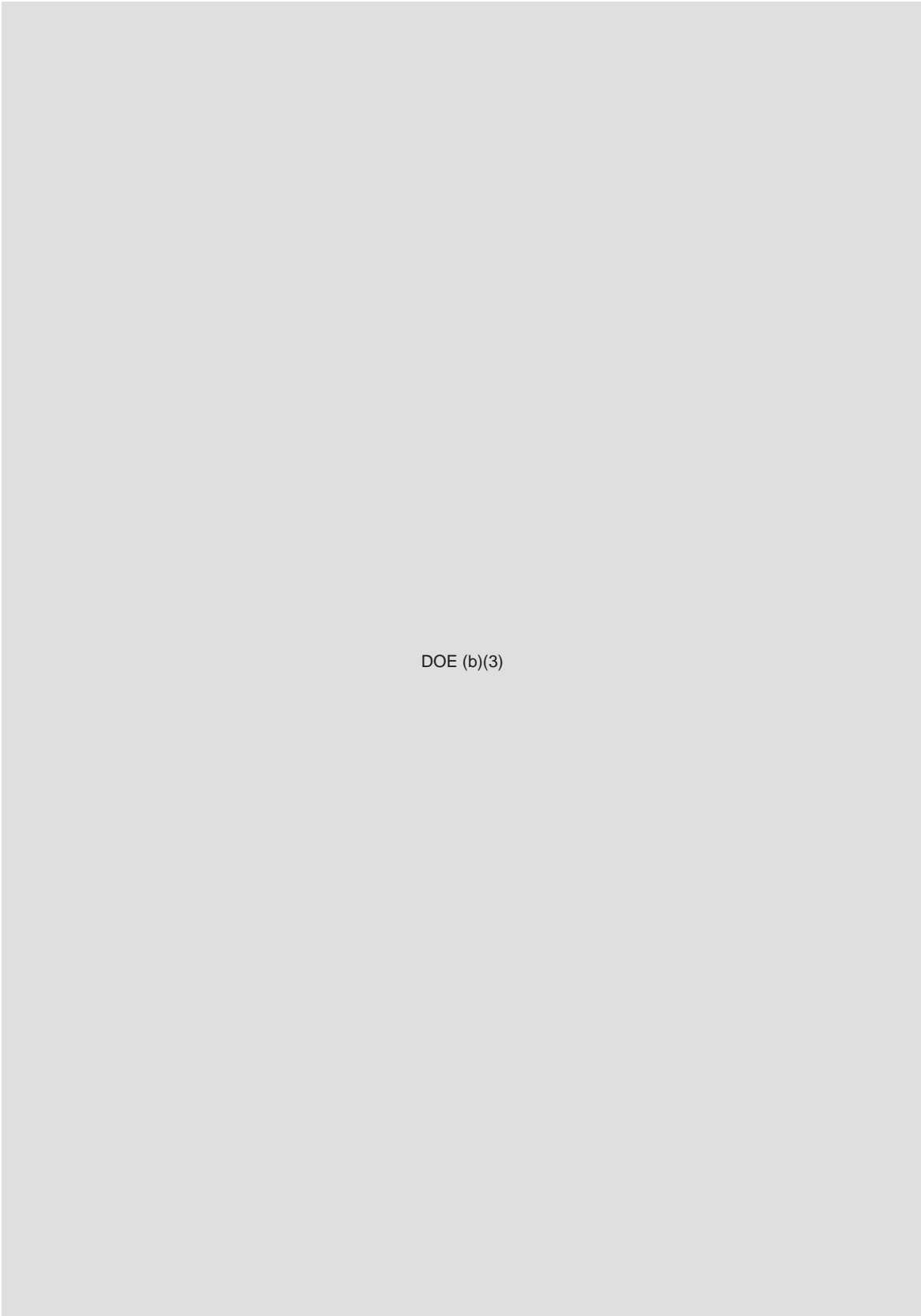
DOE (b)(3)
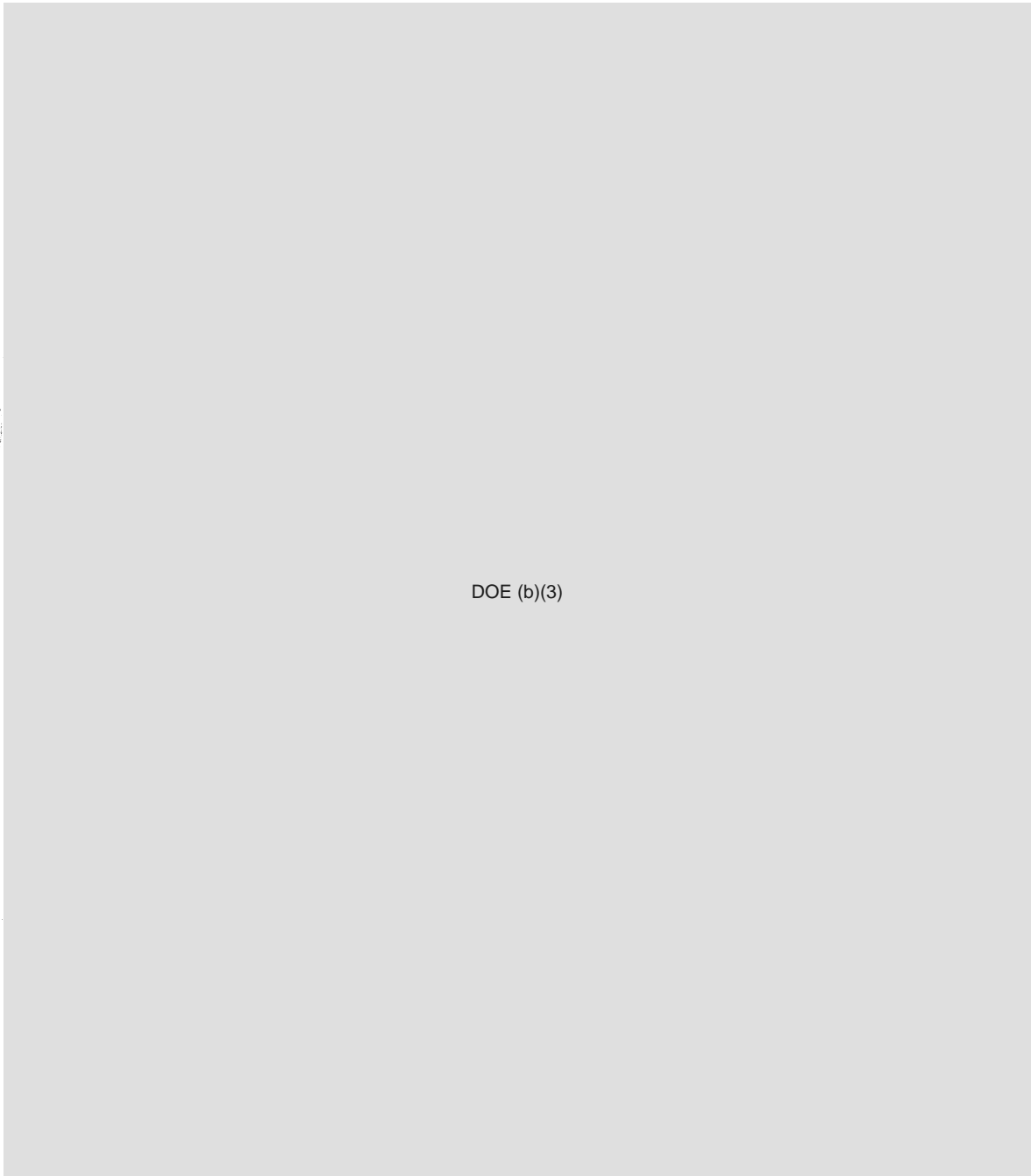
DOE (b)(3)

3.4   Entropy Generation

Beyond the P-T-ρ EOS are thermochemical properties that determine equilibrium phase stability. During most of the course of a hydrodynamic experiment the flow is nearly isentropic. It is usually nearly adiabatic (except within detonating high

explosive or in nuclear explosions) because radiative and conductive heat flow and viscous dissipation are slow compared to hydrodynamic processes under "warm dense matter" conditions (temperatures of 0.1–10 eV, densities of 0.1–10 × solid density, and dimensions of tenths of mm or greater). The flow is therefore nearly isentropic except at shocks. In metals and covalently bonded solids, whose bulk moduli are generally $\mathcal{O}(1\ \text{Mbar})$, shocks produced by high explosive are weak enough that the entropy change is usually small.

When entropy is nearly conserved in most of a flow, it is a powerful tool for thinking about the flow, and for numerical calculation. The choice of entropy as one of the independent thermodynamic variables is advantageous in reducing numerical errors. In calculation of processes that change all other variables by large factors the conservation of specific entropy is then automatic and explicit; it does not have to be enforced as an implicit constraint on the variation of two other independent variables, both of which vary by large amounts.

The use of entropy as an independent thermodynamic variable also facilitates understanding. When entropy is increased by some process, the effect of that process is immediately apparent. This would be less obvious when the variables are (for example) pressure and density, because then an increase in entropy appears as only a small (perhaps nearly invisible on a plot) shift of an element's trajectory in thermodynamic space. Sometimes small entropy differences may be important; they may determine the phase of a material, and many properties, including strength and the pressure-density relation, can be very different for two phases that are nearly in thermodynamic equilibrium.

The entropy of a substance is given by

$$S(T) = \int_0^T \frac{C_P(T')}{T'}\, dT', \tag{3}$$

where C_P is the heat capacity at constant pressure; we assume a thermodynamic path at constant (generally zero) pressure and a classical substance for which $S(0) = 0$. For an electron-degenerate metal, phonons contribute essentially all the specific heat,

which we describe by the Debye model (we ignore the more exotic excitations):

$$C_P(T) \approx \begin{cases} \frac{12\pi^4}{5} \left(\frac{T}{\Theta_D}\right)^3 nk_B & T < 0.234\, \Theta_D \\ 3nk_B & T > 0.234\, \Theta_D, \end{cases} \tag{4}$$

where the low temperature Debye approximation is taken for $T < 0.234\, \Theta_D$ and the un-quantized Dulong-Petit result for $T > 0.234\, \Theta_D$; the break point of $T = 0.234\, \Theta_D$ is chosen at the value of T at which these limiting forms are equal. In Equation 4, n is the ionic density and C_P is the specific heat per unit volume.

For $T > 0.234\, \Theta_D$

$$S(T) \approx 3k_B \left[\ln\left(\frac{T}{0.234\, \Theta_D}\right) + 0.004\right], \tag{5}$$

where $S(T)$ is the entropy per ion.

DOE (b)(3)

High explosive shocks in solids are fairly weak; their typical overpressures of 100–300 kbar are less (but not enormously less) than most solid condensed matter bulk moduli[4]. The entropy increase in an infinitesimal (acoustic) shock in a fluid is [22]

$$\Delta s = \frac{1}{12T_1}\left(\frac{\partial^2 V}{\partial P^2}\right)_s (\Delta P)^3, \tag{6}$$

where s is the entropy per gram, and must be multiplied by the atomic weight to get the entropy per ion (5), and V is the specific volume (the reciprocal of the density). The second partial derivative in Equation 6 is the first partial derivative of the compressibility (the reciprocal of the bulk modulus) with respect to pressure.

DOE (b)(3)

DOE (b)(3)

DOE (b)(3)

DOE (b)(3) Experiments such as these require simplified geometry and specific diagnostics to extract the appropriate measurements.

3.5 Transformation Kinetics and Metastability

DOE (b)(3)

DOE (b)(3)

DOE (b)(3)

DOE
b(3)
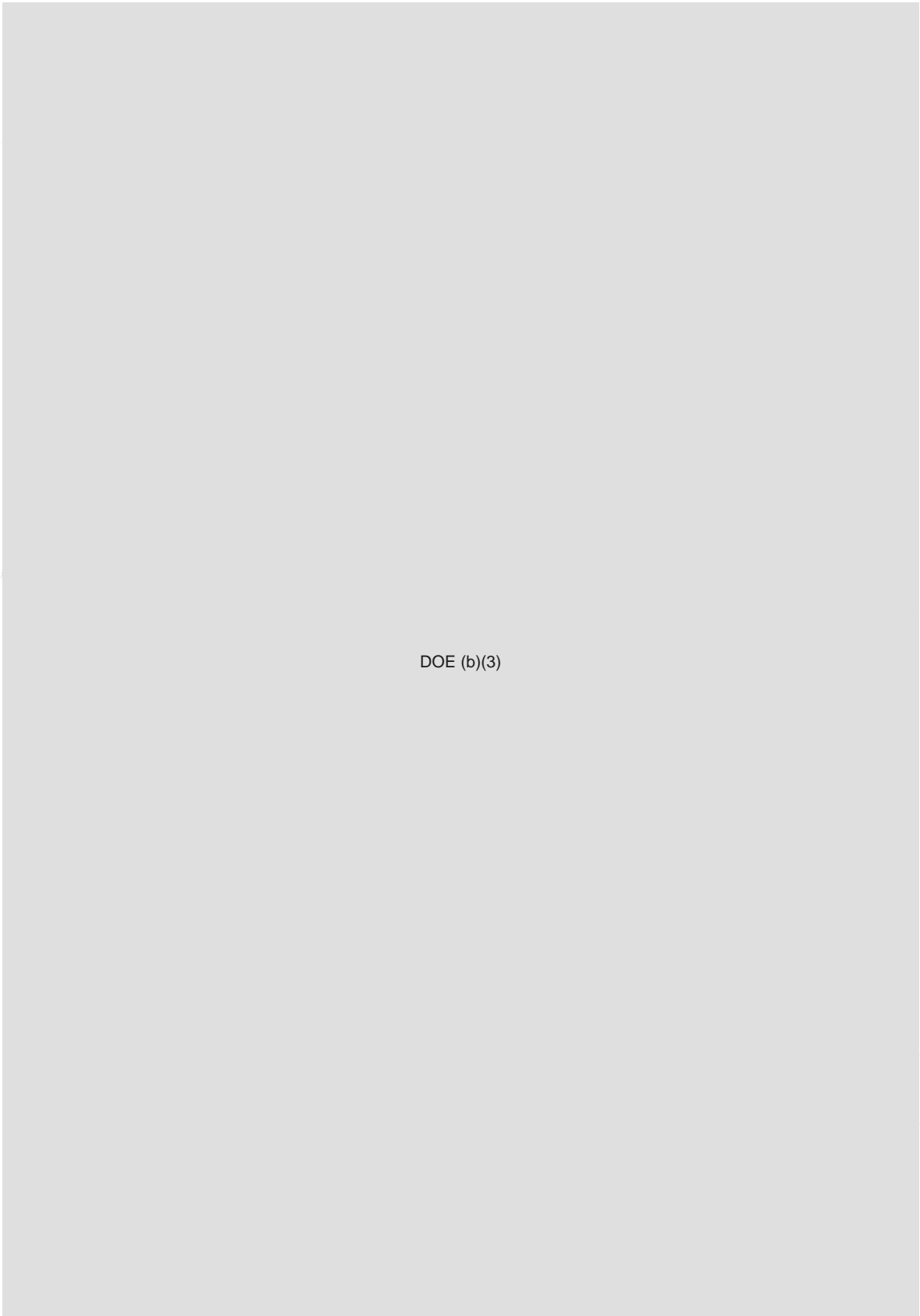
DOE (b)(3)

DOE
4(3)

DOE (b)(3)

DOE (b)(3)

DOE b(3)

DOE (b)(3)

DOE (b)(3)

DOE
b(3)
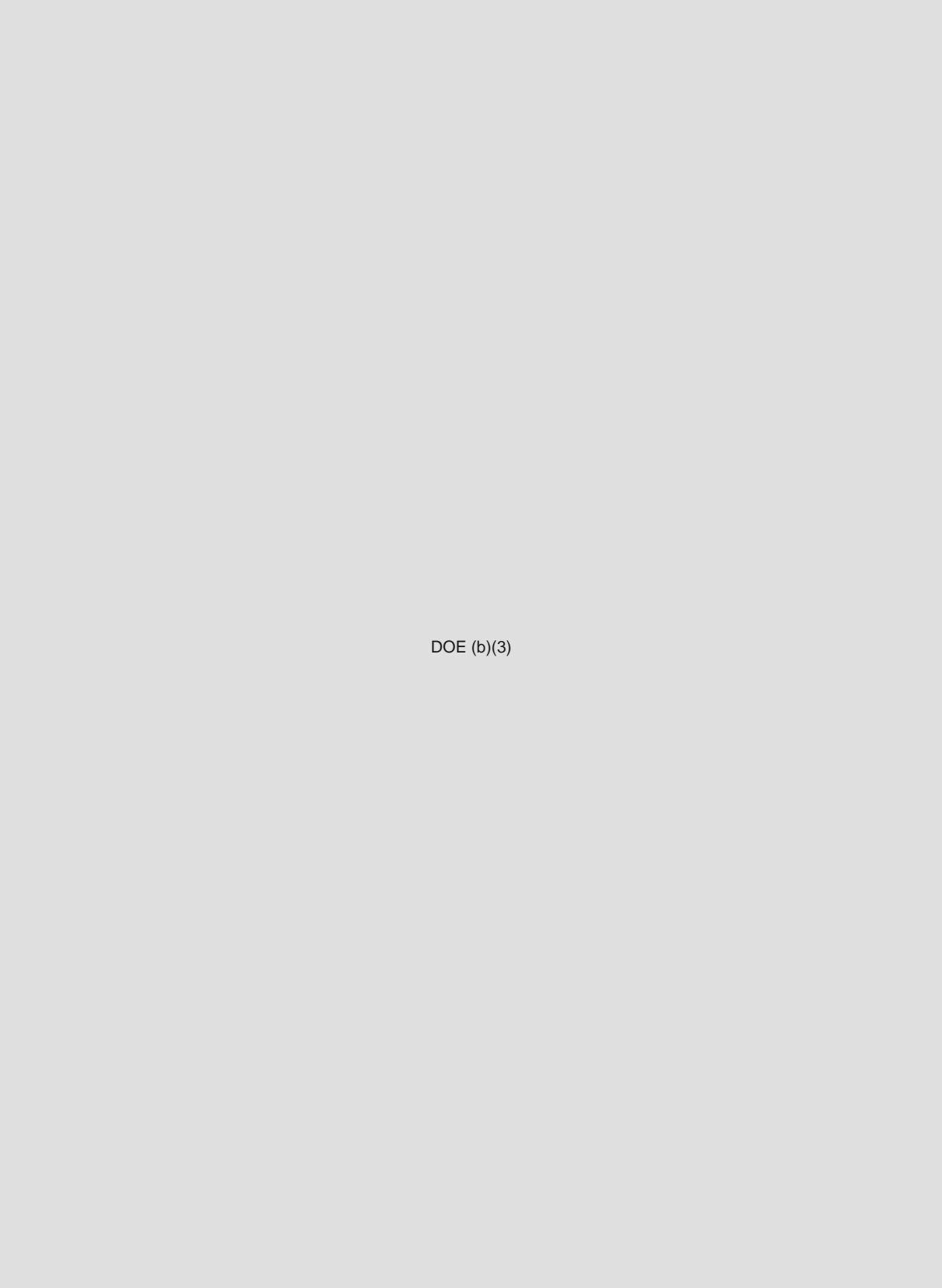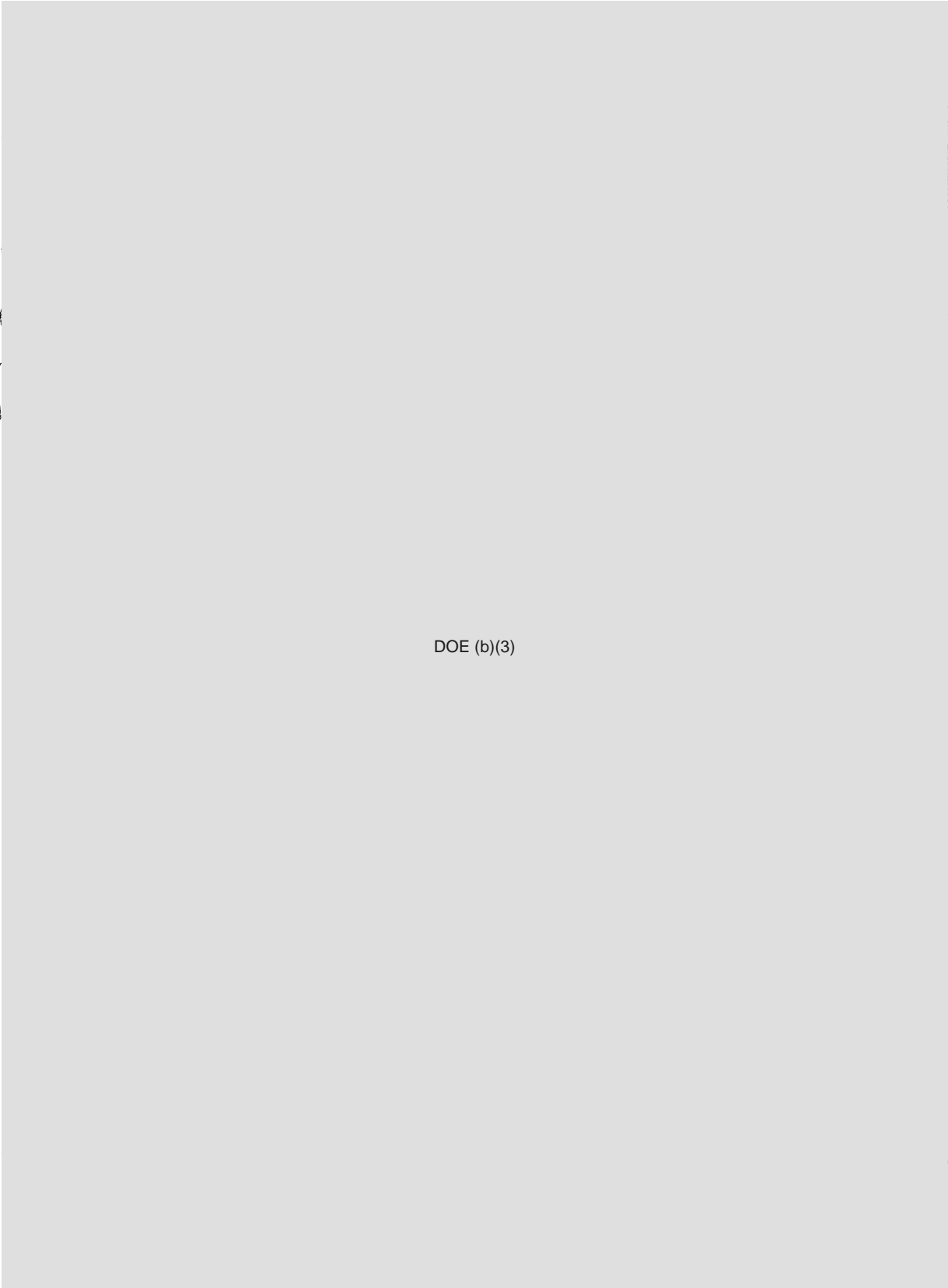
DOE (b)(3)

DOE (b)(3)

3.7   Spall and Ejecta
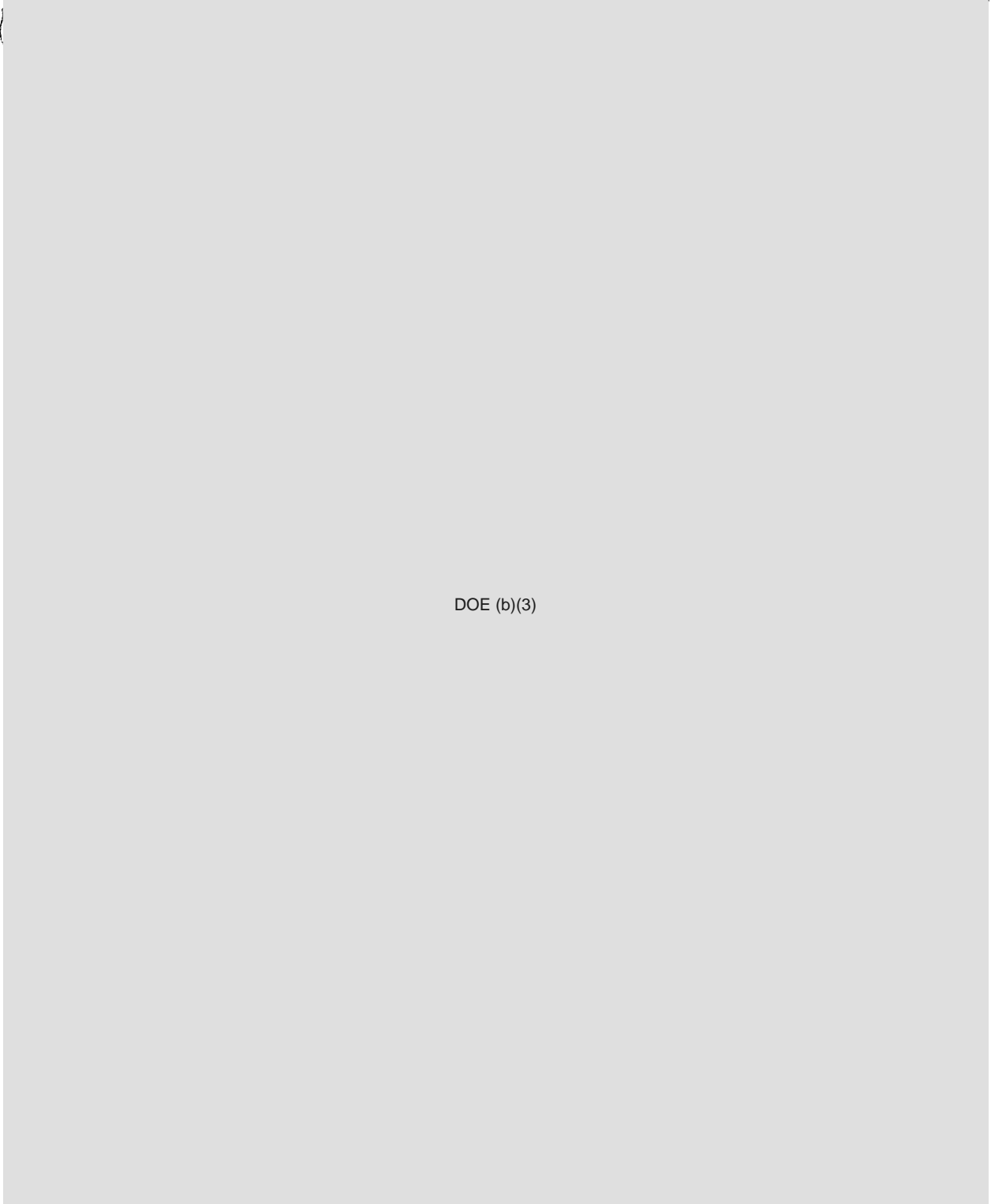
DOE (b)(3)

DOE (b)(3)

DOE
b(3)

3.8   Other Materials

DOE (b)(3)

DOE
b(3)
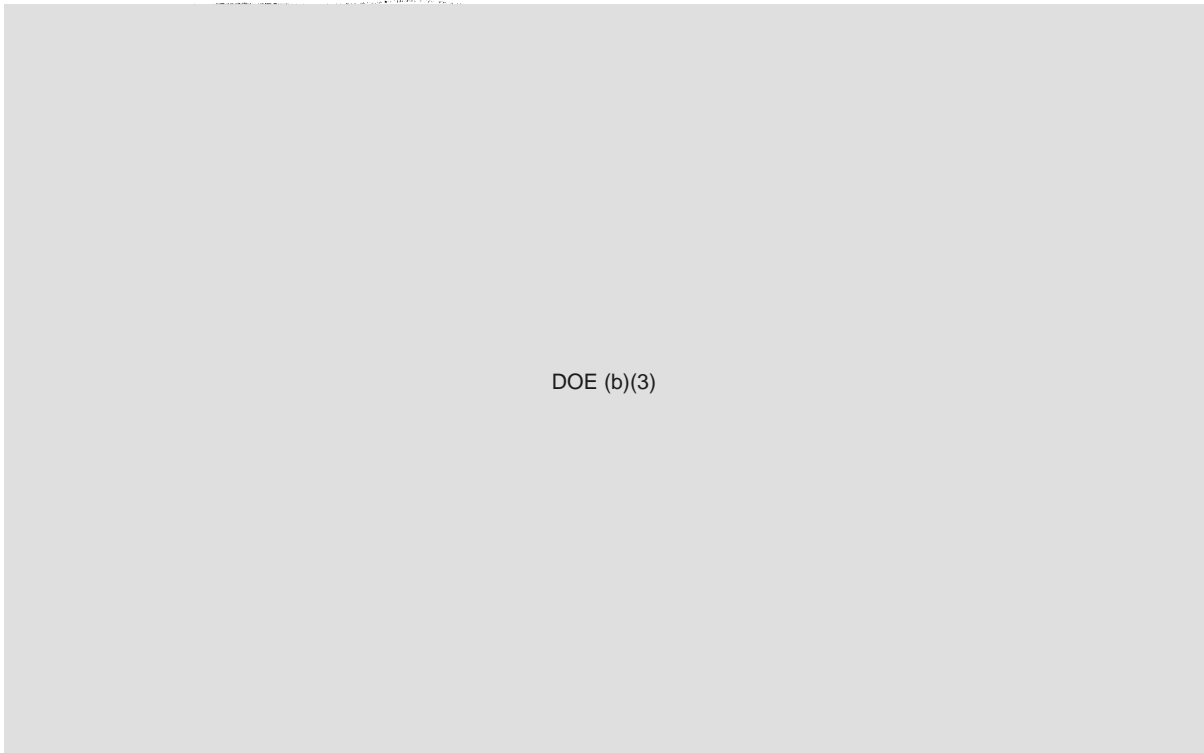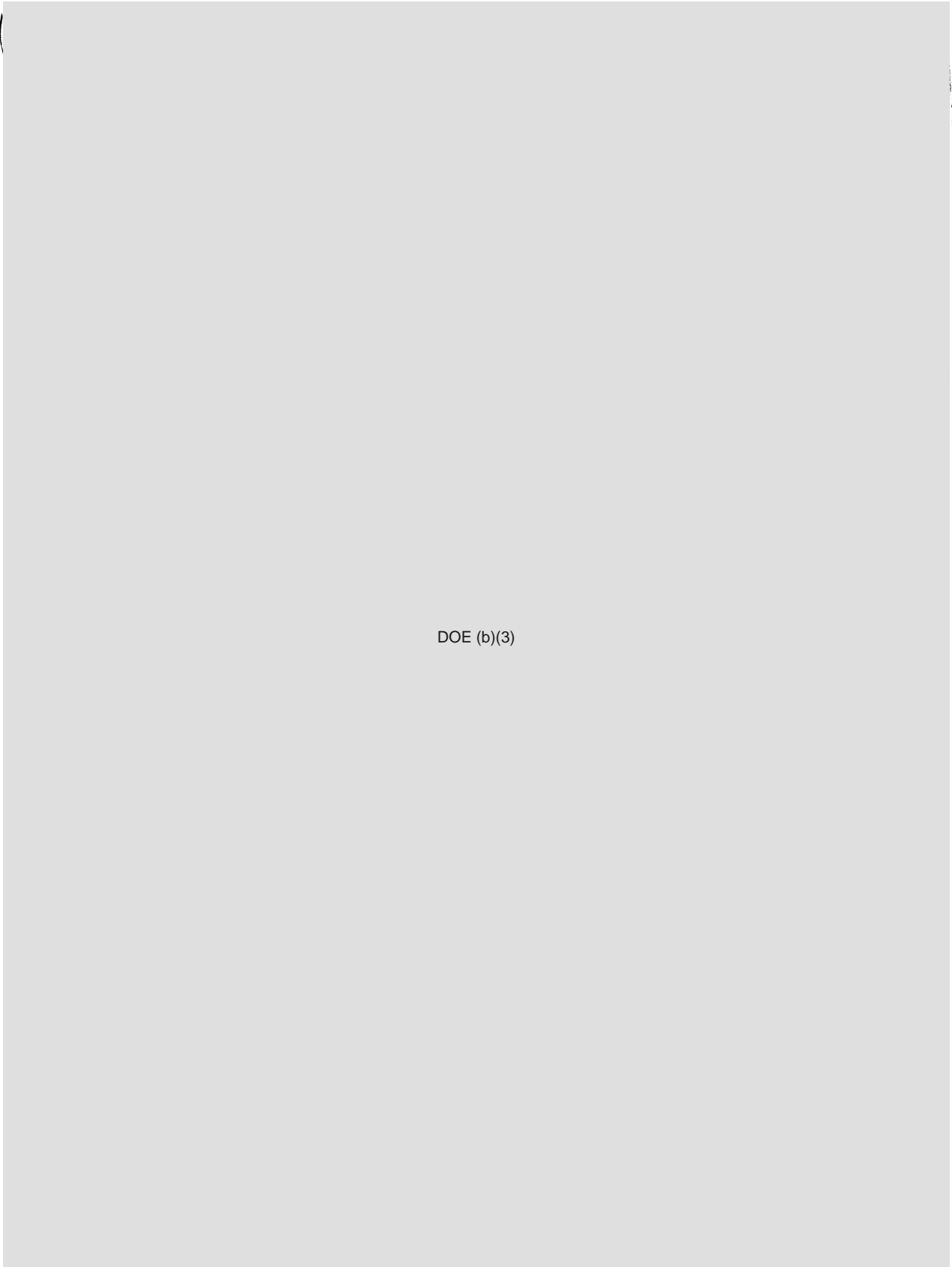
DOE (b)(3)
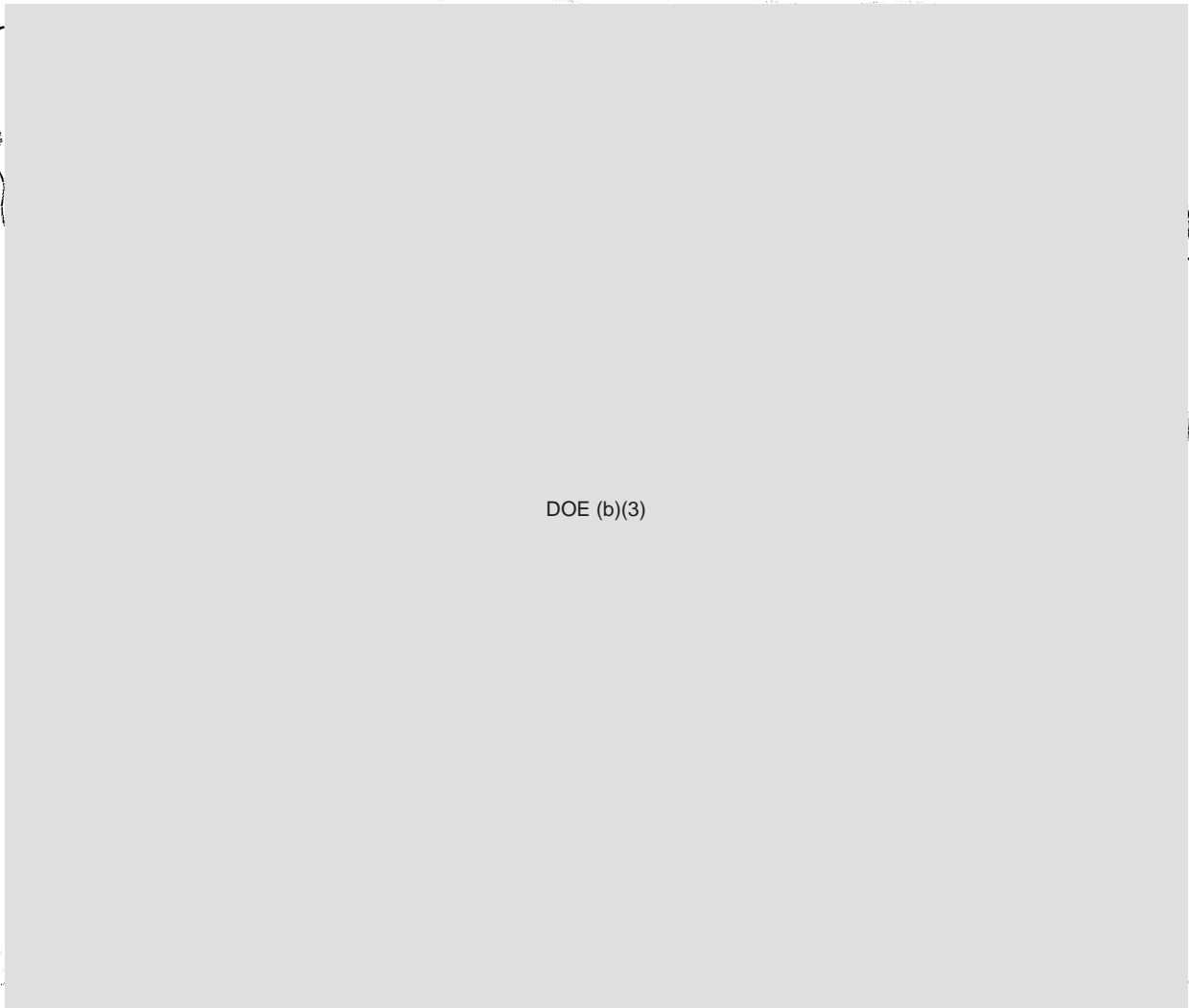
DOE (b)(3)

DOE (b)(3)

3.9   DOE (b)(3)

An important goal of the NNSA Science Campaigns is to enhance the safety and surety of the enduring weapons in the U.S. nuclear stockpile. This goal applies in particular to the B-61 and W78 Life Extension Programs, now in their initial planning stages, as well as to possible follow-on designs. Efforts to achieve such enhancements, beyond more traditional steps to strengthen and extend lifetimes of limited life components (LLCs) in current designs, are moving weapons scientists to explore design models with changes further away from those well calibrated by data from past tests. If such changes are to be incorporated as intrinsic features into future designs without re-

ducing confidence in their overall reliability, the ongoing Science Campaigns will have to provide the necessary improvements in the current level of understanding of the physics of boost and performance of the primary that meet established requirements for accurate quantitative analysis based on validated criteria for accuracy.

Achieving these improvements will require a well executed and supported program of experiments and analysis to establish and verify these requirements. DOE (b)(3)
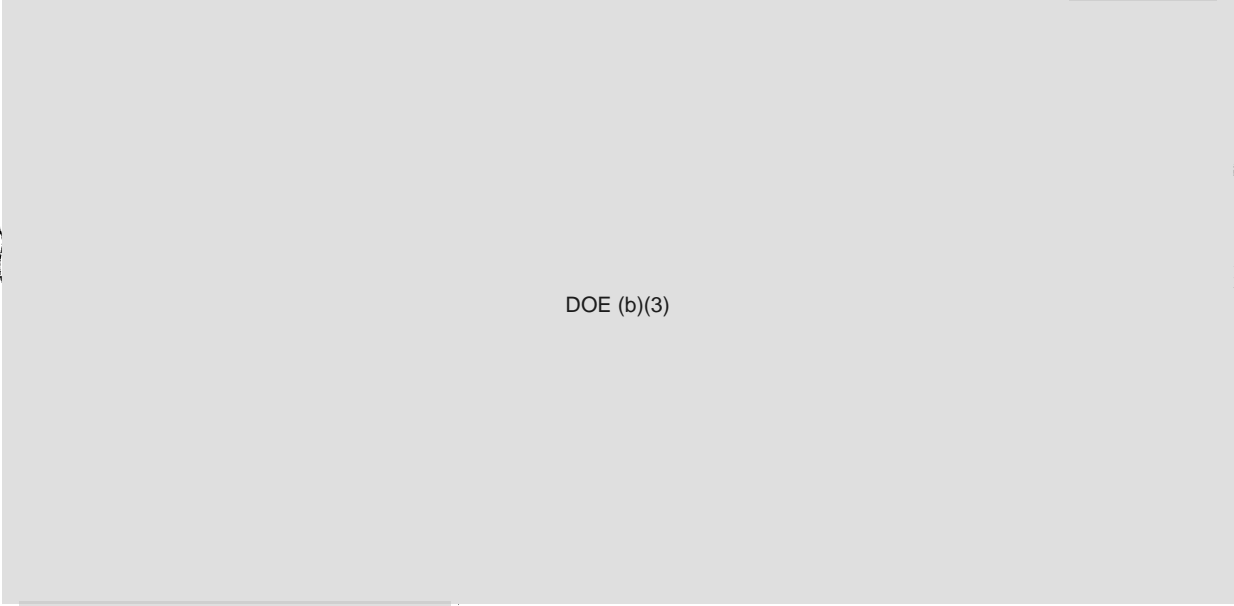
DOE (b)(3)

DOE (b)(3) Again this is important question requires fundamental experiments to obtain the basic physical behavior. These can then be followed by integrated experiments to test the overall efficacy of the various approaches.

3.10   Findings and Recommendations: Current Questions

3.10.1   Findings

1. DOE (b)(3)

DOE (b)(3)

2. DOE (b)(3)

3. DOE (b)(3)

4. DOE (b)(3)

5. DOE (b)(3)

6. DOE (b)(3)

7.

DOE (b)(3)

DOE (b)(3)   Progress has been made in identifying surrogate materials for different behavior and properties of Pu during weapon performance (*i.e.*, EOS, phase diagram, strength).

3.10.2   Recommendations

1. There are currently large uncertainties in measurements in many of the materials properties required to understand early time primary performance. A priority for stockpile stewardship is to devise fundamental and focused experiments that can provide definitive measurements of the requisite quantities.

2.

DOE (b)(3)

3.
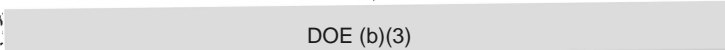
DOE (b)(3)

4 EXPERIMENTAL PROGRAM

We now examine the suite of current and planned experimental facilities and capabilities, and comment on their capacity to address the questions examined in the previous chapter. We comment on potential upgrades and augmentation to facilities that would be required as well as priorities. This includes the NNSS facilities as well as non-NNSA laboratory opportunities. We include the fundamental and focused experiments that provide information needed to interpret hydrodynamics and nuclear experiments, in particular for understanding boost. Experiments that provide fundamental materials dynamics data include magnetic pulse power experiments such as Z, high explosive pulse power (HEPP) experiments such as Phoenix, and laser driven dynamic compression experiments such as NIF. We also discuss the role of smaller scale static materials characterization experiments and developments in diagnostics.

4.1 Subcritical Experiments

Subcritical experiments involve implosion of Pu material for which the neutron multiplication rate is less than 1 ($\exp(\alpha) = k_{eff} < 1$) and have been a key element of the Stockpile Stewardship program since the UGT moratorium in 1992. There has been concern about the rate which with the laboratories have performed these experiments in recent years. We summarize the results of selected recent focused subcritical experiments in this section in order to help address the question of the appropriate balance between focused and subscale experiments, which are discussed in the next chapter. We discuss the Krakatau and Unicorn experiments as exemplars of such experiments.

The Krakatau subcritical experiment was a joint US/UK effort conducted on February 23, 2006 at U1a [45]   DOE (b)(3)
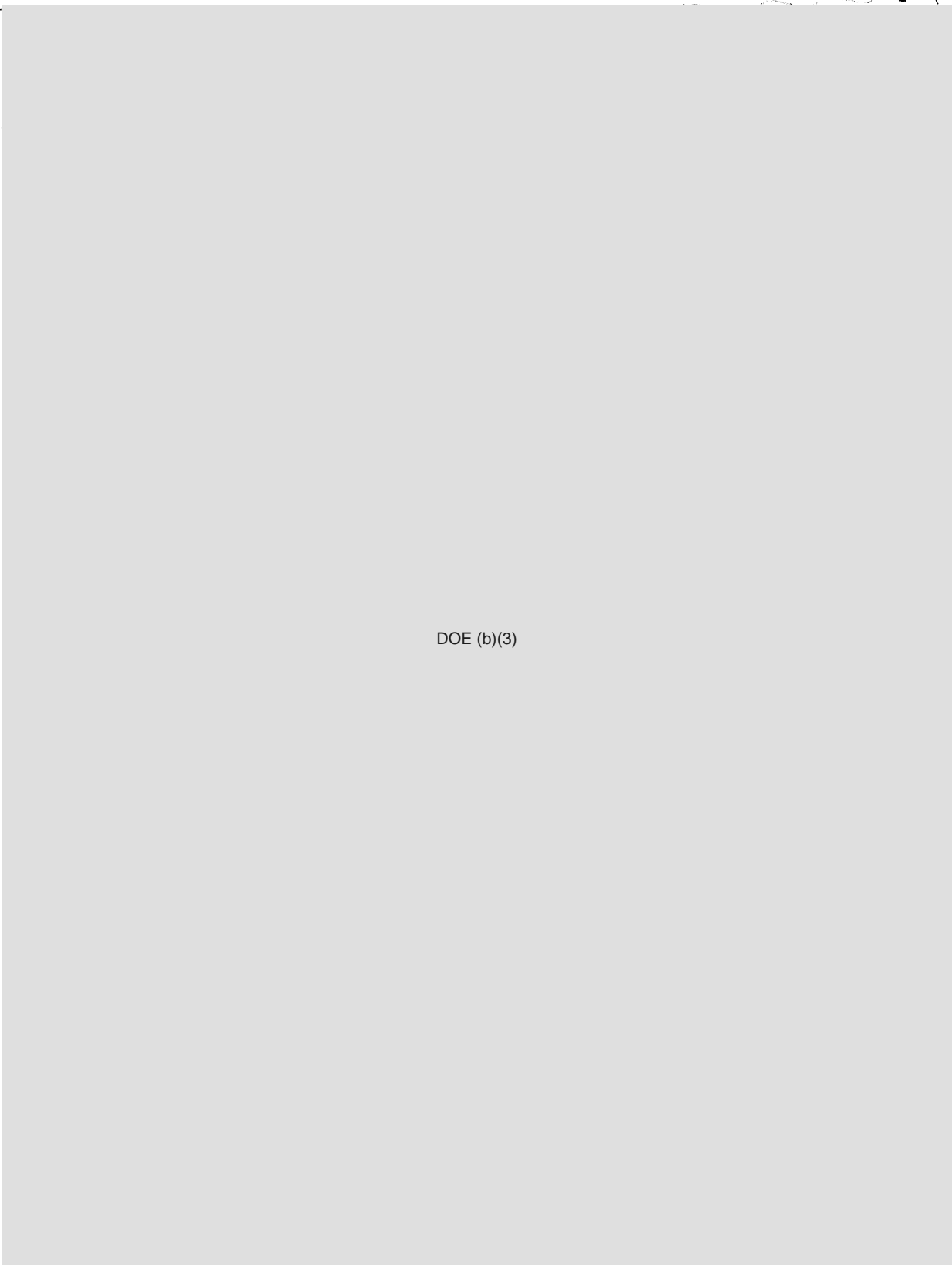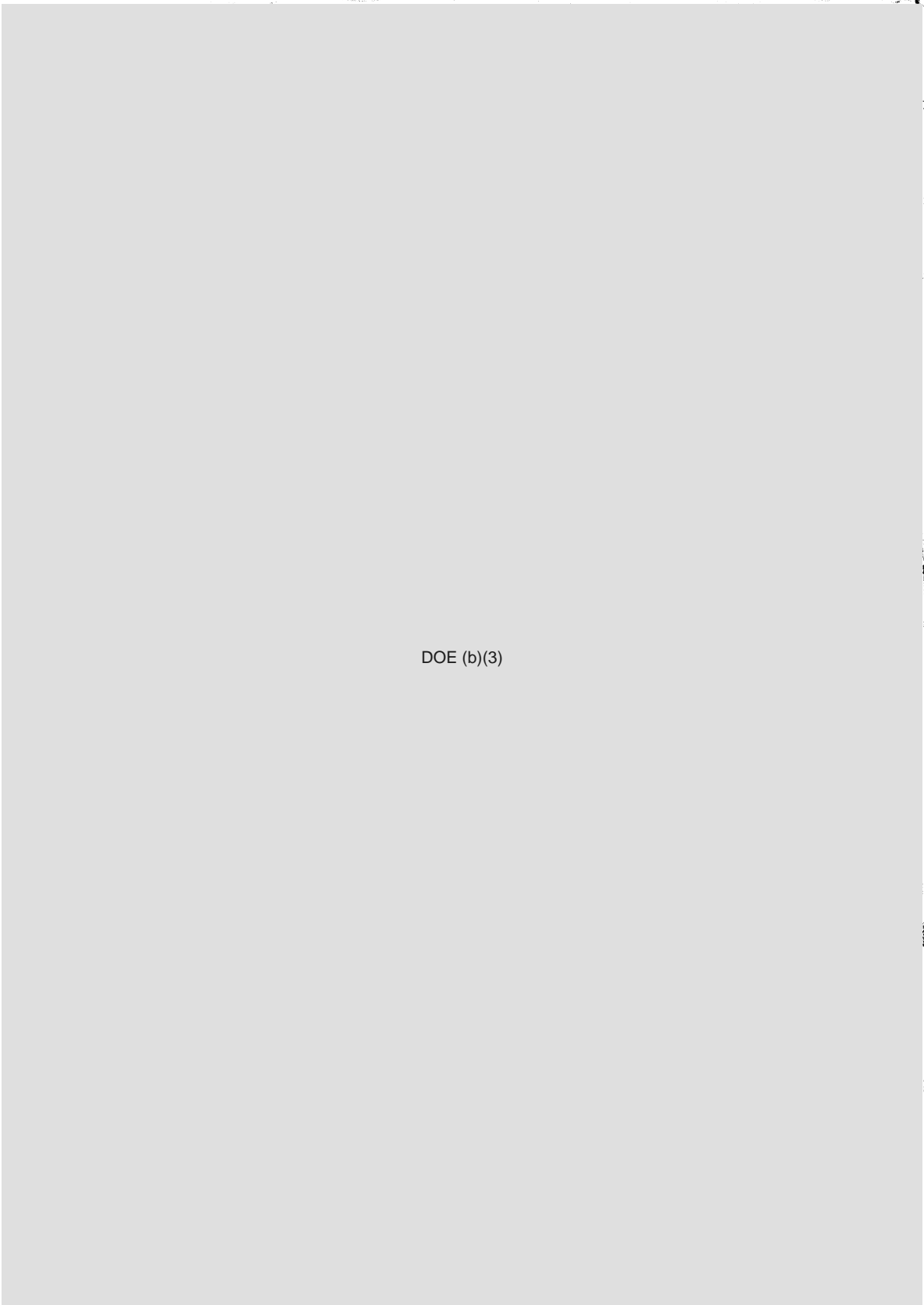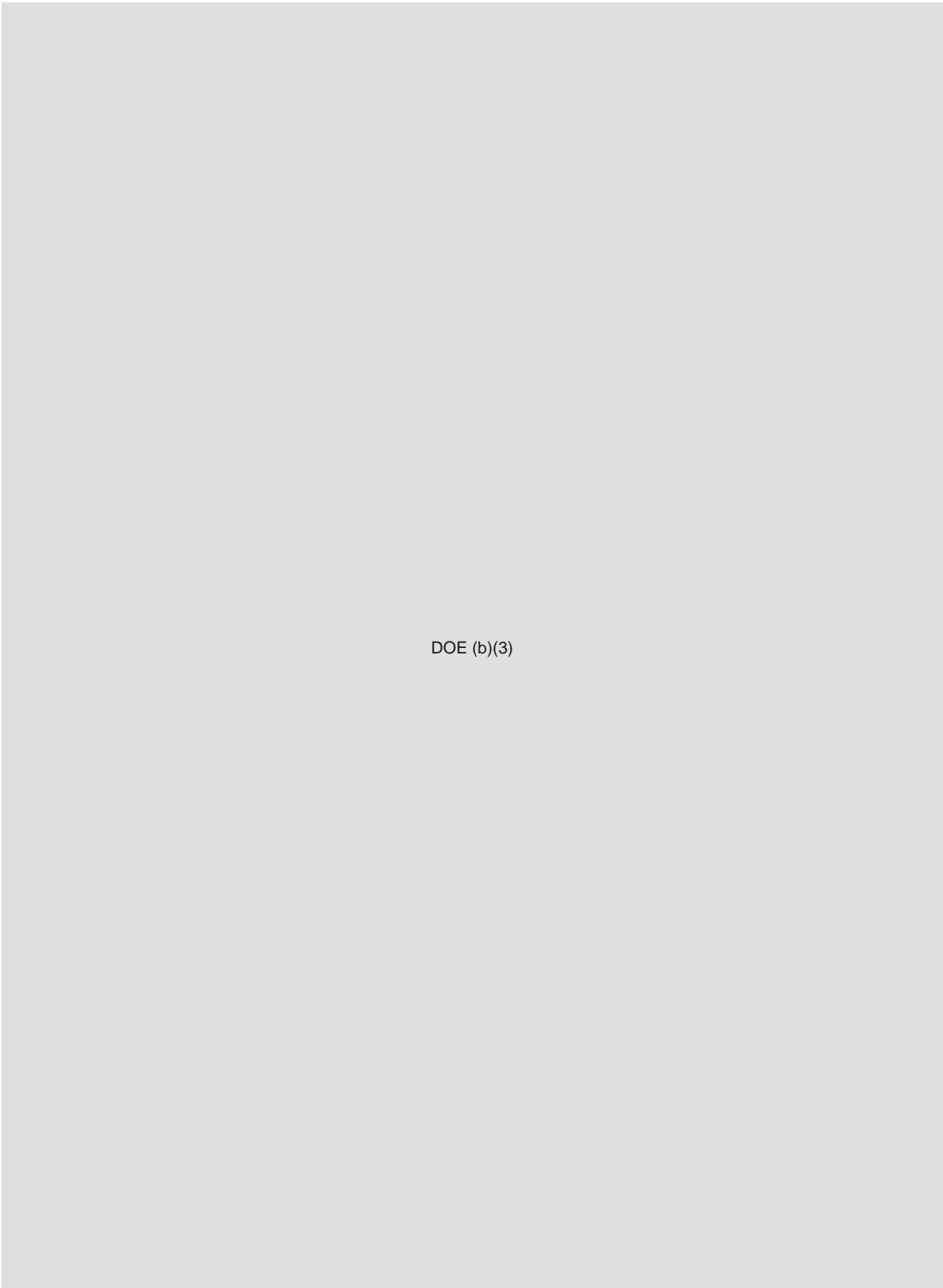
DOE (b)(3)

DOE (b)(3)
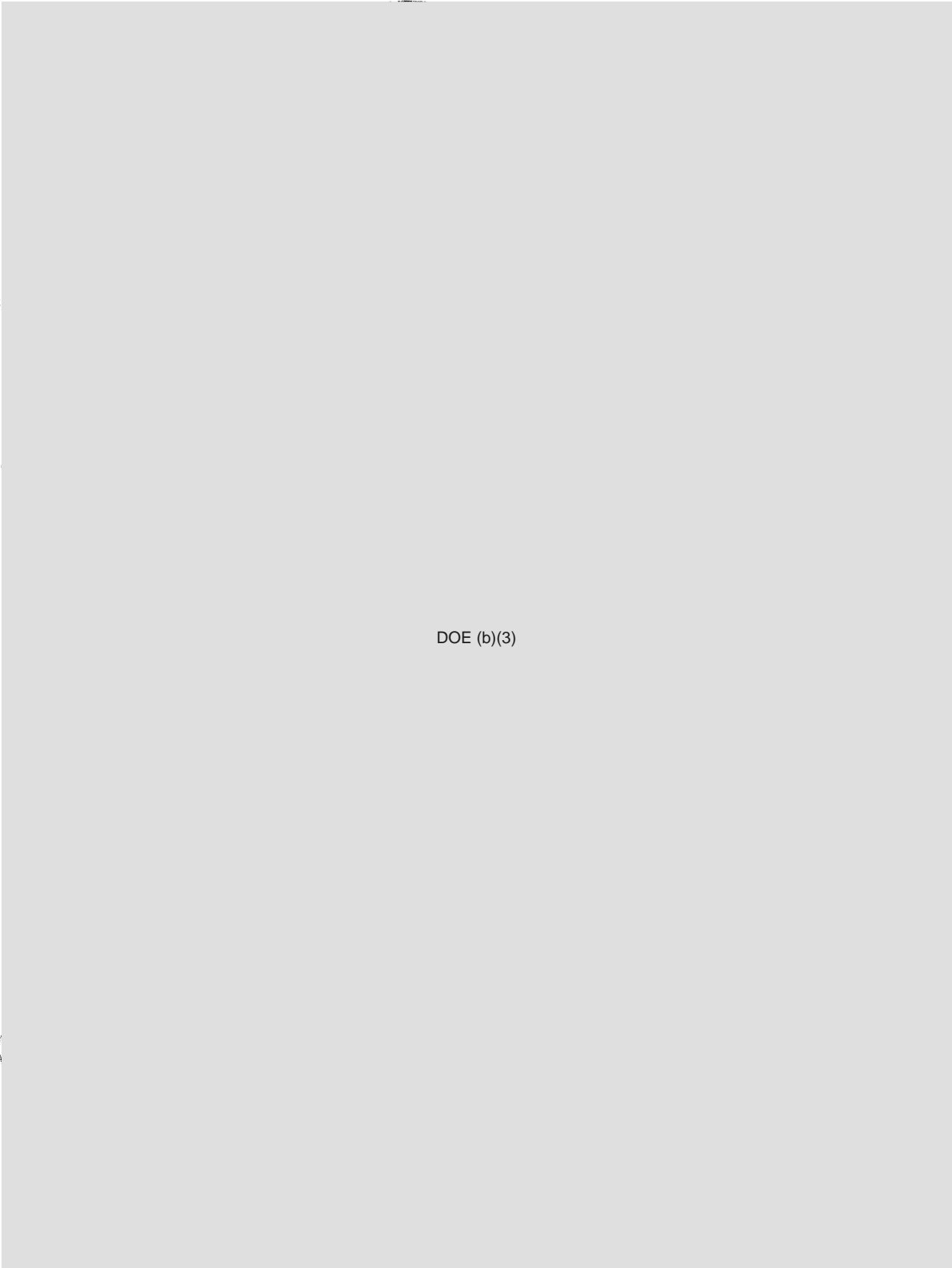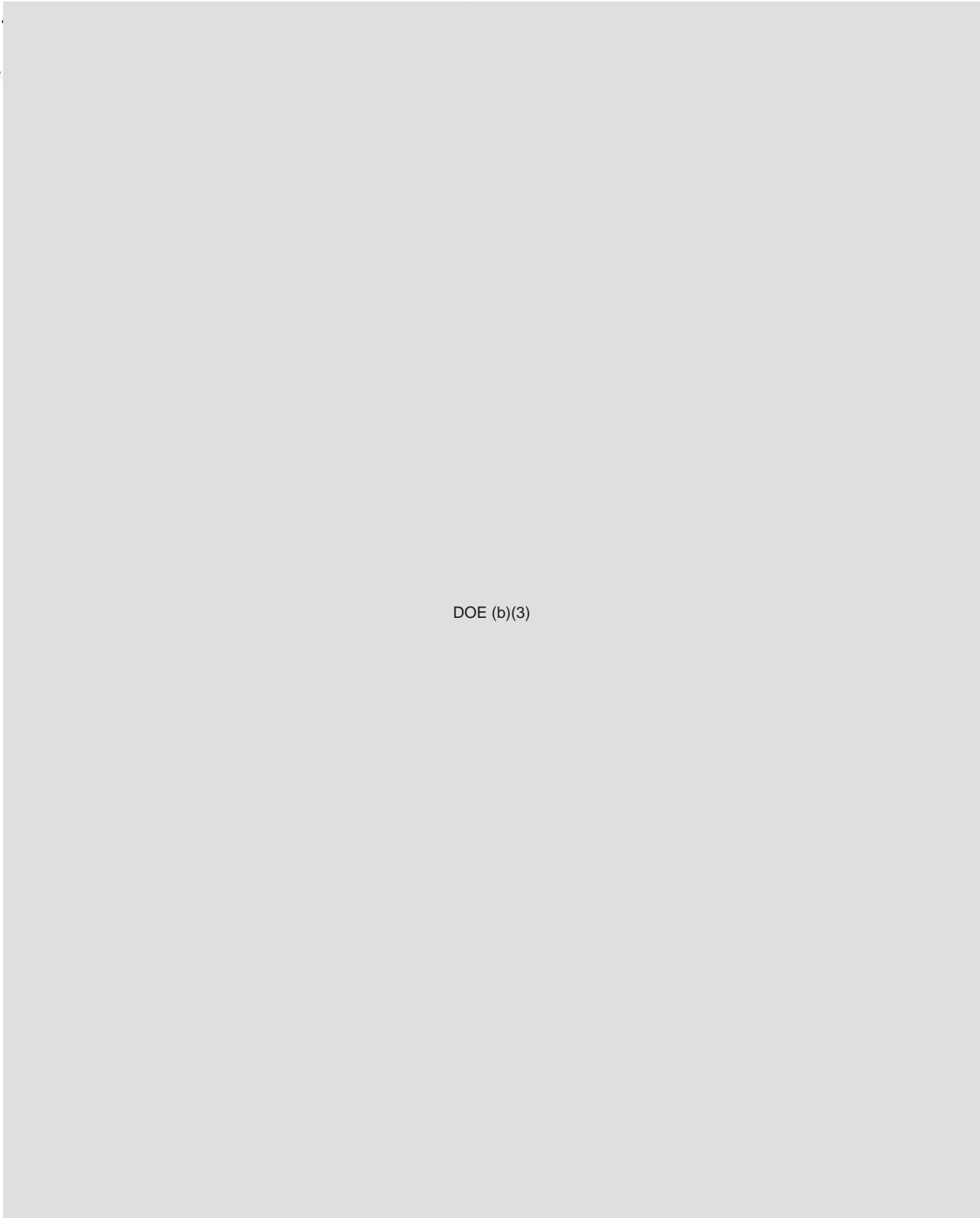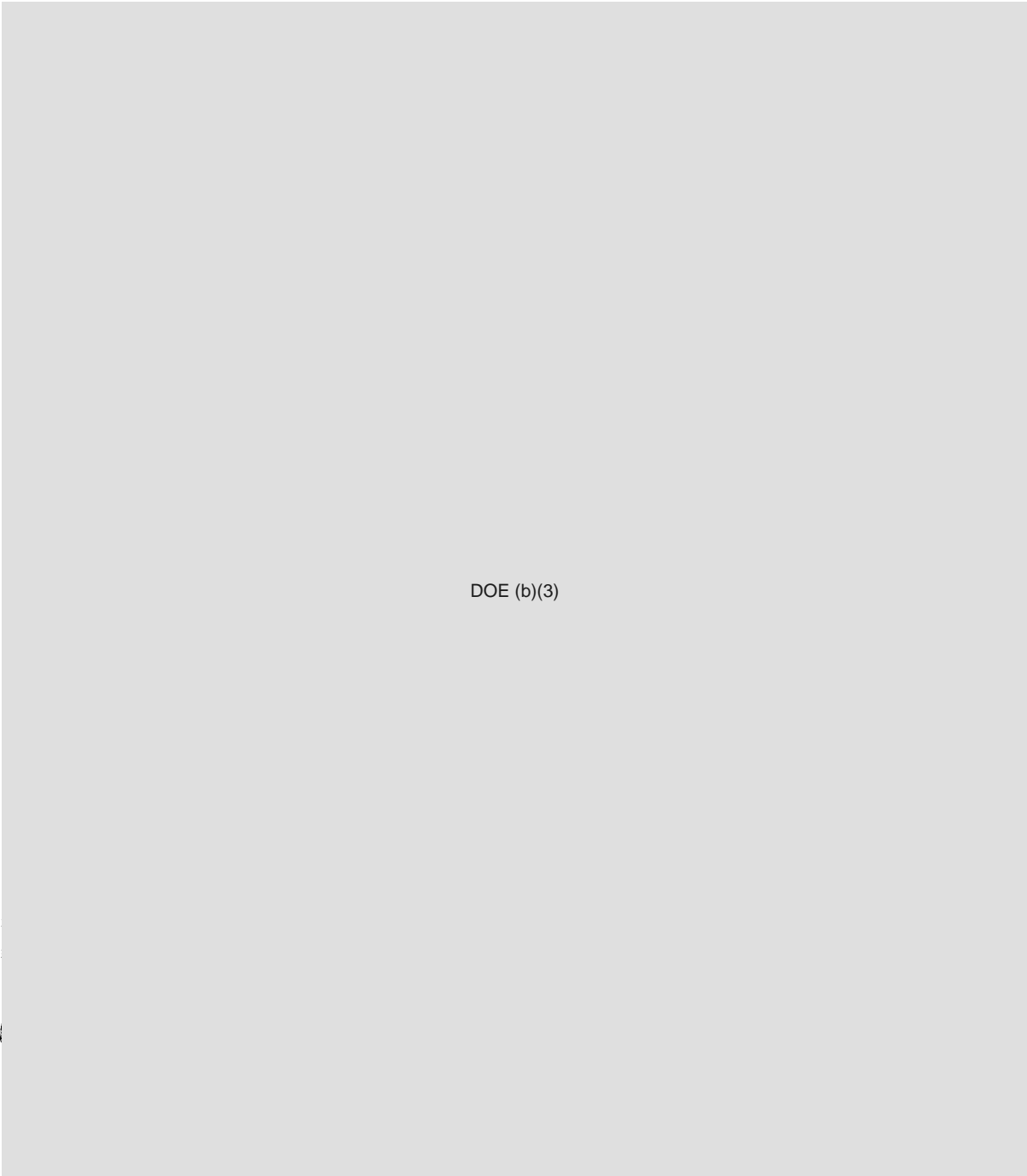
DOE (b)(3)

DOE (b)(3)

DOE (b)(3)

DOE (b)(3)

Again this is an example of the process by which fundamental experiments should be used to inform the interpretation of focused experiments.

4.2 Hydrodynamic Experiments on Surrogate Materials

Hydrodynamic experiments are conducted for weapons design and development (*e.g.* LEPs), to address stockpile issues in the form of significant findings investigations (SFIs), to improve the understanding of existing designs, and for code validation and exploration of the range of validity of models. Considering the immediate need for subscale experiments, it is useful to determine the extent to which there have been surprises in previous integrated full-weapon hydrodynamic experiments using plutonium surrogates. These surprises, for example, could lead to the potential discovery of new materials and hydrodynamic phenomena that were not evident from knowledge gained from data from fundamental and focused experiments used in simulations of performance. This aspect then would be distinct from uncovering the effects of specific design, engineering, or manufacturing issues.

DOE (b)(3)

DOE (b)(3)

DOE (b)(3)

Based on the material provided to us, it is difficult to obtain evidence for new phenomena from hydrodynamic experiments. Such experiments are integrated validation experiments and so prediction of the results will depend on the level of knowledge of the fundamental properties of the relevant materials. Hydrodynamic experiments of course do have essential value as regards engineering information and to validate various design choices.

These hydrodynamic experiments, including those on full-scale weapons configurations must rely on surrogates (or simulants) of Pu (or more precisely ^{239}Pu dominant material and relevant alloys). Thus, fundamental data are needed on these surrogate materials in order to provide a link to the behavior of Pu alloys of the pit.

DOE (b)(3)

DOE (b)(3)

DOE (b)(3)

Because of the diversity of properties exhibited by Pu as a function of pressure and temperature, different surrogate materials are required to match the behavior of the material of

the broad range of conditions relevant to primary performance. DOE (b)(3)

DOE (b)(3)

DOE
b(3)

Important hydrodynamic experiments are being carried out at pRad, for example, on ejecta formation from solid and liquid metals. DOE (b)(3)

DOE (b)(3)

4.3 Gas and Powder Guns

Interpretation of the hydrodynamic and nuclear experiments discussed above has required experiments with simplified geometries and for which additional diagnostics could be brought to bear and analyses performed. Of these, gun experiments using flat flyer plates continue to play a role. Both fundamental experiments (*e.g.*, for the EOS) and focused experiments (*e.g.*, for strength and ejecta) are performed. The 40 mm gun at TA-55 and JASPER at NNSS are dedicated to experiments on Pu materials. DOE (b)(3)

DOE (b)(3)   In addition, various

DOE
b(3)

guns are used throughout the complex on surrogate materials at a range of pressures.

There has been an unfortunate decline in the use of these facilities in recent years. A major delay associated with a change in the safety level at the JASPER facility resulted in the considerable down time, but this problem appears to have been resolved. Given the quality and uniqueness of the data possible from this facility, it is important to maintain operations at this facility. A decline in activity at other facilities has resulted from the loss of personnel as well as a shift in focus toward laser platforms for dynamic compression experiments (at LLNL). The latter has led to the use of shock-wave facilities in academia; on the other hand, the reinstallation of the LLNL gas gun at HEAF is a promising development.

We devote the rest of this section to a discussion of the Large Bore Power Gun (LBPG). The LBPG has a bore diameter of 80/89 mm, in contrast to the 40 mm powder gun. It has received additional attention because of the plan to move the gun to NNSS; it was shut down as a result of a containment incident. Two advantages of the large bore are the longer time before a release (unloading) wave from the periphery of a sample arrives at its center, and the ability to perform several different experiments on smaller samples simultaneously.

DOE (b)(3)

DOE (b)(3)

DOE (b)(3)

Larger containment required by larger test objects (the masses and kinetic energies of test objects scale as the second or third power of the gun diameter, depending on whether their thickness is assumed constant or to scale with diameter). If these larger masses require location at U1a, costs include the additional amounts for construction at a remote underground location, the operational cost of the remote site, and the implicit cost on human resources imposed by its remoteness. The programmatic decision of whether to accept these costs is beyond our charge.

A figure of merit is the radius of the bore divided by the sample thickness. In a nominal experiment a shock (weak enough that its propagation speed is close to the sound speed in the shocked material) propagates through the thickness of the sample, and is reflected as an unloading rarefaction from a free surface normal to the shock and normal to the gun axis. If this figure of merit is two then the sample is completely unloaded from its periphery in the time required for the unloading wave from the free surface to penetrate its full depth. The minimal figure of merit for an experiment that only needs to study the loading wave, or the beginning of the unloading process, is unity.

DOE (b)(3)

DOE (b)(3)

DOE (b)(3)

The 40 mm bore powder gun provides this with margin to spare.

If the experiment includes a tamper or a fire-resistant shell. then the requirements may be more stringent. Sound speeds in most such materials are higher than in Pu (the thin rod sound speed is 5.1 km/s for stainless steel, 12.9 km/s for Be and 2.26 km/s for α-Pu). By itself, this imposes no further requirement on the bore diameter because both longitudinal and transverse loading and unloading occur at the same speed in each material. For example, a shock will traverse a steel tamper much faster than a plutonium shell, but neither the loading shock nor the release wave from its periphery will begin to enter the steel until it has passed through the plutonium. However, because of its lower density a tamper may be thicker than the plutonium. This is particularly so for Be, with density 1.85 (less than one tenth that of α-Pu).

4.4 Laser Platforms

As we have noted repeatedly above, there is a dearth of data to constrain the predictions of the dynamic behavior of Pu above 4-5 Mbar. Shown in Figure 23 is a notional path of Pu particle as the primary implodes. Note that constraints on the location

DOE (b)(3)

of phase boundaries as well as the location of the Hugoniot is only constrained by experiments up to pressures of 4-5 MBar. DOE (b)(3)

DOE (b)(3)

Gas gun facilities such as JASPER have been used to generate Hugoniot data up to about 5MBar and it has recently been possible to generate off-Hugoniot data in this regime as well. Beyond this regime it is necessary to use platforms such as Phoenix, NIF and Z. These facilities are important components of the 10 year DPE program plan.

We describe in this section the potential for Pu experiments on NIF to explore both the EOS and also investigate strength effects. The advantage of NIF will be the ultra-high pressures beyond 30 Mbar that can be reached. The idea is to tailor the laser drive so as to create ramp compressions that can either drive the target material onto the Hugoniot via shock compression or can be used to explore off-Hugoniot isentropes. Indeed it may be possible to use specially designed loadings to
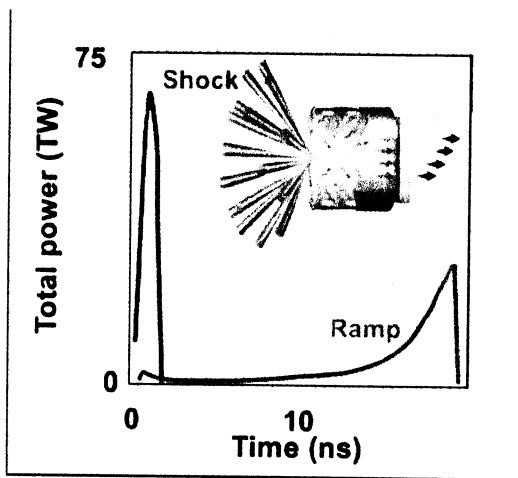
Figure 24: Left: the use of pulse shaping on NIF to produce either shock compression or ramp compression.

DOE (b)(3)

DOE (b)(3)

initially shock compress Pu and then drive it isentropically in a way similar to the environment experienced by a Pu particle in an imploding primary. The concept is shown graphically in Figure 24. Of course, the actual design of the appropriate pulse shape requires careful measurements but the initial experience with the NIF laser is encouraging. It has been repeatedly demonstrated that one can "program" a pulse of a given shape and the laser produces the desired pulse with impressive repeatability.

Questions have arisen regarding the accuracy of the measurements that will be achieved, and the extent to which ramp compression will be possible. For example it may not be possible to maintain isentropic compression at very high pressures without suffering formation of a shock in the material. This will require further investigation. On the other hand, the recent work on diamond to 50 Mbar and Ta to 6 Mbar is encouraging. In Figure 25 we show results from explorations of the Ta EOS on several platforms. The results shown correspond to isentropic compression As can be seen the new NIF data are in good agreement with previous data from the Omega laser and are also in agreement with data obtained on the Z pulsed power platform at SNL. The results are the highest pressure off-Hugoniot data achieved to date.
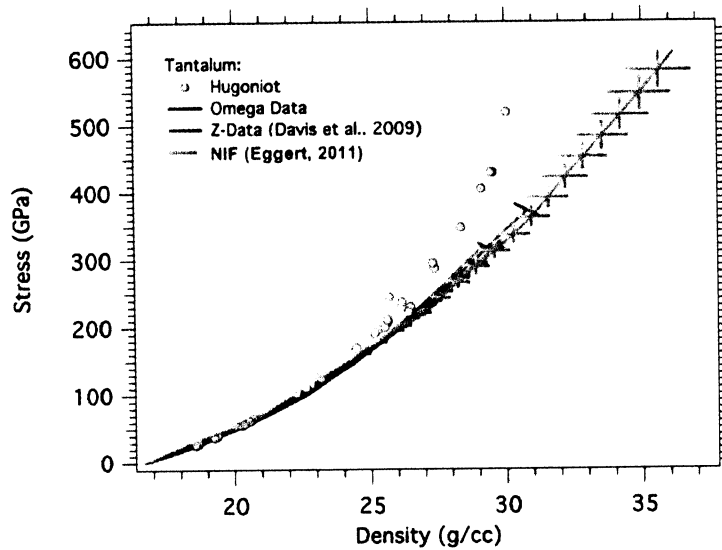
Figure 25: Measurements of the off-Hugoniot Ta EOS on several high pressure platforms.

No Pu experiments have yet been performed on NIF or Omega. Clearly this will require work to ensure that the appropriate safety issues can be addressed. Concerns have been voiced that the type of Pu that could be investigated is not weapons grade material which typically is alloyed with Ga, has various levels of impurities, and has differing isotopic compositions. In addition, it is likely that the microstructure of Pu samples on NIF also will not match that of weapons grade Pu used in primaries. However, in our view this is not a compelling objection. Indeed, from the point of view of fundamental measurements it is important to get a baseline on the pure material (both with and without Ga) as this high pressure data is very useful for informing theoretical approaches to characterize the more complex weapons grade material. Ultimately, of course, it will be be necessary to investigate the more complex weapons grade material and these issues will have to be addressed.

We next discuss the possible use of laser platforms in validating strength models at high pressure. Remington et al [54] have developed a laser-based platform to investigate various strength models. The basic idea is shown in Figure 26. A laser is aimed at a gold hohlraum which then produces X-rays that impinge upon an impactor which becomes a plasma after absorption of the X-ray flux. This plasma then
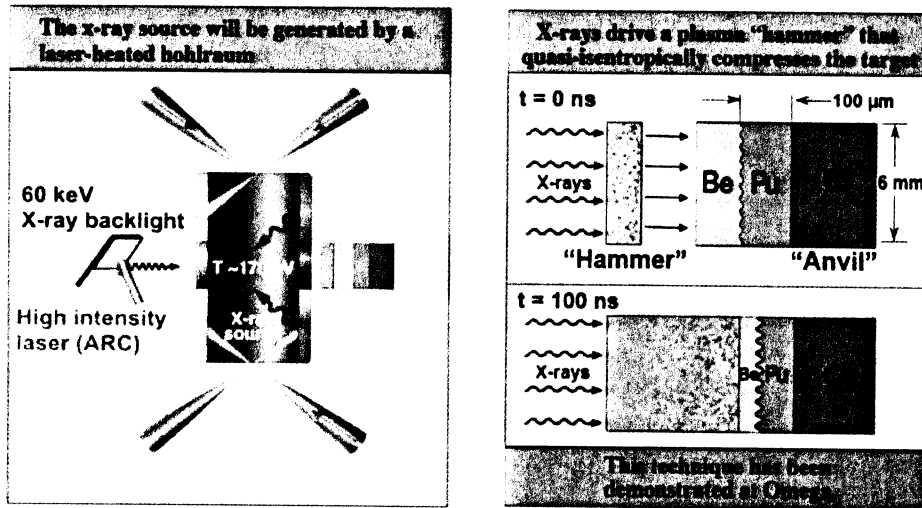
Figure 26: Laser platform for strength investigations

expands and transfers momentum to a target that creates a ramp-like compression on a layered target with a rippled interface. The interaction of the compression wave with the ripples interface produces baroclinically generated vorticity and thus an acceleration-induced instability known generically as Rayleigh-Taylor instability; that is, the rippled disturbance will grow at a rate that depends on the loading it receives but also on the nature of the materials across the interface. The growth rate in the absence of high pressure strength effects is different (larger) than that in the absence of such effects. Typical results are shown in Figure 27 where simulations of the instability both with and without strength are compared. Experiments of this type have been successfully carried out using high explosives at pRad as well as at the Omega laser and thus differing strain rates can be explored. With the advent of NIF even higher strain rates can be examined. The results have been used to validate various strength models. Shown in Figure 28 is the amplitude of the instability as a function of time for Ta as predicted by various strength models. Results are shown for material driven by HE loading as well as by laser drive on the Omega facility. As can be seen none of the current models in use for weapons simulation accurately predict the growth vs. time but of greater significance is the fact that the results are sensitive to the type of model used and this difference can be measured. Recently
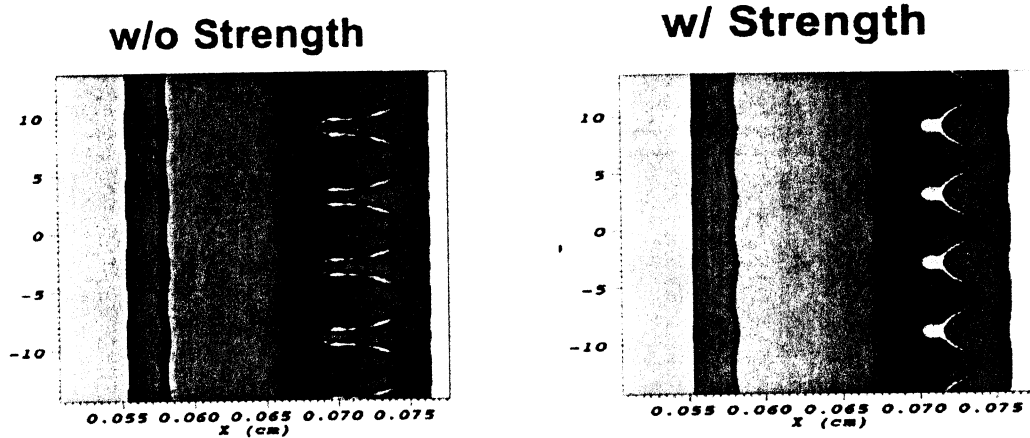
Figure 27: Comparison of strength effects on solid-solid Rayleigh-Taylor (R-T) instability.

Barton et al [34] have developed a multiscale strength model which attempts to model the mesoscopic processes such as dislocation dynamics. This model produces differing responses depending on the dislocation mobility.

Two experiments using R-T instability to infer strength on Ta have already been performed at NIF and more are scheduled. This will allow investigation of strength effects at upwards of 5 Mbar and will hopefully provide data which can further constrain strength models in use in weapons simulations. DOE (b)(3)

DOE (b)(3)

Overall, this type of approach holds promise for improving physics-based materials models for weapons materials that can be further validated in larger scale integrated experiments; however, the development of diagnostics with the requisite sensitivity and revolution will be challenging.
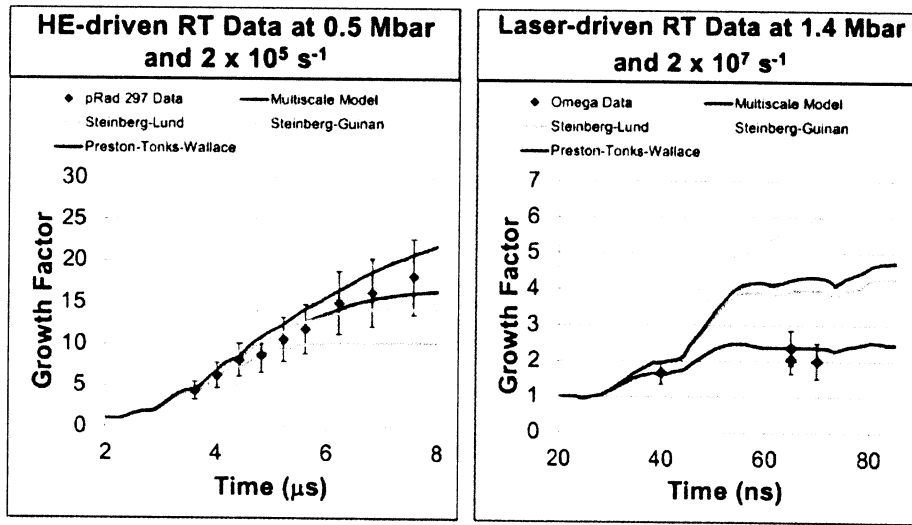
Figure 28: Growth rates for Rayleigh-Taylor (R-T) instability with strength effects. Loading is produced via high explosives (left) or the Omega laser (right). The predictions of various phenomenological models are also included as well as the prediction of a new multiscale model.

4.5 Pulsed Power

Pulsed power facilities provide the ability to examine materials under extreme P-T conditions and high strain rates of 10^5-10^6/sec, in principle in convergent or flat plate geometries. Because of the volume of material subjected to extreme conditions (linear dimensions of order 1 cm), multiple samples can be measured. The key facility for this work has been the Z machine at SNL, which was refurbished to increase its power by 50%. Z is now capable of both shock-wave compression to ~10 Mbar and ramp (*i.e.*, quasi-isentropic) compression to pressures of order 5 Mbar [55], generating the highest accuracy and precision data to date on materials at these conditions.

DOE (b)(3)

DOE (b)(3)

Pulsed power can also be driven by high explosives (HEPP), and plans have been underway for several years for the construction of an HEPP facility at LLNL for this effort. This facility, called Phoenix, should could be complementary to that of Z with

the ability to reach higher pressures with longer dwell times (see Figure 4). As such, it would also have a niche for EOS measurements relative to NIF. However, no EOS data have yet been reported from this facility, and the viability of the diagnostics fielded at the facility has not been established and thus the accuracy of the data (*e.g.*, for the Pu EOS discussed above) cannot be assessed.

4.6 Static Compression

A broad range of static (and quasi-static) characterization experiments support the above hydrodynamic and nuclear experiments. These experiments include static compression methods such as those based on diamond anvil cells. The importance of these methods has been recognized since the inception the Stockpile Stewardship Program. They have provided the identification of the high P-T phases of Pu and Pu-Ga alloys, their phase boundaries and EOS to pressures of several megabars and temperatures of 2000–3000 K, as described above.

DOE (b)(3)

Static compression methods are readily can be combined with x-ray and neutron scattering and spectroscopy. Most recently, there have been important developments in examination of the development of texture and microstructure in situ at high P-T conditions using x-ray imaging methods. These imaging methods are useful for general characterization of materials recovered to ambient conditions as well.

4.7 X-Ray and Optical Diagnostics

A variety of X-ray characterization tools exist for the above focused and fundamental experiments. A number derive from advances in synchrotron radiation techniques using storage rings from 3rd generation synchrotron facilities. For static compression, upgrades in facilites (Advanced Photon Source, APS) and new facilities (National Synchrotron Light Source II, NSLS II) will provide capabilities for hard X-ray experiments. The utility of these sources for understanding weapons performance is evident fo the recent Pu EOS measurements [8], and the ability to examine texture development with submicron x-ray imaging techniques under pressure needed to understand high-pressure strength. Recent X-ray tomographic imaging experiments carried out at the Advanced Light Source (ALS) reveal texture development (*e.g.*, Ref. [56]). These are important for the development of improved high P-T-strain rate strength models.

There are prospects for extending these storage-ring based X-ray techniques for in situ measurements of materials on dynamic compression (*e.g.*, through the proposed Dynamic Compression Sector, DCS, at the APS). Improved measurements could be performed using significantly more intense free-electron X-ray laser diagnostics (*e.g.*, above 20 keV), which would in principle allow dynamic imaging of Pu material at weapons relevant strain rates. Facilities would need to be built for dedicated experiments on Pu.

It has been realized for many years that there could be differences in phases sampled on implosion versus that obtained on static compression (*i.e.*, based on the known P-T phase diagram). These variations could arise from different strain rates sampled or different phase transformation kinetics associated with different P-T paths. Moreover, the implosion of a pit samples P-T regimes beyond the range of current experimental data; thus there is a need to determine the equilibrium boundaries at more extreme conditions. Conventional methods of structure determination by X-ray diffraction are precise and accurate, but generally require integration of the

scattered radiation over an extended time. They are not applicable to experiments in which the sample is stressed for very short times (often $< 1\,\mu s$).

In addition, many phase transitions are affected by kinetic effects (otherwise known as hysteresis or metastability), as described above. Hysteresis in phase transitions affects a material's properties (the pressure-density relationship and strength differ for different phases), and relaxation of a metastable phase to thermodynamic equilibrium is irreversible and generates entropy. Even if a phase transition were to nucleate immediately at a phase boundary, if it involves a volume change (or any crystal lattice deformation) the surrounding material must flow to accommodate the volume or shape change of the nucleated region, a flow that necessarily involves irreversible plastic work analogous to creep. It should be remembered that any material in shear stress is in a non-equilibrium state and its relaxation to equilibrium (creep is one mechanism by which this occurs) is irreversible.

Calculation of an equilibrium phase diagram from first principles is a deterministic problem, but in general not feasible to the required accuracy with present methods, as discussed above. Very small free energy differences between phases may have important consequences for the P-ρ relationship as well as for strength. Dynamic X-ray diffraction can be a powerful tool to study them. A sample is subjected to a transient high stress, such as that produced by high explosives or a flyer plate, and an intense pulse of X-rays is used to obtain its diffraction pattern. This technique is difficult because the sample is in the desired state only briefly, and the X-ray fluence obtainable during that short interval is small. However, it has been used for many years, and offers promise as a diagnostic in hydrodynamic experiments on any material. Because the duration of loading is short, and strain rates may be high, dynamic X-ray diffraction may probe regimes, including short-lived metastable phases in which kinetic effects are important, inaccessible by other means. In particular, they may provide direct access to parameter regimes encountered in other explosively loaded systems.

An example of dynamic X-ray diffraction has been reported for Sn and Zr using a 37 stage Marx bank as a high voltage source to excite Kα radiation from a Mo anode, producing a 40 ns X-ray pulse [57]. Shock-induced phase transitions creating mixtures of phases were observed but the signals were were weak and noisy. This technique can be applied to Pu, but because of its higher atomic number, the diffraction is best performed at higher X-ray energies than for Sn or Zr. More promising is the use of a laser-generated X-ray backlighter. This latter method is particularly well-suited to experiments performed at NIF, where laser energy is available and targets would necessarily be thin. It is among the standard suite of NIF diagnostics used in a wide range of experiments. Indeed, X-ray experiments to date at Omega have been able to examine phase transition kinetics associated with solid-solid transitions and melting have been examined. Both X-ray diffraction and spectroscopies (*e.g.*, extended X-ray absorption fine structure, EXAFS) have been performed.

DOE (b)(3)

DOE (b)(3)

X-rays from a synchrotron storage ring or energy recovery linac are possible as well. The latter needs to be matched to the instrinsic time structure of the source, allowing for example measuring the material through a shock front. The use of X-rays from a storage ring has been tested on selected materials on shock loading with a powder gun [58]. Indeed, even at low pressure this could be used to study liquids. Feasibility studies at the APS have been encouraging, leading to the possibility of a dedicated beamline at that facility. The facility will be used to investigate weapons materials including Pu surrogates; the appropriate authorization will be needed for experiments on Pu.

Dynamic X-ray imaging with sufficient spatial and temporal resolution can in principle be used to investigate the evolution of microstructural changes that control strength and damage. These kinds of measurements will require a significantly brighter X-ray source such as an X-ray free electron laser. Studies of high-Z materials such as Pu and its surrogates in turn will require photon energies above 40 keV.

Such facilities have not yet been built and are technically challenging, though developments at the Linac Coherent Light Source, which plans to deliver photon energies as high as 20 keV, provide promising prospects. A facility for weapons science within the NNSA hydrodynamic and nuclear experiment program could provide information that is crucial for understanding high-pressure strength and developing testable and predictive models at $P\text{-}T$ – strain rate conditions relevant to weapons implosions.

4.8 Findings and Recommendations: Experimental Program

4.8.1 Findings

1. Subcritical experiments have returned useful data, but the rate of these experiments has decreased in recent years as a result of a number of factors.

DOE (b)(3)

2. The hydrodynamic program continues to provide tests of surety concepts and designs, and we applaud the feedback between planning hydrodynamic tests and focused experiments carried out at supporting facilities (*i.e.*, DARHT and Z)

3. DOE (b)(3)

   DOE (b)(3)

   Hence the 40 mm powder gun is adequate for most purposes. The increase in bore from 40 to 80-89 mm in going to the large bore powder gun will provide only a marginal increase in capability.

4. Experiments with large laser platforms such as NIF have the potential to reach the highest pressures for fundamental EOS measurements, for example using ramp compression.

   DOE (b)(3)

   DOE (b)(3)

DOE (b)(3)

5. Pulsed power methods now play a critical role in tracking the dynamic response of materials in relation to weapons performance. The pressure range, accuracy, and diagnostics developed on Z provide important new constraints on Pu behavior. Reconciling controversies with earlier data, developing a fundamental understanding of the results, and incorporating those results in codes are essential for improving weapon performance.

6. Static compression experiments provide highly accurate measurements, including imaging complex multiphase systems.

7. Dynamic X-ray diffraction experiments performed with X-ray sources from free-electron lasers or even synchrotron storage rings have the potential to provide accurate fundamental data at relevant P, T, and strain rates. Experiments include time-resolved X-ray measurements of phase transition kinetics and imaging. Dynamic tomography could in principle provide direct information on the time dependence of the development of damage. These experiments are likely to be informative about Pu on shock or ramp compression, and it would be straightforward to develop and implement the required apparatus.

4.8.2   Recommendations

1. The experimental program has brought into focus a number of important materials problems that need to be resolved within the hydrodynamic and nuclear experiment program. Newly developed techniques for fundamental and focused experiments should be brought to bear to solve these problems.

2. Prior to undertaking any subcritical experiments, the science value of those experiments needs to be established by scientists at the laboratories and at

NNSA headquarters. Fundamental and focused experiments offer the best near-term approach to obtaining the data essential for planning and interpreting integral subcritical, including subscale, experiments as well as validating theory and simulation. They will also help attract, develop and retain scientific and technical expertise.

3. We recommend development and implementation of extended temperature measurement capability for dynamic compression experiments. For ramp compression experiments, these measurements will provide additional constraints on the closeness to isentropes.

4. Technical issues associated with further development of explosive pulsed power need to be addressed and resolved. Build dynamic X-ray diffraction apparatus for contained Pu samples at a suitable site (TA-55 for small samples, NTS for larger samples).

5 SUBSCALE EXPERIMENTS

In this section we discuss some of the recently proposed scaled experiments to be performed with Pu at the U1a site at NNSS. The idea behind such experiments is to explore the implosion of a primary at a scale chosen to be small enough so that the Pu assembly never becomes critical. The advantage of such an experiment is that one can explore the stages of primary performance as discussed in Section 2.3 up to, but not including, the stage of fission heating and boost. Such an experiment is attractive for a number of reasons:

- As we will show, the densities and pressures achieved in such an experiment are comparable to those encountered in a full scale primary.

- The Pu experiences a thermodynamic trajectory that is very similar to that in a primary.

- There is no concern in such an experiment with the differences in material properties between Pu and surrogates as is the case with full scale hydro experiments since one is working directly with Pu.

- Based on the type of high explosive loading applied, it is possible to capture much of the structure of the gas cavity formed as a result of implosion.

- Realistic loadings will drive ejecta into the cavity.

- Because the assembly remains subcritical, it is possible to separate the effects of compression from the effects of fission heating.

In principle, such an experiment displays in an integrated way almost all of the physics that one wishes to understand at early time. On the other hand, there are some challenges associated with this type of experiment :

- It is essential to ensure that the initial loading from the high explosive is also identical under scaling. We will discuss this issue further below.

- All of the physical issues under consideration in this report (EOS, strength, phase change, damage, etc.) are of course operative simultaneously during the implosion. This raises the issue of how one discriminates among various proposed models, many of which are phenomenological in origin and therefore have parameters that can be tuned in nonunique ways to explain given data.

- Appropriate diagnostics must be designed so that it is possible to make inferences regarding at least integral measures like cavity shape etc.

DOE (b)(3)

DOE (b)(3)   In July of FY12 an engineering test called Leda with a Ta surrogate pit will be performed. This will test the use of PDV diagnostics which are the primary diagnostics to be used for the Gemini experiment. As discussed below in Section 6, the Cygnus facility at U1a will provide radiogrpahic data at very early times just after the HE detonation completes. In September of 2012, a confirmatory test again using Ta will be performed to verify the experimental operations and, if successful to collect PDV data on implosion of Ta. Finally, in November of 2012, Pollux, the scaled experiment in Pu will be performed at U1a.

This study did not review these experiments, which are already underway. Rather, we were presented with overviews of these plans, which were in turn used as a basis for assessing future subscale experiments. Moreover, in this study JASON only examined the technical aspects of the subscale experimental program, and focused on the science value.

DOE (b)(3)

DOE (b)(3)

DOE (b)(3)   These aspects of the scaled experiment program are outside the study charge and we do not comment on them here.

5.1 Historical Background

DOE (b)(3)
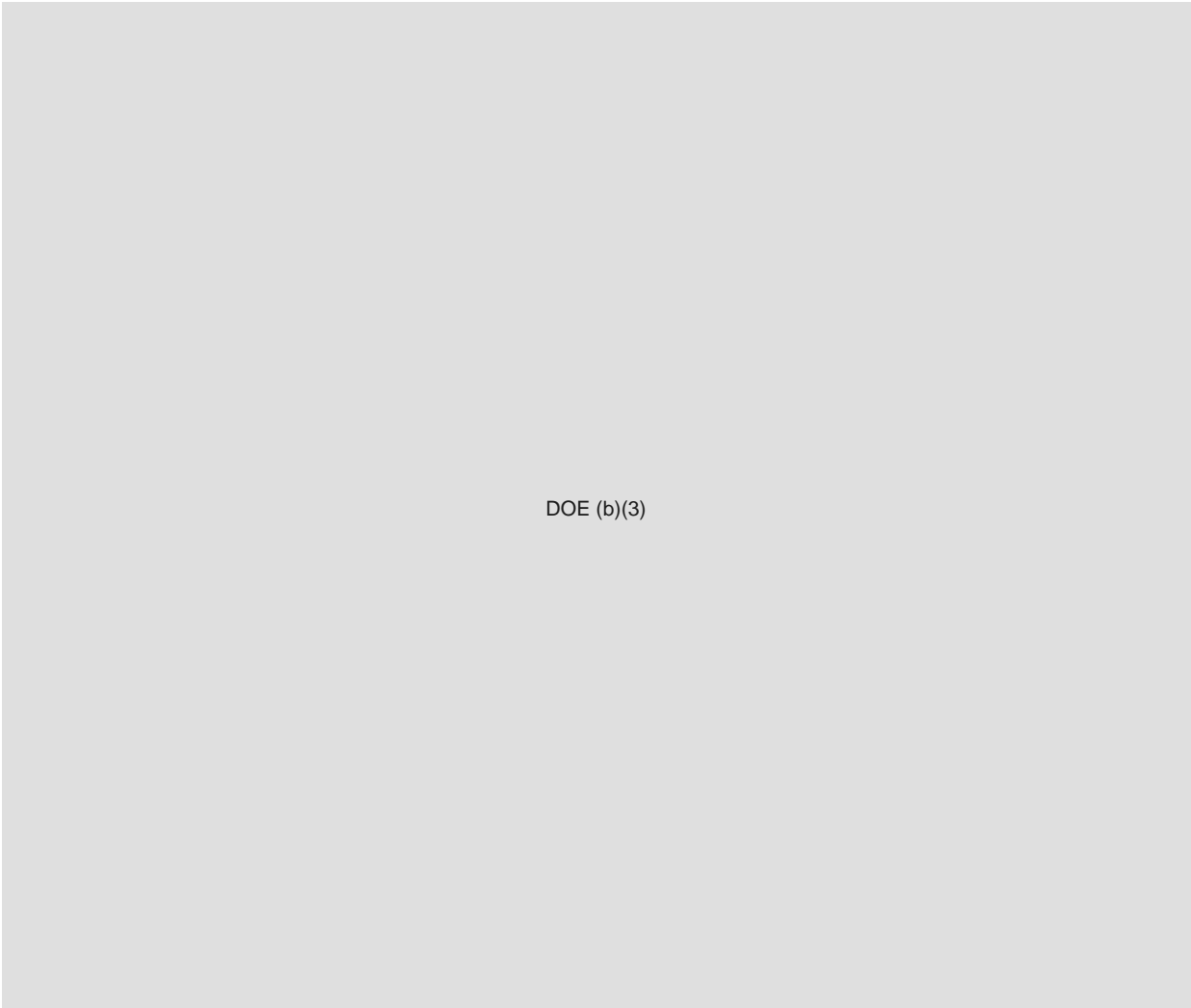
DOE (b)(3)

5.2 Why Scaling (sort of) Works

Consider the motion of a continuum (either solid or fluid). In the Eulerian frame the equations of motion are

$$\frac{\partial \rho}{\partial t} + \frac{\partial (u_j \rho)}{\partial x_j} = 0$$

$$\frac{\partial \rho u_i}{\partial t} + \frac{\partial (u_j \rho u_i)}{\partial x_j} - \frac{\partial \sigma_{ij}}{\partial x_j} = 0$$

$$\frac{\partial E}{\partial t} + \frac{\partial (u_j E)}{\partial x_j} - \frac{\partial u_i \sigma_{ij}}{\partial x_j} = 0$$

where ρ is the density, u_i is the velocity, σ_{ij} is the Cauchy stress tensor and

$$E = \frac{1}{2}\rho(u_i u_i) + \rho e$$

is the total energy density with e representing the internal energy per unit mass. All the physics is in the stress tensor.

If we scale lengths by some factor (call it β) and scale time by the same factor, that is

$$x_j \rightarrow \beta x_j \qquad t \rightarrow \beta t$$

it is not hard to see that the equations of motion are invariant with respect to this transformation provided

$$\sigma_{ij}(x_k, t) = \sigma_{ij}(\beta x_k, \beta t)$$

and, that the initial and boundary conditions are identical as well under the scaling transformation.

For the Euler equations for pure inviscid fluid motion we have

$$\sigma_{ij} = -P\delta_{ij},$$

where P is the thermodynamic pressure given by the equation of state. it can be seen that the equations are indeed scale free. For more complex constitutive relations scaling does not necessarily hold. Two important examples where scaling can fail to hold exactly come about when one uses rate dependent strength models or has a rate dependent energy release which may occur for certain reactive materials like high explosives. For example, if one uses a strength model to relate the stress tensor to strain and rate of strain, the strain tensor will in general not exactly scale. Similarly, the reaction zone of a high explosive may not scale properly and so the loading from the HE will modify the implosion so that it does not scale properly.

Scaling is also directly related to dimensional analysis and it can be shown that the presence of dimensionless quantities is directly related to measures of the violation of pure scaling. For example, the fact that viscous effects in fluids do not scale leads

to the development of the Reynolds number. Scaling or the lack thereof can be a powerful way to get insight into various physical effects and properly applied can be used to isolate and examine various effects separately. Indeed, an example of this is the fact that the contribution from fission energy becomes irrelevant provided the experiment is scaled so that the critical areal density is never reached during the implosion.

5.3 Scaled Implosions of a CHE Primary
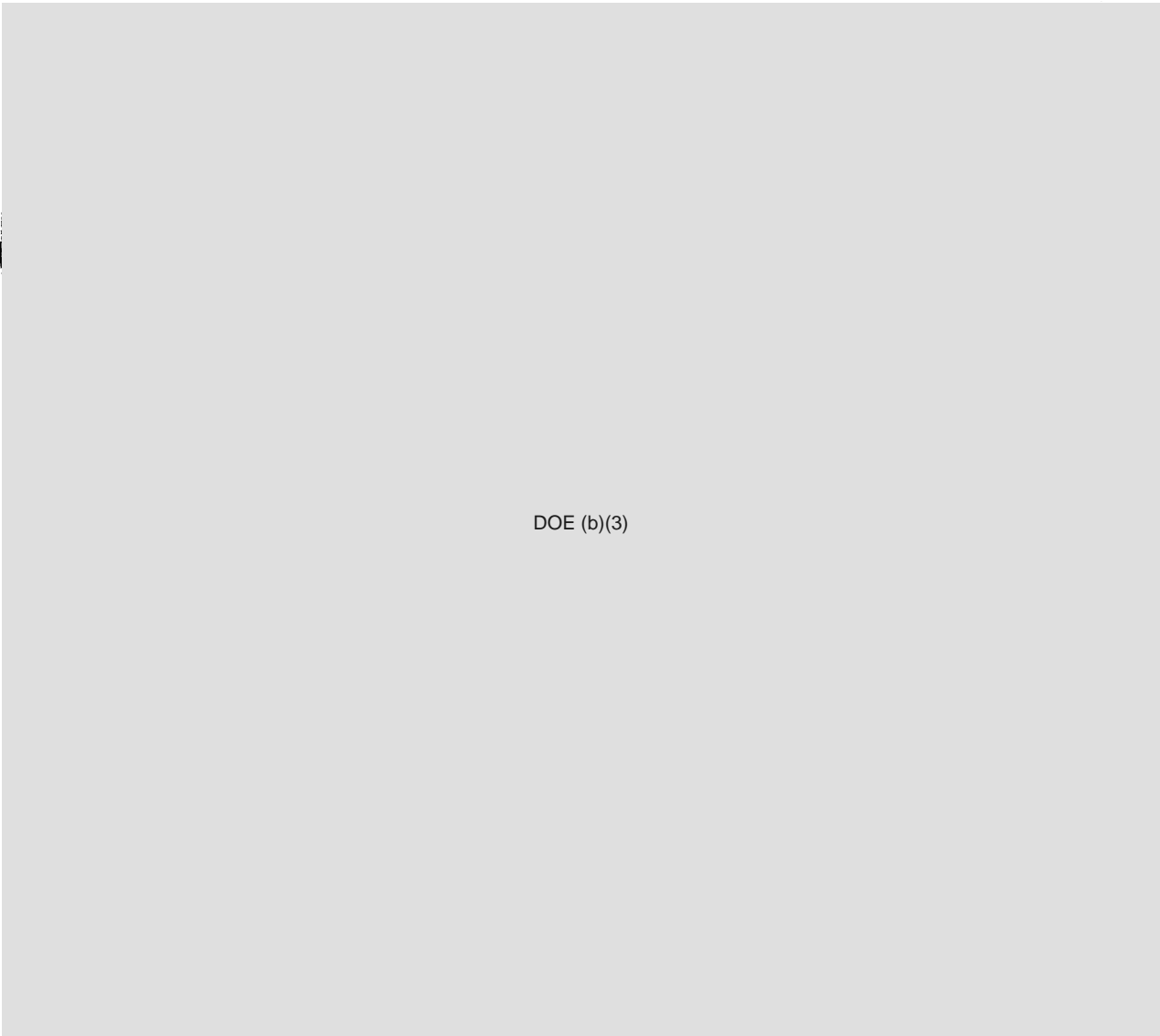
DOE (b)(3)

DOE (b)(3)
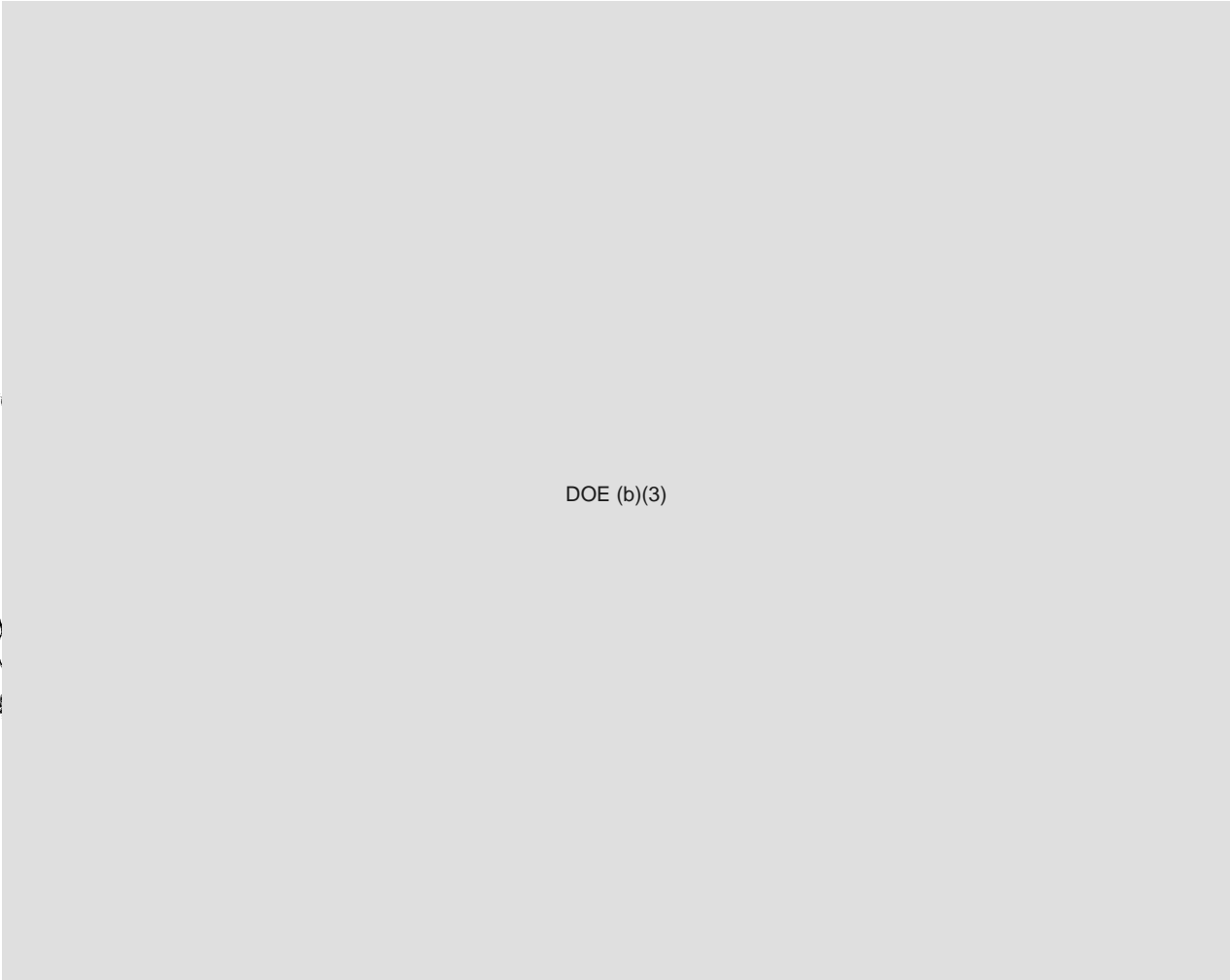
DOE
b(3)

DOE (b)(3)

DOE (b)(3) However, the challenge of actually measuring those conditions remains. We discuss this further below.

5.4   Scaled Implosions of an IHE Primary

DOE (b)(3)

DOE (b)(3)
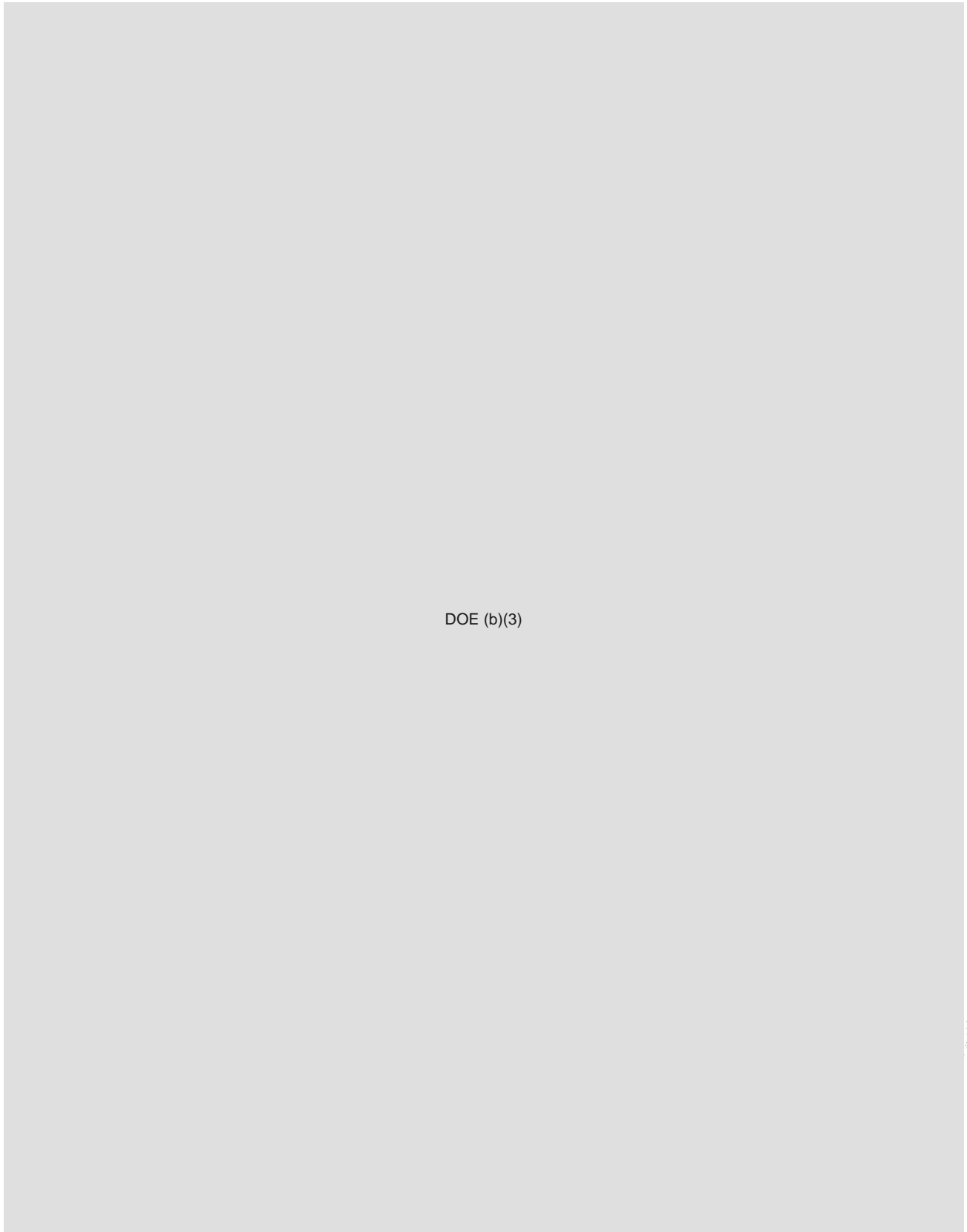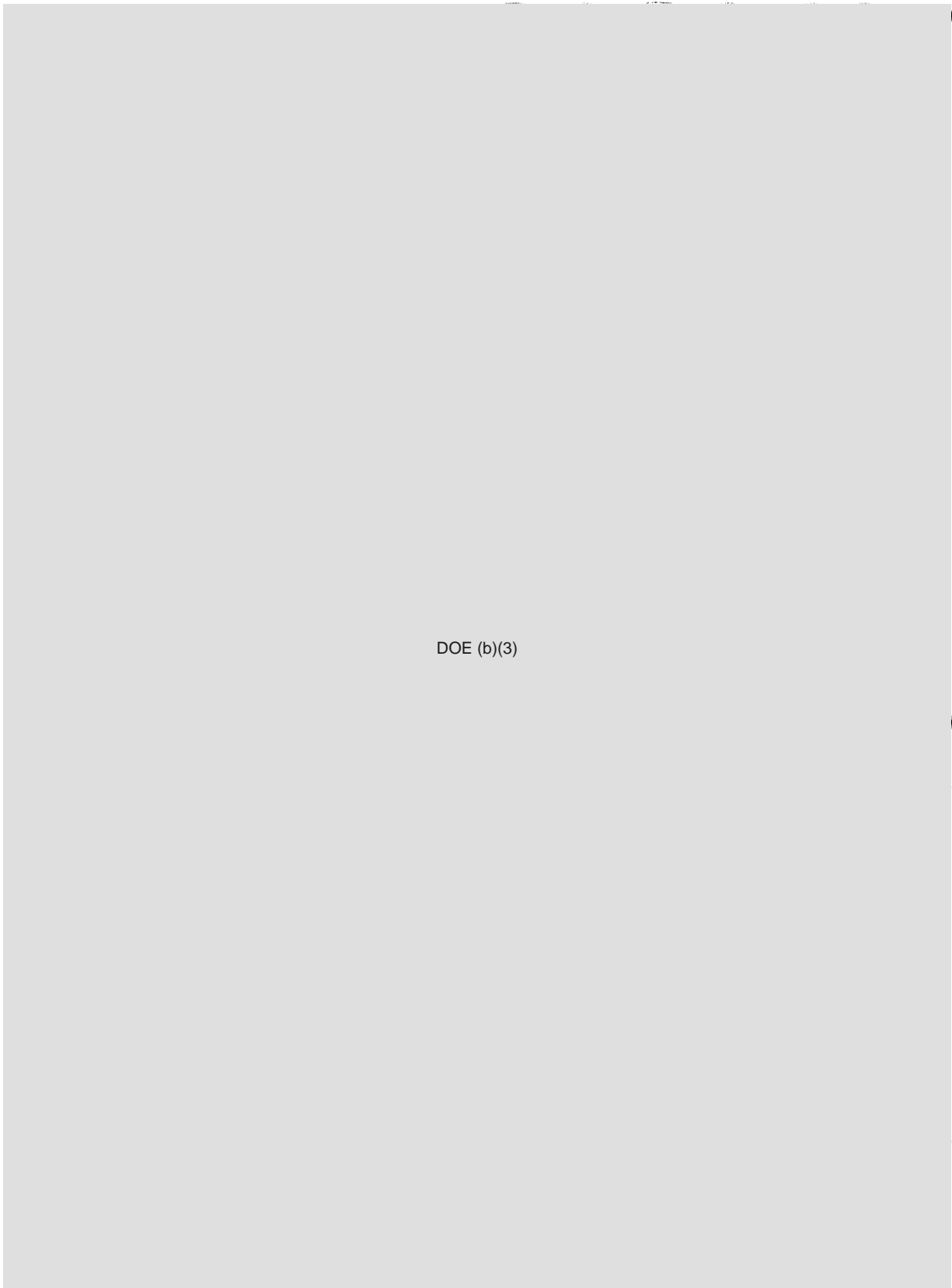
DOE (b)(3)

DOE (b)(3)

DOE
(b)(3)

DOE (b)(3)

Scaled experiments have value in validating implosions. Where simulation and scaled experiments disagree, the results of such experiments will most likely not provide a way of assessing which aspect of our understanding is at fault.

DOE (b)(3)

DOE (b)(3)

DOE (b)(3)

DOE b(3)

5.5 Surrogacy

Another important aspect to be explored as part of the scaled experiments is the ability to make the link from surrogate materials that are used in full-scale hydrodynamic experiments to the corresponding behavior in Pu. This is a critical issue as one cannot do hydrodynamic experiments with Pu at full scale. Designers therefore use surrogate materials to make this connection. Typically the way this is done is to perform the hydro with the surrogate and then see if the simulation using the surrogate matches the results of the experiment. A designer considers general features
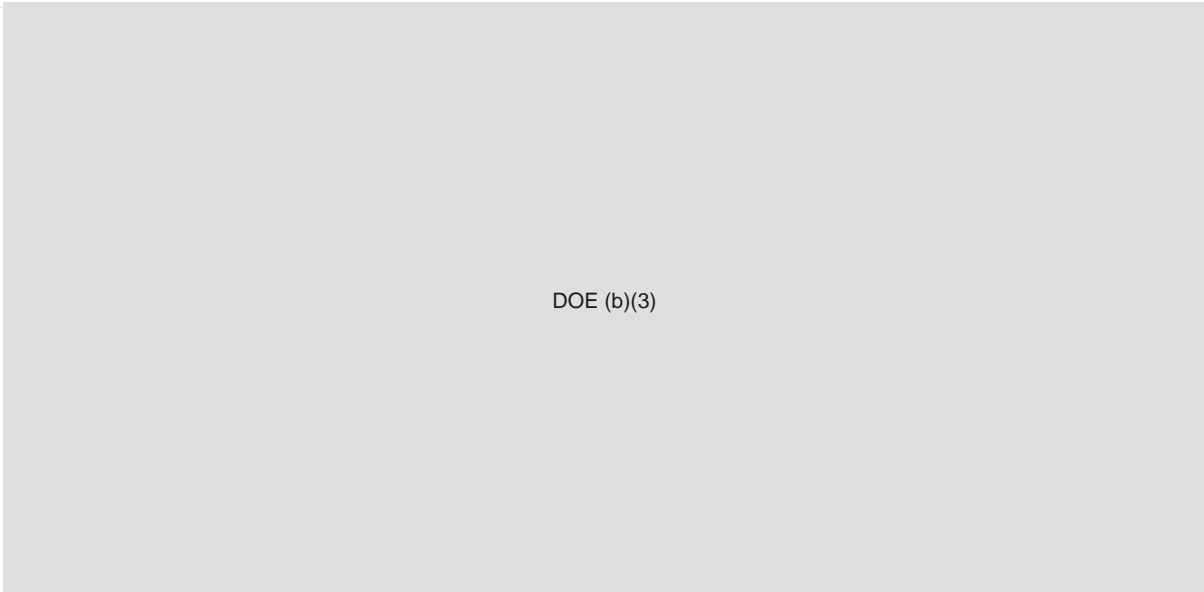
DOE (b)(3)

of the results to see if a proper match has been achieved. DOE (b)(3)
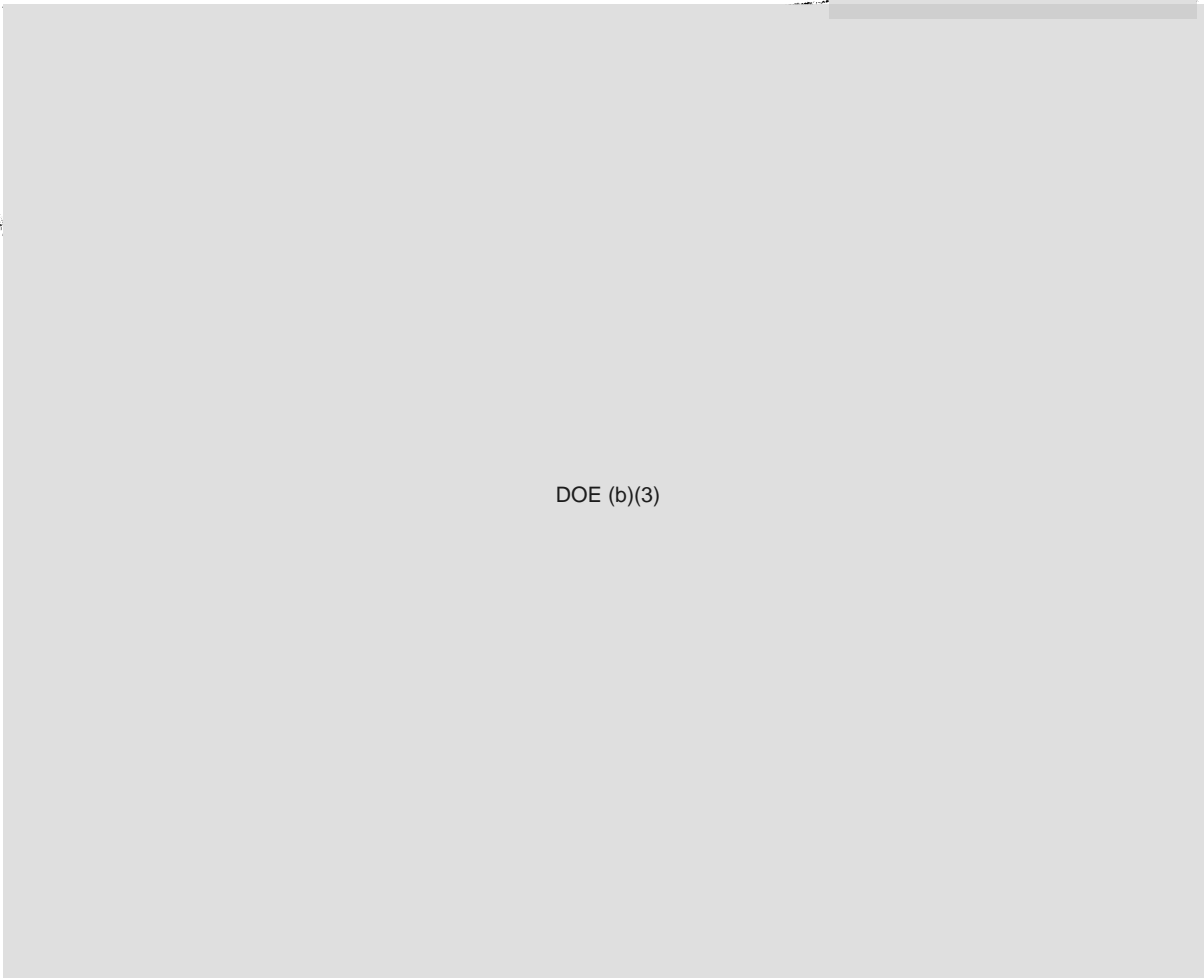
DOE (b)(3)
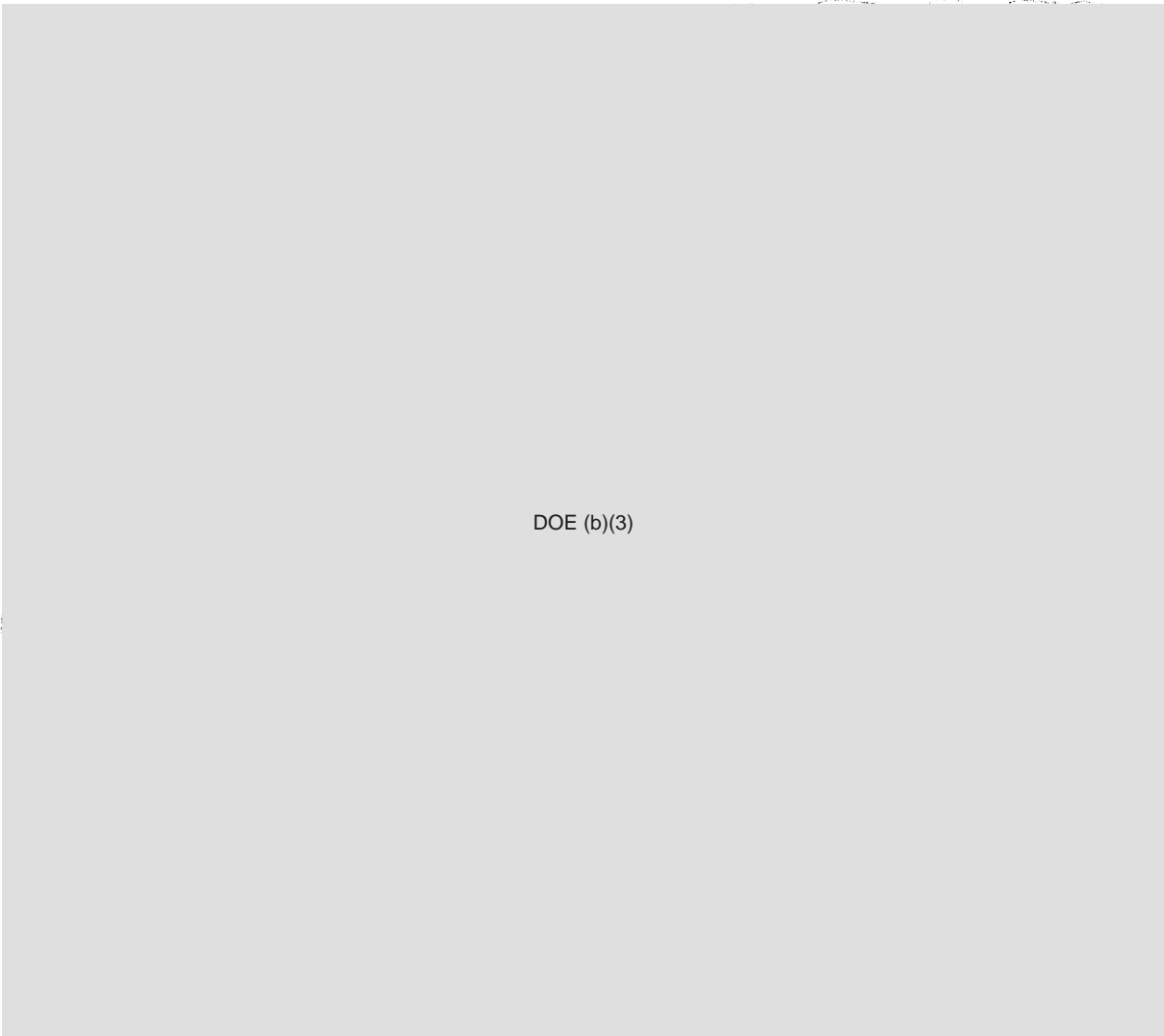
DOE (b)(3)

DOE
b(3)

Our reservation with this approach is that the data may never be good enough to make the connection with the requisite sensitivity. We are not persuaded that conclusions can be drawn given the quality of the cavity radiographs and PINEX images we were shown. In addition, this approach could require data at a variety of scales and with a variety of systems to get meaningful correlations.

An alternate approach to making the connection to surrogates would be to continue fundamental and focused experiments on Pu as well as all relevant surrogates, Ta, DU, etc. so as to characterize these materials as completely as possible including the pressure and temperature regimes accessed prior to nuclear time in the primary.

DOE (b)(3)

This would entail measurements of EOS, strength, phase etc. for all relevant materials. With this in hand it is then possible to explore surrogacy first via computation and then, when sufficient confidence in the results is in hand, to perform a scaled experiment with diagnostics that can provide data of the requisite quality to draw conclusions.

5.6 Improving Predictive Capability

Another motivation for the scaled experiment program is the improvement of predictive capability. G. Maskaly and G. Wall described a plan that includes   DOE (b)(3)

DOE (b)(3)

- "Follow-on gas cavity radiographic experiments will provide data to further validate plutonium models at high pressure and to look for quantitative links to full scale performance."

- "Calculations indicate the data offered by PDV may allow the ability to uniquely differentiate models"

One example of this approach as presented by Maskaly and Wall would be to use PDV to measure the Pu free surface velocity at early time and compare the measurements with predictions of differing spall models, one that was Pu phase aware versus one that was not.   DOE (b)(3)

DOE (b)(3)

DOE (b)(3)

While there have been significant accomplishments in our ability to simulate implosions in Pu, it is likely that a blind preshot simulation will fail to match the PDV results of the proposed first subscale experiment given the detailed information that may be possible with the new PDV probes that will be fielded. In the absence of data from other experiments it will be difficult to to make improvements in the modeling of the unit processes associated with the implosion. This is a challenging intractable inverse problem. One envisions that as knowledge from fundamental and focused experiments improves, the ability to predict subscale experiments (viewed as validation exercises) will also improve. Of course, from the standpoint of weapons performance it is only necessary to achieve agreement within the requirements set by QMU studies.

5.7 An HE Driven Test Bench

For several materials including uranium and plutonium, data in the P-ρ plane are essential for weapon design and for the improvement and validation of theoretical and semi-empirical EOS. By definition, the Hugoniot is accessible via the application of a single strong shock, although more energy is required to reach a given ρ than along the adiabat passing through the initial state of the material. DOE (b)(3)

DOE (b)(3)

The P-ρ trajectory as well as the trajectory in physical space depends to some extent on strength, and it would be good to measure strength and to develop theories of strength for comparison, over a broader range of parameters than is involved in the trajectories that are exploited in order to increase confidence in the values (or in limits, if the effect is very small) along the trajectories that are actually traversed. Diamond anvil cells and the two stage gas guns provide access to pressure regimes important to weapon design and performance, but it would be valuable to access a much broader state space, with appropriate, affordable diagnostics.

From the early days of weapon programs, pin shots have played an essential role in understanding weapons implosions, PDV now provides a great deal of additional information, effectively making pin domes obsolete. Radiography has been essential to the US program, culminating in the 2-axis multi-time capability of DARHT, which unfortunately, has not been used with Pu, but only with simulants. Regulatory difficulties costs impede the use of even small amounts of Pu in contained firings at DARHT.

DOE (b)(3)

Of course, there is no such material to replace symmetry, but it may be possible to use simulants to provide at least an approximate boundary condition on the Pu sector that would obtain in a full Pu implosion.

The problem can be broken into two parts:

1. If it is possible, how would such a low-Pu full scale system be used to obtain data on a weapon configuration?

2. How can one establish the feasibility of low-Pu firing and diagnostics

As for (1) one would design the weapon or candidate configuration to be investigated, identify a substantial sector to be built with Pu, and then redo the hydrodynamic calculation until the rest of the system to be built with simulant allows even the boundary of the Pu sector to follow the original trajectories. The entire system (Pu plus simulants) would be shot and diagnosed to "explosion" (*e.g.*, in principle at DARHT)

DOE (b)(3)

DOE (b)(3)

DOE (b)(3) . These calculations of experimental design, with appropriate choice of "sector" should be carried out in 2D, not 3D. This is a challenging idea and there may not be a straightforward path to develop such an HE driven test bench. But the idea is very similar in spirit to the modifications made in D. Roberts' calculations. One would still need additional materials information to even do these types of calculations but they do allow one can work with Pu at relevant pressures without criticality.

5.8 Safety Requirements

We now turn to the potential use of subscale experiments to examine safety features. Here a number of engineering issues remain to be resolved[8]. DOE (b)(3)

DOE (b)(3)

)

However, modeling the effect of such a design change on the boost process

DOE (b)(3)

is work in progress with 3D ASC codes and has yet to achieve the required high fidelity. The value of $\alpha_{\max}$ and the boost efficiency are recognized as of major importance in modeling boosting.

DOE (b)(3)

DOE (b)(3)

Finally, there are also proposals for improving intrinsic safety in current designs that rely on conventional high explosives (CHE) to drive the primary implosion by introducing insensitive high explosives (IHE).

DOE (b)(3)

DOE (b)(3)

DOE (b)(3)

Concepts for substituting IHE for CHE are under active evaluation at the laboratories. This was also examined in the 2010 JASON study on nuclear weapon surety Ref. [59], which came to the following conclusion:

DOE (b)(3)

Any such change would require an extensive experimental program, involving both sub-critical tests as well as full-scale tests in surrogate materials. Since the properties of IHE do not scale simply, a sub-scale experiment in Pu may not properly mimic the behavior of a full-scale weapon. The utility of such experiments for safety is currently unclear, and should be evaluated. Potentially such experiments could provide an integrated test of the ability to model IHE in 3D geometries relevant to safety, but the case has not yet been made.

5.9 Findings and Recommendations: Subscale Experiments

5.9.1 Findings

1. Subscale plutonium experiments are integral validation exercises, and enable assessments of the ability to predict the integrated dynamic response of materials during the implosion of a primary. Such experiments, which also address issues of surrogacy and scaling, can be a component of the long-term plan for hydrodynamic and nuclear experiments for Stockpile Stewardship. In the absence of other experiments, the near-term subscale experiments, as currently planned and with proposed diagnostics, cannot be used to determine material properties to the accuracy required to distinguish between competing materials models.

2. Subscale plutonium experiments can have scientific value to the weapons program provided they are performed as part of a weapons science experimental program continuously informed by data from ongoing fundamental and focused experiments.

3. The subscale experiment plan, including the Gemini series is challenging the laboratories and attempting to enhance responsiveness to adapt to new kinds of experiments. On the other hand, the interpretation of these experiments will require the results of continued fundamental and focused experiments. From the results above we see that very similar material conditions are sampled in scaled implosions as those in full scale implosions. But because all of the relevant phenomena (EOS, strength, phase change, etc.) are active simultaneously, these integrated experiments will not provide definitive measurements on any of these properties individually.

4. It has been claimed that the measurements on a scaled system will facilitate the ability to differentiate among various phenomenological models now in use in weapons simulations. We agree that the added data provided by PDV measurements may make it possible to develop better choices of parameters or models,

but we are concerned that this exercise will lead to the same ambiguity encountered in our attempt to infer the importance of strength models from the use of the PMP which uses a collection of models that are similar to those being diagnosed in the proposed experiments.

5. For IHE systems the detonation properties do not scale well and these timing differences have to be taken into account. Work is underway to address these issues. Nevertheless, there is an interesting correspondence between the results that should be understood as it will have an important bearing on understanding the differences between full scale and half scale results in IHE systems.

6. It should be noted that the concept of exploring scaling need not rely on the use of plutonium. Scaling of implosions will most likely work as well for any of the surrogates of Pu. This has the advantage that experiments are much easier to execute because the authorization issues are far less onerous and the premier radiographic diagnostics of DARHT can be brought to bear.

7. In testing models in subscale experiments, it is important to use models in forward calculations that are appropriate to the problem being addressed. If an hypothesis is being tested, the question is the extent to which the subscale experiment can provide the appropriate test of two models that cannot be decided by another (e.g., focused) experiment.

8. Enhancing intrinsic safety (and surety) of U.S. nuclear stockpile requires a well executed and supported science campaign that includes subcritical experiments. These must use realistic geometries (with and without Pu), Pu "coupons", full-scale experiments with surrogates.

5.9.2   Recommendations

1. A key goal of the subscale program is to be able to make connections among hydrodynamic experiments in Pu and experiments in surrogate metals. However, this too does not require the use of scaled primary implosions. One can develop

a detailed understanding of dynamic materials properties in Pu as well its surrogates by completing the experiments of the DPE plan and executing in parallel a similar program for surrogates. Here too the best way to make measurements is to execute fundamental and focused experiments on the surrogates.

2. Once a reasonable understanding of the dynamic behavior of surrogates and Pu is developed, it would be possible to execute simulations using the best available understanding of each material and make a series of predictions on full scale Pu implosions, full scale surrogate implosions, subscale surrogate implosions and subscale Pu implosions. These experiments would then serve as integrated validation experiments to be compared with the best understanding of material properties as embodied in the simulation codes. We would argue this is a better way of making connections between Pu and surrogates than the development of empirical correlations because it exercises many capabilities at once.

6 DIAGNOSTICS FOR SUBSCALE EXPERIMENTS

In this chapter we examine selected diagnostics for the proposed subscale experiments including some issues specific to their implementation in these experiments. We begin by discussing some radiographic issues associated with the subscale experiments. We then discuss some of the proposals for addressing these issues. We also provide some discussion on methods to assess radiographic uncertainties. We close with some suggestions for further diagnostics that might be considered.

6.1 Radiographic Issues for the Subscale Experiments

The ability to infer results from scaled experiments will depend on the quality of the diagnostics. There are two types of diagnostics planned - radiography and velocimetry using PDV probes. We discuss in this section some of the issues associated with radiography. Because scaled experiments must be performed underground at U1a it will be necessary in the short term to use the Cygnus radiography facility. The capabilities of Cygnus were discussed in Section 2.5.

We were briefed by LLNL on the potential performance of Cygnus for scaled experiments. The current state of the art as regards radiography is the DARHT facility at LANL which provides unparalleled dose and resolution as well state of the art detector technology. An example of its capability is shown in Figure 41 where we show a comparison between a DARHT radiograph and a simulated version for a hydro fired with surrogate material.

We can use such simulated radiographs to assess the type of image quality that would be available at U1a. First there is a fundamental limitation in that since the features of the experiment might be as small as half the full size twice the resolution is required for the radiograph. A comparison of how spot size affects the quality of the image is shown in Figure 42. The Cygnus spot size is comparable to that of DARHT
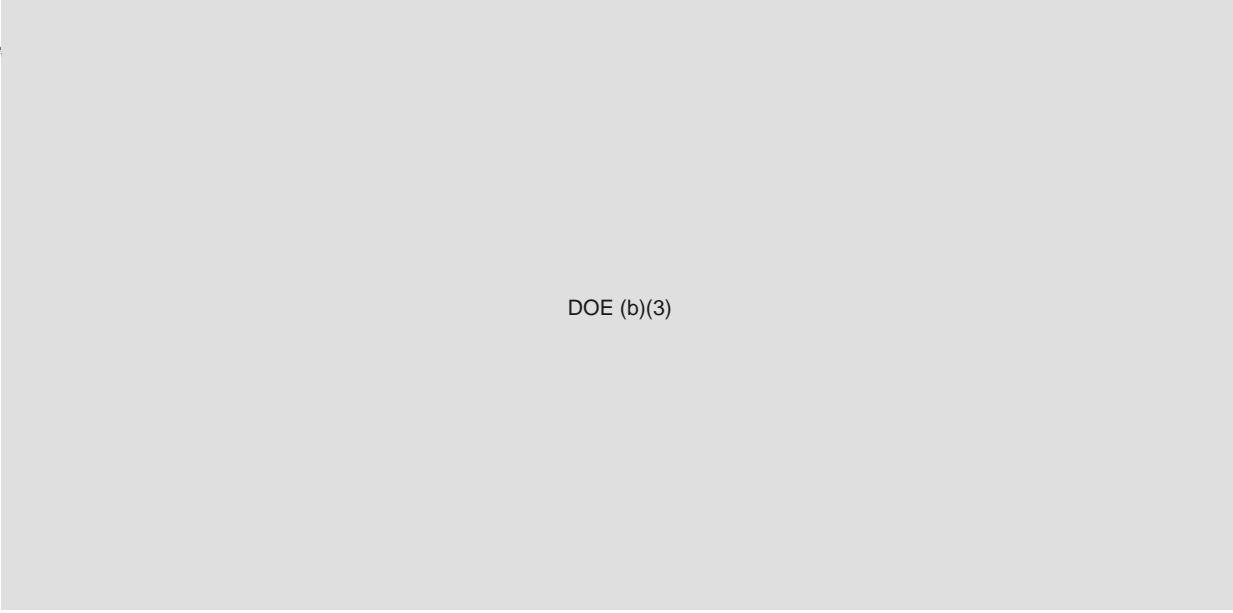
DOE (b)(3)

and so there will be a fundamental limitation for half scale experiments on the level of detail that can be seen.

There are also issues arising from the reduced end-point energy of Cygnus as well as the performance of the detector at the facility. In the discussion below we show that with appropriate improvements the Cygnus facility can be used to produce images although without actual tests although it is not yet possible to tell precisely how well one can diagnose the subscale experiments. We focus on the potential utility of the two radiographic machines, Cygnus-1 and Cygnus-2 at U1a, each with an endpoint of 2.25 MeV. These provide doses of the order of 4.4 R at 1 m from the target, where the object to be subject to dynamic radiography is placed. In comparison, DARHT provides 400 R for its single pulse on Axis-1, and 100-300 R on each of the four pulses on Axis-2. With its endpoint energy of 2.25 MeV, it is not obvious that Cygnus could produce useful radiographs of weapon-relevant systems, in particular of half-scale devices. This message was reinforced in a presentation by LLNL where simulated results of the Cygnus radiography system were presented as applied to a half scale experiment. In Figure 43 the effects of spot size, dose, end-point energy and detector sensitivity were taken into account and this results in the radiograph on the right dominated by noise.

DOE (b)(3)

A JASON analysis indicates the situation is not quite so dire. A modest modification of Cygnus will make it possible to produce meaningful images, although not with the quality DARHT. The problem is that the analysis even of the half-scale system, in which the projected mass per unit area is precisely half that of the full-scale system, and the transparency therefore much greater, provides a signal that in each pixel was calculated to be less than the measured noise in the DARHT camera, although the DARHT camera has not been used down-hole with Cygnus. We focused on this image, and communicated with LLNL, in particular, with B. A. Jacoby, who had done the analysis resulting in this image. Jacoby's analysis [60] begins with the measured dose of 4.4 R at 1 m from the target, as described in Ref. [61] and propagates the calculated photon spectrum through the test object at 100 cm, and to the camera at 534 cm, as is the case with DARHT. But the image could be improved by substituting the DARHT camera itself for the somewhat simpler one in use at Cygnus. In particular, Cygnus uses a uniform plate of thickness 2.5 mm of the highly efficient fast scintillator cerium-doped lutecium silicate (LSO), in contrast to the individual crystalline prisms of LSO used in DARHT, 1.0 mm square and 40 mm long. In fact, the DARHT camera uses 135,000 such pixels, which are all oriented toward the target at a distance of 534-cm [62]. Axis-1 of DARHT has also a tour de force

DOE (b)(3)

Bucky grid to reduce contrast loss by limiting the scattered x-rays in the target. This is a 30-cm thick structure of tungsten-polymer with density of 11.4 g/cc (compared with tungsten metal at 19.3 g/cc).

At our request, Jacoby recalculated the low-dose half-scale image, now with the assumption of the DARHT camera at 534 cm, which improves the signal by a factor 3.69 with the substitution of 40 mm of LSO for the 2.5 mm of LSO. A re-run of the transmission through the half-scale test object improves the fluence through the thickest part of the object by a factor 2.5, probably because the thicker LSO increases the detection of the highest-energy gammas that are the most penetrating through the object. The resulting simulated image is shown in Figure 44.

In addition, the Cygnus camera usually operates at distance of 200 cm instead of the DARHT camera at 534 cm. Cutting the DARHT distance from 534 to 260 cm will increase the energy density on the LSO by a further factor 4, but at poorer spatial resolution. Thus, despite the great handicap of a 2.25 MeV X-ray endpoint, Cygnus can provide quite a respectable image of the half-scale object.
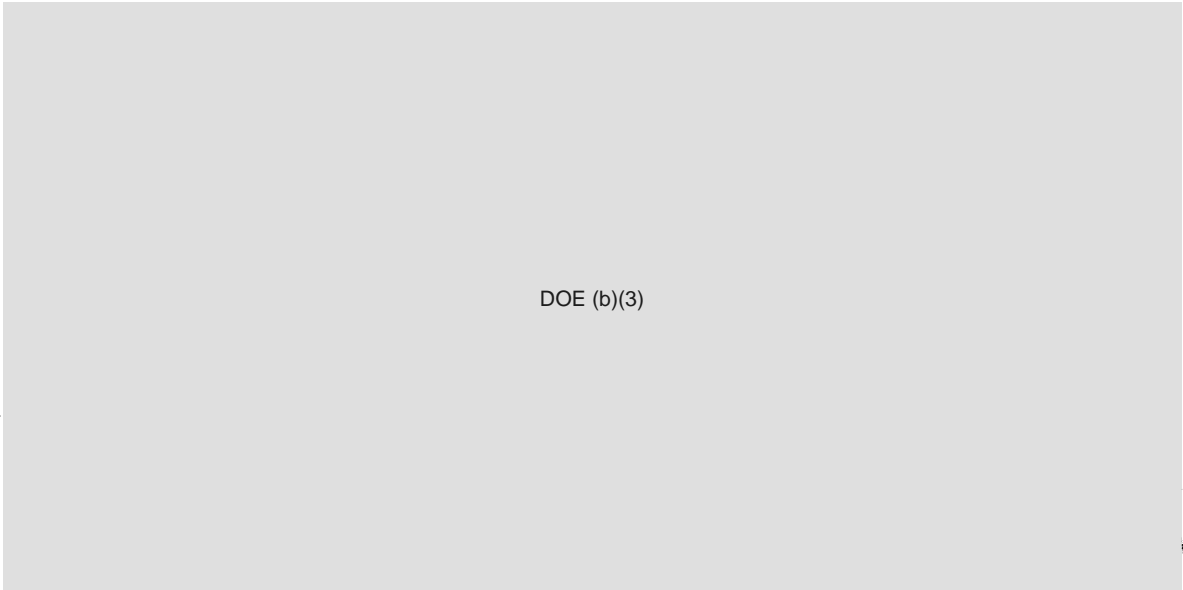
DOE (b)(3)

*DOE
b(3)*

Of course, things are not so simple as just moving the DARHT camera to 260 cm from 534 cm, because the individual LSO crystals are aimed at the target, in order that the spatial resolution not be degraded by the X-rays entering at an angle to the axis of the pixel. So a new LSO plane would be required. It would, in principle, be cheaper than the DARHT camera in that only a single optical system would be used, in view of the half-scale object and the assumed factor 2 reduction in magnification, so the linear extent of the LSO plane would be reduced by a factor 4 and its area by a factor 16. This would, in principle, allow the use of faster (*i.e.*, more efficient) optics for gathering the scintillation light onto the CCD focal plane, which could increase the signal by about a factor 4.

We emphasize that a figure such as that of C. Tomkins (Figure 45) which shows 2.5% standard deviation for pixel thickness measurements in thick tantalum, does not limit the use of meaningful radiographically derived densities to errors on the order of 2%. For instance, in the estimate of areal density, it is not the individual pixel areal density that counts, but an average over many pixels. If there is a region of area of 4 cm^2 that is relevant to a particular aspect of the calculation, this comprises almost 400 pixels, so that the standard deviation of the measurement with 2.5% S.D. per pixel, is reduced by the square root of 400, to about 0.12

We described this approach in considerable detail in Appendix D of the 2006
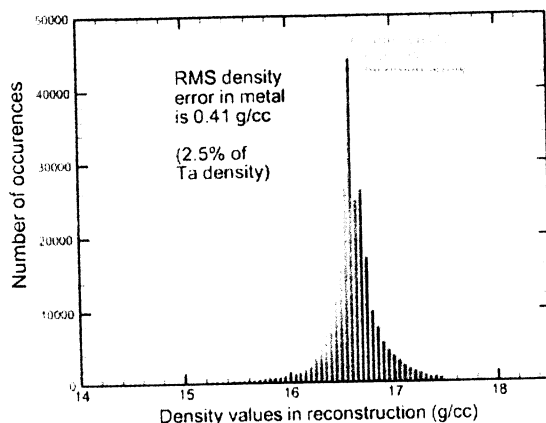
Figure 45: Statistics of density measurements at DARHT

JASON DARHT report [63].   DOE (b)(3)

DOE (b)(3)

DOE (b)(3)   We also described, in passing, the estimate of density from simulated radiographs that show noise to the extent that it is hard to recognize the contrast.

Yet the averaging procedure we have described does an excellent job. We also advise against the widespread use of a "line-out" to determine a boundary, preferring, instead, to fit the entire image, at least in the region of the anticipated discontinuity. Work done for this study (described in section 6.3) includes the influence of the graduated collimator on the radiographic image, and extends the simple MATLAB code used in Ref. [63]. We support the kind of work in this field that we see, usually teamed with the term "BIE" or Bayesian Inference Engine (*e.g.*, Ref. [64] in which this is done extensively).

Of course, much calibration needs to be done to make this approach quantitative and most useful. This begins with "flat fielding" of the LSO, optics, and CCD imaging system, by the use of guaranteed uniform (or measured) illumination on the LSO, most readily obtained initially either in static measurements or with a microtron. Other calibration that needs to be done is to image the graded collimator, and to fit that. Similarly, overlying material could be imaged with a known object. DARHT shots

and even Cygnus shots are costly, but the program of quantitative radiography can succeed only if one provides the basic information to make use of the performance of which DARHT and now Cygnus are capable.

Discussions with S. A. Watson (LANL) about the construction of a Bucky grid for Cygnus radiographs indicate that this is a much simpler problem than for the 45-cm "tungsten" Bucky grid (BG) at DARHT. DARHT's BG is 30-cm thick, cast of tungsten powder in polymer with a density of 11.4, in contrast with pure tungsten of 19.3 g/cc or heavimet with density of 17.95. There are several ways of providing such a Bucky grid, probably at considerably smaller feature scale than the 1.1 mm pitch and 0.90 mm apertures for the BG at DARHT. In particular, the Cygnus BG might be made of 11-cm diameter tungsten foils, photo-etched with the requisite pattern, differing in scale on each of the successive foils. Thus, if the apertures are 0.22 mm, the tungsten foils might be of thickness 0.07 mm. Uniform thickness could be assured by a preliminary measurement and broad-area photo-etch or chemical-mechanical polishing under radiographic control.

6.2 Proposals for Future Radiographic Capabilities

As indicated above, radiographic diagnostics for the near term subscale experiment are limited to the capabilities of the Cygnus facility at U1a. This system was not originally designed for experiments with high areal density and so at best only very early time images could be obtained using Cygnus. As indicated above, some improvement in radiographic image quality can be had by improving the detector and altering the imaging geometry. But in the longer term, it will be necessary to develop improved radiographic capabilities at U1a if data on late time cavity geometry is desired.

All three laboratories (LANL, LLNL, and SNL) have developed proposals for radiography upgrades at U1a. We briefly summarize these proposals below. NNSA requested an assessment of the relative merits of the various approaches but we were

not able to provide a comprehensive analysis owing to time constraints. What follows is a cursory review of the proposals. We do relate the stated capabilities of the various approaches to the measurement requirements that were outlined in Section 3, but we caution that a complete study of the requirements and capabilities of the various proposed systems should be carried out to evaluate fully the various proposals. We also do not take into account the costs of the various proposals.

Currently in the US the main radiographic facilities are DARHT at LANL, Cygnus at U1a and FXR at LLNL. The DARHT facility provides dual axis views as well as the ability to radiograph a target up to five times so as to provide time sequence information. Cygnus which we have discussed above has two axes and provides two pulses. It was designed for subcritical experiments. FXR has a single axis and provides a single pulse but has a very large format so can provide a larger field of view.

SNL has proposed two approaches. The first uses a 7 MeV linear transformer driver coupled to an SMP diode. The second uses a 7 MeV indication voltage adder coupled to an SMP diode. Either system would provide 2 or perhaps 4 pulses on two separate axes. The dose is about half that of DARHT (300 Rad versus 600 Rad for DARHT). At present however, the technology is still in development and there is no estimate of important metrics like spot size and the attainable accuracy of density measurements. These would have to be in hand to properly assess this technology.

LLNL has also proposed two approaches based on their previous development of the FXR system in which a linear induction accelerator (similar to what is used at DARHT) drives a DARHT-like target. The system would provide at least 2 pulses on one axis and could provide 4 if a two axis configuration is pursued. The dose is similar to the SNL proposal. The spot size is comparable to that of DARHT (1.6 mm). The first option would use current FXR technology while the second would use a solid state linear induction accelerator. The technology of the first option is quite mature except that a double pulse capability has to be developed and there are

questions about spot size reproducibility. The second option offers the advantage that the number of pulses is limited only by the target and detector but the technology is not completely proven.

LANL presented three approaches. The first would be to install a DARHT-1 type linear accelerator. This is proven technology that can provide one pulse along one axis at high dose (580 Rad at 1m). The second approach is to install a DARHT-2 linear accelerator. This would allow for up to four pulses along one axis at up to 300 Rad at 1 m. The spot size for both approaches is < 1.7 mm. This too is proven technology but, because of space limitations in the U1a drifts, it would be necessary to redesign the accelerator cells, an issue which arose during development of the DARHT second axis at LANL as well. The capabilities of a DARHT-like facility are summarized in Figure 46. The figure shows the actual abilities of DARHT as demonstrated through its use in current hydrotests on surrogate materials at LANL.

The third LANL approach is the most ambitious. The idea is to build a proton radiography facility at 20 GeV at U1a. This would require the construction of a 20 GeV proton accelerator at NNSS. The capabilities of pRad imaging are impressive. Up to 10 images can be produced at intervals of 10 ns. Such a system can image at the requisite areal density for subscale experiments ($\rho \Delta r \approx 160 - 180$) with an accuracy of less than one per cent. The capabilities for pRad are summarized in Figure 47.

All approaches presented by the laboratories constitute impressive applications of modern radiographic technology. There are of course issues of technology readiness and cost but we have not assessed these. Deployment of any of the proposals would certainly improve upon the current capabilities at Cygnus and would provide higher quality imaging of the cavity formed in a subscale experiment. But it is not possible given the information presented to date to make a clear choice among the various ideas. The difficulty is that we have not seen analyses of the subscale experiments that provide actual requirements for radiography. We have seen what can be done but we have not seen what is actually required. In turn such requirements are connected

Scale	ρdr[1] (g/cm²)	Δρdr (%)	Δx[2] (mm)	Δt (μs)	T[3] (μs)	# Images[4]	# Axes[4]	Point-spread FWHM[5] (mm)	Comments
DARHT Axis I	315-360	~1.0	0.3-0.4	NA	NA	1	1	0.9	Demonstrated Capability
~0.7-0.8	250	0.6	0.15	NA	NA	1	1	0.9	Demonstrated Capability
~0.5-0.6	180	0.4	0.10	NA	NA	1	1	<0.8	Demonstrated Capability
DARHT Axis II	250 315-350	NA	<0.20	0.5	1.6	4	1	0.9-1.1	Demonstrated Capability To be demonstrated this summer
1.0	315-360	0.6	0.15	0.5	3.0/20	4-8	2-4	0.4-1.2	Current DARHT Axis I and II can meet all these requirements as shown. Axis II can provide 4-8 pulses, the 2 axis variant will have capability for 4-8 pulses on each axis
0.8	250-290	0.6	0.12	0.4	2.4/16	4-8	2-4	0.3-1.2	
0.5	160-180	0.6	0.075	0.2	1.5/10	4-8	2-4	0.2-0.75	

Figure 46: Capabilities of DARHT

Scale	ρdr (g/cm²)	Δρdr (%)	Δx[1] (mm)	Δt (μs)	T (μs)	# Images	# Axes[2]	Point-spread FWHM[3] (mm)	Comments
~0.7-0.8	250	0.6	0.15	NA	NA	1	1	0.9	Current capability
~0.5-0.6	180	0.4	0.10	NA	NA	1	1	<0.8	Current capability
1.0	315-360	0.6	0.15	0.5	3.0/20	4-8	2-4	0.4-1.2	For DynEx, full-scale capabilities
0.8	250-290	0.6	0.12	0.4	2.4/16	4-8	2-4	0.3-1.2	Largest scale that remains sub-critical
0.5	160-180	0.6	0.075	0.2	1.5/10	4-8	2-4	0.2-0.75	0.5-scale is lowest practical for retaining physics fidelity
1.0	315-360	0.25	0.020	0.2	100	≤10	1	0.2	20 GeV/c pRad single axis
0.5	160-180	0.25	0.014	0.2	100	≤10	1	0.14	20 GeV/c pRad single axis
0-1	0-400	0.1[4]	0.005[5]	0.2	100	≤10	4	>0.02[5]	20 GeV/c pRad multiple axis

Figure 47: Capabilities of pRad

to the goals of the experiment.

For example, the first subscale experiment will use Cygnus radiography to get early time images. The main diagnostic to be used will be the PDV probes which will provide velocity information at early to intermediate times on the Pu gas interface.

DOE (b)(3)

DOE (b)(3)

Thus for this experiment there is little to no radiographic requirement. The Cygnus system will presumably provide early time interface information but this will at best provide a consistency check for the PDV measurements.

DOE (b)(3)

DOE (b)(3)

It will also be important to make density measurements but again some notion of the level of precision has not been completely defined. There is reasonable agreement on the quantities of interest that may be inferred from radiography. For example in D. Roberts' presentation the following list in rough order of priority was given:

DOE (b)(3)

2. Jet and cavity formation for nuclear safety applications

3. Position vs. time of outgoing shock

4. Position of the outer boundary of the SNM

Next in priority are

1. Jump in density across the outgoing shock

2. Outer boundary of the tamper

3. Change in density across the SNM-tamper boundary

4. Dynamic density mapping of the entire pit.

We are unaware at this point of any studies that inform what measurement precision is required to assess these metrics. On the other hand, we understand that a quantitative assessment of the requirements has been undertaken, and the final results will be mutually agreed upon by the design laboratories. Once these are in hand the radiographic options can be compared as regards their fitness for purpose and a choice can be made that also takes into account the various trades such as cost and additional engineering complexity associated with construction at U1a.

6.3 Assessments of Radiographic Uncertainties

This section describes a simple analysis procedure for extracting quantitative information from radiographs such as those produced in hydrotests performed at DARHT; it extends work reported in Appendix D of the 2006 JASON report on DARHT [63]. The main difference between this and the earlier work is the introduction of concentric spherical objects to be radiographed. The forward-modeling and parameter fitting are performed using MATLAB.

DOE (b)(3)

DARHT is modeled by a bremsstrahlung target having a 2 mm × 2 mm beam spot, a graded collimator located 1 m from the bremsstrahlung target to balance

118

DOE (b)(3)

the dynamic range of the radiograph exposure[9], the concentric spheres to be imaged located at 1.33 m from the beam spot, and the scintillator detector plane located about 5 m from the bremsstrahlung target. This setup results in a target image magnification $M = 4$. We do not simulate the scattering from containment vessel windows or other sources, nor do we simulate the "Bucky" grid, which helps shield the detector plane from scattered X-rays[10]. We model the detector as a close-packed array of 1 mm square scintillator towers oriented normal to and centered on the beam line.

Figure 48 shows the integrated material density assumed in the simulation described here. The average power in the bremsstrahlung spectrum is delivered by 5 MeV X-rays, which is near the energy where absorption lengths of most elements cross over at a value near $\rho\lambda \approx 22$ g/cm^2; our analysis assumes this simplified attenuation

---

[9]We thank D. Funk and S. Balzer of LANL for providing us with drawings of the graded collimator. Briefly, it is a 6 inch block of tantalum with a bi-cone bored in it to give a nearly linear increase in column mass density from an inner radius on the detector plane (radiograph plane) of about 45 mm.

[10]It would be relatively easy to include such effects in a more complete simulation.
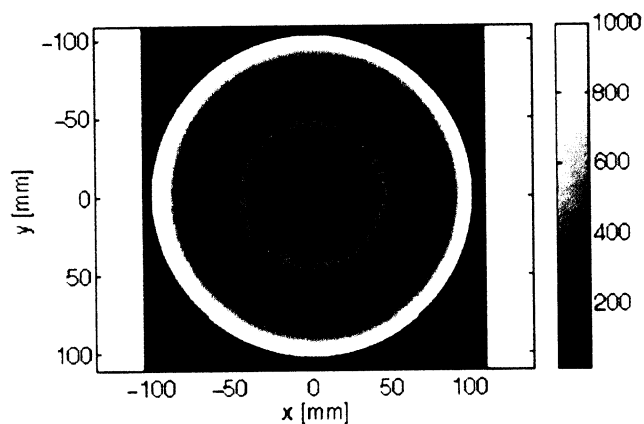
Figure 49: Simulated radiograph of the target object, including a beam-spread of ± 1 mm, for an exposure of 25 R. The units of intensity are detected photons per 1 mm^2 pixel. The dynamic range was restricted to a range of 1:100, or 10 to 1000 photons detected per pixel, for producing the radiographic image.

model and counts photons accordingly in the description of the image intensity and corresponding statistical fluctuations. A sample radiograph based on the preceding model, including a convolution over the beam spot and a Monte Carlo instance of photon fluctuations, is shown in Figure 49. The contrast range in this image is restricted to a range of 1:100 to show features in the vicinity of the core/outer sphere interface.

Our fitting algorithm for parameters describing the core compares the number of photons detected in each pixel in the active region (*i.e.*, the pixels inside the radius of the outer spherical shell of the model target) radiograph shown in .Figure 49. Let the matrix R represent the number of photons detected in the array of scintillator pixels making up the radiograph to be fitted and the matrix $F(\{p\})$ be the results of a forward-model calculation of a radiograph described by the set of parameters $\{p\}$. For the present study, we fit for 4 parameters describing the core sphere (its radius, mass density relative to the outer sphere, and 2D coordinates of its center on the radiograph) and the overall dose delivered to form the radiograph.
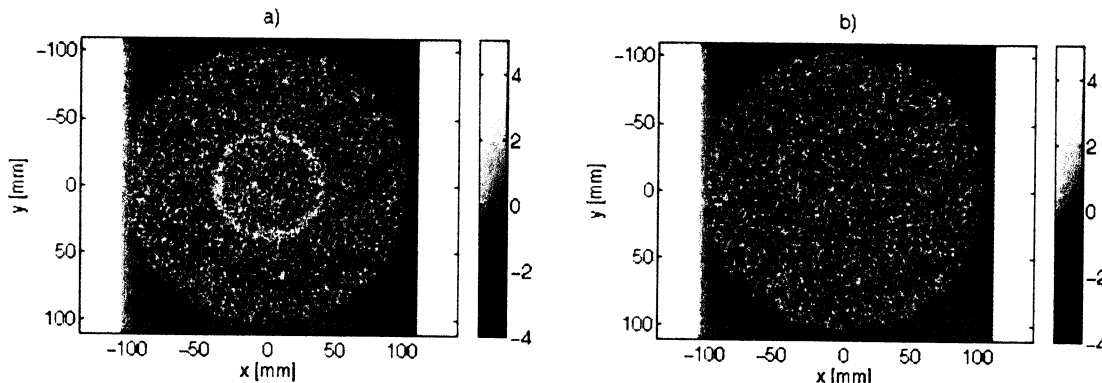
Figure 50: Image a: difference between the radiograph shown in Figure 49 and the forward-model calculation of a target object where the central core is larger in radius by 0.1 mm compared to that simulated in the radiograph where the core object radius is 10.0 mm. Image b: difference between the radiograph and the forward-model calculation with identical radii. Differences between the radiograph (r) and forward model calculations (f) are plotted as the statistical weight S_{pixel} of the difference in numbers of photons detected each pixel, $S_{\text{pixel}} = (n_r - n_f)/\sqrt{n_f}$.

We describe the statistical significance of the comparison between actual and model radiographs by the matrix S, with elements given by:

$$S_{i,j} = \frac{R_{i,j} - F_{i,j}}{\sqrt{F_{i,j}}} \tag{13}$$

where i, j label the pixels. From S, we can define a "cost" function χ^2 by:

$$\chi^2 = \text{Tr}(S^T S) \tag{14}$$

A gray-scale representation of the statistical significance matrix is shown in Figure 50. In this case, one fitting parameter–the radius of the core sphere–is increased by 0.1 mm while the others are held at the values used to produce the simulated radiograph of Figure 49. This image is instructive because it illustrates the large number of detector pixels that are impacted when one parameter of the forward model is varied, thus indicating qualitatively the statistical power inherent in this approach for extracting quantitative results from image data.

The variation of χ^2 with core radius (while other fitting parameters are held
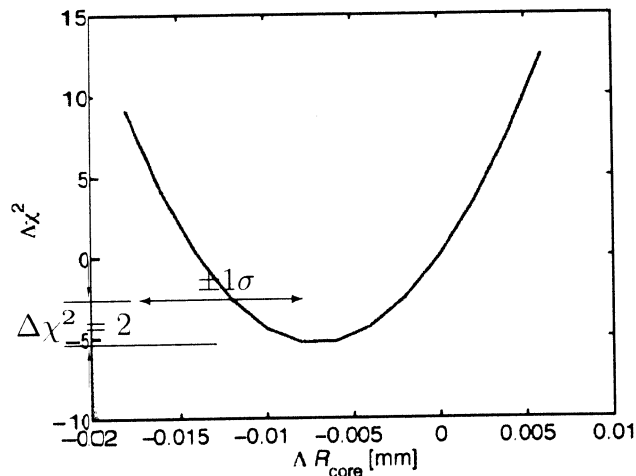
Figure 51: Variation in χ^2 as a function of departure of the model core radius from the value simulated in the radiograph shown in Figure 49. For this plot, the other parameters describing the core region are fixed at their nominal values. Also indicated in the figure is the width of the χ^2 curve at the level $\Delta\chi^2 = 2$ units above the minimum value. This width is an estimator for the standard deviation σ in the parameter R_{core} for the particular radiograph being fit by the forward model.

fixed) is shown in Figure 51. With this plot, the power of this analysis can be quantified. Notice that comparison of the forward model to the particular statistical instance captured in the simulated radiograph results in a best-fit to core radius about 7 μm smaller than what was used in the model. This is consistent with the variation observed in χ^2 where one expects 1 standard deviations in fitting parameters to result in a change $\Delta\chi^2 = 2$. The estimated covariance matrix of the fitting parameters can be found by examining $\Delta\chi^2 = 2$ contours in the full space of the fitting parameters. In this particular case where only the core radius is being varied, the estimated statistical error in the determination of the core radius is $\sigma_R = 5\,\mu$m.

To check the statistical power of this analysis, we generated 100 radiographs from the same forward model and separately fitted the radiographs to all 5 parameters used in the forward model. The means and RMS spreads in the parameters fitted are given in the table below:

Parameter	Input Value	Mean Fitted	RMS Spread
R_{core}	10 mm	10.0027	0.0041
ρ_{core}	1.5	1.4972	0.0010
X_0	0 mm	0.0000	0.0002
Y_0	0 mm	0.0000	0.0002
Dose	25 R	25.0250	0.0063

It is seen that the fits to the 100 radiographs reproduce the actual input parameters to a high degree of precision. In particular, the density of the core relative to that of the surrounding sphere is determined to much better than 1% accuracy. In our model, there is a correlation between the density of the core region and the dose assumed for the radiograph. This has the effect of shifting the mean fitted values for these two parameters slightly outside the expected statistical spread. The RMS spread in fitted values for the radius of the core region, 4.1 μm agrees well with the expected error 5 μm derived from the width of the χ^2 curve shown in Figure 51.

Real-world effects in actual radiographs, such as scattering, non-uniform detector response, and more complex images will certainly reduce the accuracy of parameters determined by fitting from these admittedly idealized estimates. Nevertheless, using forward models that capture the important physical constraints of the test object and experimental setup can yield excellent accuracy because of the large number of detector elements independently contributing to the radiograph.

6.4 PDV and Asay Plates

Photon Doppler Velocimetry (PDV) is a powerful tool for diagnosing early-time implosions [65]. We were told that PDV will provide initial jump off data for the first time in the Gemini series experiments.We were informed about continued developments and extensions of PDV diagnostics, notably multiplex PDV, as part of the Gemini project [66]. These optical dome diagnostic contains, for example, 72 points mounted into probe with multiplexing capability for each probe. Such development will be useful for a broad range of hydrodynamic experiments, including focused experiments.

DOE (b)(3)

A velocimetry image from PDV that identifies ejecta is shown in Figure 52

One can measure not only bulk pit motion, but also to some extent one can see and measure spall and ejecta. However, there are limits on such measurements, because at a certain size scale the spall may become optically-thick. One possible amelioration is to combine PDV with Asay windows [67], which are transparent Asay plates that can measure the total ejecta momentum impinging on the plate while allowing some ejecta and possibly the pit surface to be seen by the PDV.
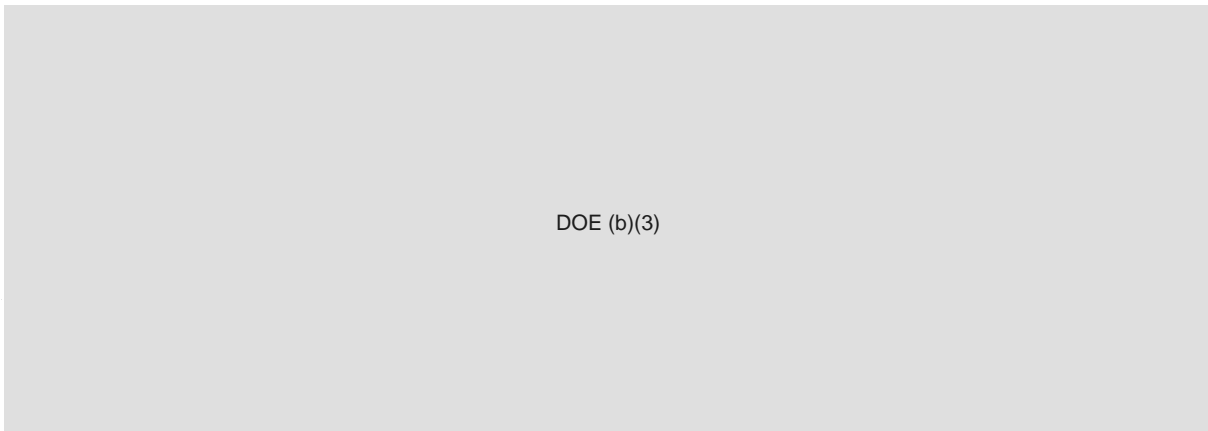
DOE (b)(3)

DOE (b)(3)

6.4.1 Optical depth analysis
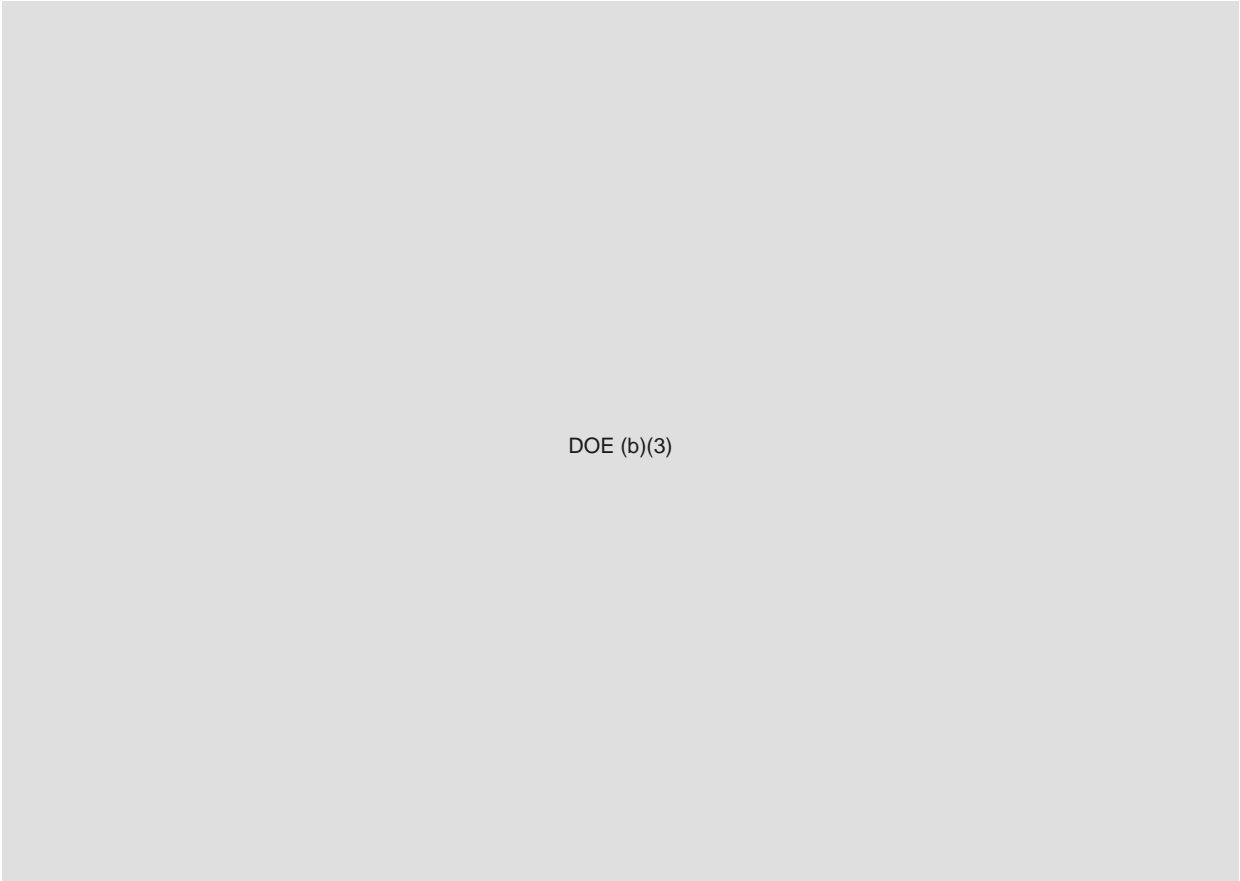
DOE (b)(3)

DOE (b)(3)
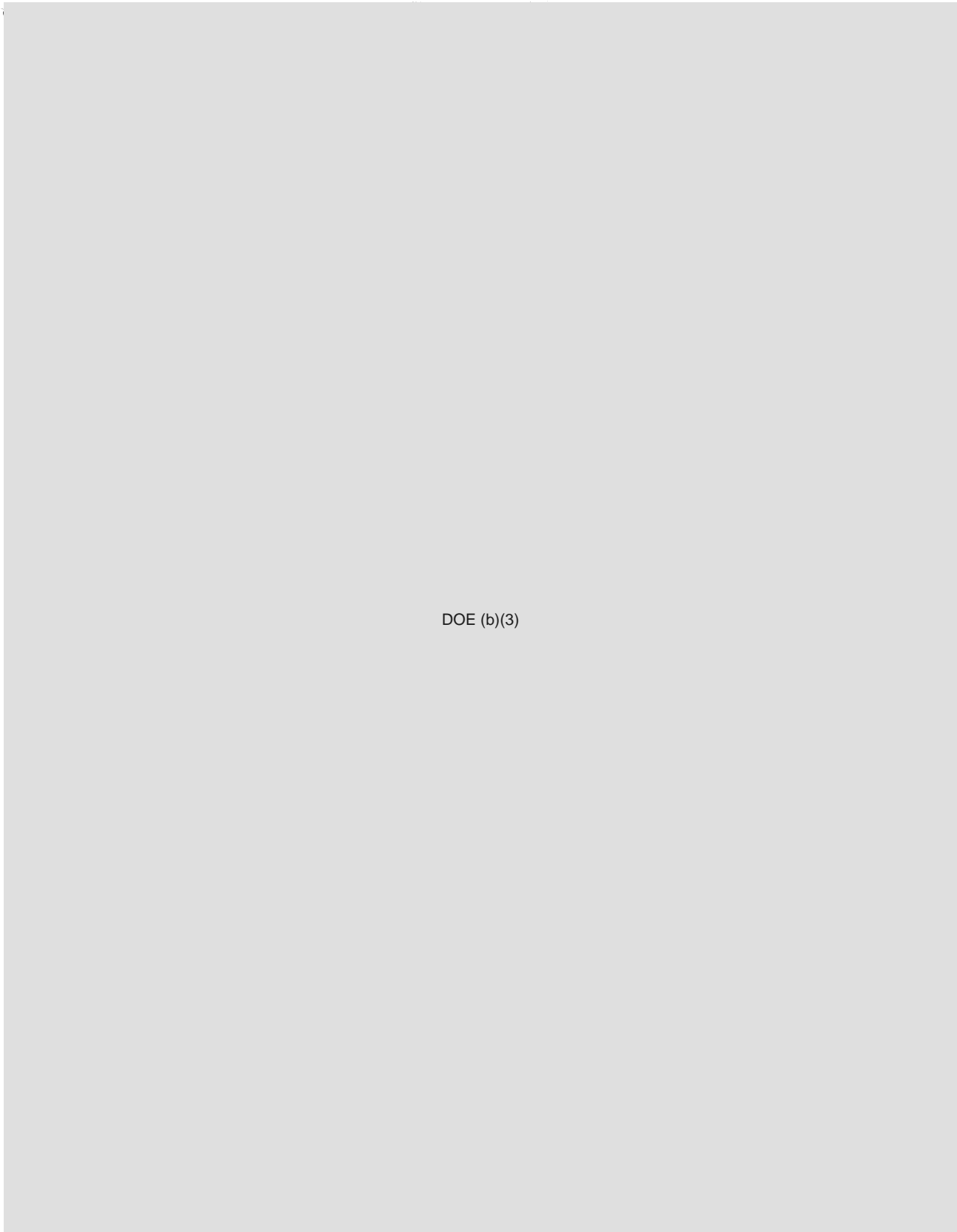
DOE (b)(3)

6.4.2 Asay windows

An Asay window is simply a transparent Asay plate that can be used in conjunction with VISAR or PDV in experiments for shock-generated ejecta, and can furnish valuable constraints on the total ejecta. They have been used at the labs and other sites for some years [67]. Materials for Asay windows include LiF and polymethyl methacrylate (PMMA), otherwise known as plexiglass. LiF remains transparent at shock pressures of order of 1-2 Mbar, while PMMA loses transparency at a few hundred kbar. However, LiF, which is crystalline, tends to crumble under stress, which can cause it to become opaque at lower pressures. Either material is useful for pressures associated with high-explosive-driven shocks. In principle, it is possible to analyze the ejecta momentum distribution from the velocity-time history of the Asay window, but there is not enough information to deconvolve the separate mass and velocity distributions. Combining Asay window information with PDV diagnostics can be a powerful tool.

6.5 Additional Diagnostics

6.5.1 Pyrometry

The free surface of a shocked and unloaded plate or shell is at essentially zero pressure because the extreme acoustic mismatch between gas and solid implies an almost free surface boundary condition The temperature of this free surface may be determined pyrometrically if its emissivity is known. Such a temperature measurement is useful because it provides an independent check on the equation of state and on entropy

generation by irreversible processes other than the shock. The free surface of an imploding incomplete shell is accessible to pyrometry from inside; pyrometry need not be limited to flat plate or coupon experiments. Pyrometric sensors can be placed on a pin dome along with VISAR or PDV.

DOE (b)(3)

DOE (b)(3)

DOE b(5)

One consequence is that the surface temperature is sensitive to additional irreversible processes. Another consequence is that nearly all the emitted thermal radiation is infrared. A briefer pointed out to us that emission by a small quantity of hotter ejecta, as has been observed, would mask thermal emission in visible and near-infrared light (such as that detectable by Si photodiodes, which are sensitive only for $\lambda < 0.8\,\mu$m, or InGaAs, sensitive for $\lambda < 1.8\,\mu$m). For both reasons it would be necessary to perform pyrometry at longer infrared wavelengths. In the Rayleigh-Jeans portion of the black body spectrum ($\lambda > h/k_B T$) the emission is proportional only to the first power of the temperature, so that radiation from a small solid angle filled by hotter ejecta would not overwhelm the emission from the surface. In addition, at long wavelengths the emissivity of small particles (with radii $a < \lambda/2\pi$) is also low, whatever their material properties.

At a nominal surface temperature of 1000 K the peak of the black body spectrum is at a wavelength of about $3\,\mu$m. To minimize the masking by hotter ejecta and because we may need to measure even lower temperatures it is desirable to observe at yet longer wavelengths. Fortunately, HgCdTe detectors are fabricated with long-wave cutoffs of $5\,\mu$ or $10\,\mu$m (these particular values are chosen to take advantage of atmospheric transparency windows, but also serve our purposes). These detectors

have response times of 10–100 ns, far faster than is typically needed. If necessary, thermoelectric or liquid nitrogen cooling can be provided within a pin dome, provided the experiment is done in dry air or gas to avoid condensation of ice on the detectors or if all exposed surfaces are kept warm. This is a problem faced by all users of cooled detectors, and is solved routinely. Fortunately, our sources of infrared radiation are strong, filling detectors' fields of view, and neither great sensitivity nor great accuracy are required.

6.5.2 Mouse-holes

"Pin domes", consisting of an array of sensors mounted on radial "pins" or their optical equivalents, placed at the center of an implosion system, are used to measure the symmetry and rate of implosion. These pin domes are necessarily mounted on a column that carries the wires that transmit the measured signals (or optical fibers performing the same function, or radiation to be measured for pyrometry as described in Section 6.5.1 of this report). This column penetrates the implosion system through an aperture colloquially known as the "mouse-hole". The pin dome column and the gaps in the high explosive and in the imploding shell that accommodate them disturb the implosion.

The source of hydrodynamic disturbance is at the mouse-hole, where the supporting column is in contact with the implosion system. Some of this disturbance is local (in angle). Here we argue that it is unlikely to propagate around the imploding shell.

DOE (b)(3)

DOE b(3)

DOE (b)(3)

It is natural to ask if there is evidence for such propagating disturbances in the "loser" plots that compare the calculated and measured pit motion as determined from pin impacts or VISAR. We think this unlikely for several reasons:

1. The possible radial displacements of such a propagating wave must be a very small fraction of the shell thickness if the shell is to remain in the elastic regime. This would not be true for a thin sheet, in which small material strains lead to large displacements, but it is true for a shell (accounting for their stiffness), for which the fractional displacement is of order the local dimensionless strain.

2. The Poisson ratio of Be, the thickest component of such an implosion system, is 0.032. Hence any propagating longitudinal wave produces very little transverse displacement of the surface, and would have very little effect on the measured motion of the inner Pu surface.

3. In a material beyond its elastic limit and undergoing plastic flow, the forces of strength oppose all strains. These shells undergo rapid plastic flow. In simple models of plastic flow the elastic response depends on the strain rate, not on the strain. Under such conditions there are no propagating waves; all disturbances are exponentially damped with a purely imaginary velocity of propagation. We cannot be sure that there is no additional elastic response in these materials undergoing plastic flow, but there is no reason to expect or evidence for it.

6.5.3 Neutronics diagnostics

Subcritical, surrogate and scaled experiments cannot, by definition, become critical. Despite this, it may be possible to perform experiments that test our ability to calculate neutronics. The calculation of neutronics requires the identification of nuclear properties (neutron scattering and absorption cross-sections) of the materials

involved, the ability to calculate the material configuration (determined by the hydrodynamics and the equations of state of the materials involved), and the ability to calculate neutron transport

All of these are tested by a neutronics experiment. None of them need require a configuration resembling a weapon, scaled in size or with surrogate materials. Testing our ability to calculate some other configuration also tests some of the tools needed to calculate a weapon. Testing our knowledge of the nuclear properties of some material requires using that material. Testing our understanding of its hydrodynamic properties can be done with isotopic surrogates. Testing our ability to calculate neutron transport can be done with any material and in a broad range of configurations.

The first requirement for a neutronics experiment is a source of neutrons.

DOE (b)(3)

We consider three possible sources:

Hedgehogs – Sources that use an α-emitting radioactive isotope, typically ^{210}Po, and the low-threshold reaction $^9\text{Be}(\alpha,\text{n})^8\text{Be}$ DOE (b)(3)

DOE (b)(3)

DOE (b)(3) The required α source is formidable, and the neutron production inadequate for obtaining significant data, allowing for the finite solid angle coverage of neutron detectors (1 sterad is a likely upper bound), loss in a subcritical or (for most surrogate materials) entirely non-fissile assembly. The neutron source would continue to emit following initiation,

131

probably making it impossible to distinguish propagated neutrons from the continuing source.

DOE (b)(3)

DOE (b)(3)

DOE (b)(3) This latter factor would be larger in a nearly-critical assembly, and smaller in an assembly of non-fissionable (non-actinide) surrogate material.

DOE (b)(3)

Zippers are small electrostatic accelerators, used to initiate weapons and in oil well logging, generally producing 14.1 MeV neutrons by the $D(T,n)\alpha$ reaction. They must be placed outside the hydrodynamic experiment. Timing is at the choice of the experimenter, and it is possible to provide a number of pulses at suitable times, either by repeatedly firing one accelerator or by using several. The time of interest (usually that of central convergence) must be known in advance from hydrodynamic calculation; this has been done successfully for weapons for several decades and is not at issue. Neutron yields may be as large as 10^{10}.

Plasma Focus a company called Del Mar Ventures advertises its model ING-103 plasma focus neutron generator producing pulses of 10^{10} neutrons in a pulse width of 10–15 ns. Plasma focus machines, some with much larger neutron

output, are potential candidate external sources for neutronics experiments. Only a fraction of these neutrons will enter the experimental assembly, and many of those will be reflected from its outer layers.

Both zipper and plasma focus sources would be external, making reflection by the environment a particular problem; unless the experiment is separated from major external masses it may be difficult to distinguish neutrons propagated in the experimental assembly from those externally scattered. Measurement of neutron energy may help; neutrons elastically scattered by heavy surrogate or fissile material will not be significantly moderated, while those scattered by lighter environmental nuclei will be. Unfortunately, scintillators provide only a very crude indication of neutron energy (because the deposited energy depends on scattering angle), and time of flight measurements convolve the energy distribution with spatial transport. A particular advantage of these external neutron sources is that they would not require insertion into the experimental assembly of a neutron generator that would not be present in a modern weapon.

It was pointed out to us by R. Hanrahan that if an experiment is being diagnosed by proton radiography, spallation reactions are a source of neutrons within the experimental assembly. The beam current at LANSCE is about 1 mA at 800 MeV, or 6×10^{15} protons/s. Each proton would produce $\mathcal{O}(30)$ neutrons by (p,n) reactions before stopping. These neutrons have a very broad distribution of energies; a few have hundreds of MeV, but most have energies roughly comparable to nucleonic binding energies lesssim 10 MeV. Of course, there would be no proton radiography were they to stop in the target, so we assume 10 neutrons per proton in a thick target. In an effective beam integration time of $1\,\mu$s, $\mathcal{O}(6 \times 10^{10})$ neutrons may be produced. The beam stop is a source of neutron background, but if it is spatially removed from the target its contribution to detectors near the target will be geometrically reduced to low levels. Spallation neutrons are produced throughout the target volume, and their source distribution can be obtained from a calculation of the proton transport. LANSCE is the source of neutrons for the Lujan Neutron Scattering Center, so these

133

processes have been studied and are likely to be well understood. For experiments diagnosed by proton radiography, spallation neutrons are likely the best neutron source. Their presence cannot be avoided.

A second requirement of a neutronics experiment is a fast neutron detector. It is necessary to discriminate on the basis of arrival time against neutrons reflected from the environment or arriving late after moderation. Plastic scintillators, available in large sizes at low cost, meet this requirement.

6.6 Findings and Recommendations: Diagnostics for sub-scale experiments

6.6.1 Findings

1. Modest modifications of Cygnus will make possible meaningful radiographic images, although not with the quality of systems like DARHT. Despite the lower photon energy of 2.25 MeV, Cygnus can provide quite a respectable image of a half-scale object. Additional calibration of the detector, optics, and imaging systems needs to be done to make this approach quantitative and useful.

2. Approaches considered by the laboratories constitute impressive applications of modern radiographic technology. Deployment of any of these would improve upon the current capabilities at Cygnus and would provide higher quality imaging of the cavity formed in a subscale experiment. But it is not possible given the information presented to date to make a clear choice among the various ideas. We were not presented with sufficient analyses of the subscale experiments that provide actual requirements for radiography. In turn such requirements are connected to the goals of the experiment.

3. The areal densities of scaled experiments are proportional to the scaling factor. This is beneficial for penetrating radiography but it also has to be taken into account that the feature size is scaled as well so that the resolving scale of

2. Given the importance and challenge of diagnosing properties of the implosion in the subscale experiments, additional diagnostics such as those suggested in this section should be considered.

7 STRATEGIC PLAN

Maintaining a safe and secure nuclear deterrent in the absence of nuclear underground testing as described in the 2010 Nuclear Posture Review (NPR) must rely on a robust experimental program consisting facilities and techniques that cover a range of scales. As described above, filling gaps in our knowledge of nuclear weapons performance requires these experiments. The 2007 Dynamic Plutonium Experiments (DPE) program is a proposed multi-laboratory effort of experiments that need to be performed for the Stockpile Stewardship Program [5]. This plan, representing the consensus view of scientific experts at the relevant laboratories, is fine as far as it goes. However, it has two limitations that need to be addressed as soon as possible.

First, the program is about three years behind schedule for a variety of reasons, many of which are not technical (*e.g.*, the result of unexpected scientific findings). The plan is thus less effective than its strong technical basis would warrant, suggesting that the description of experiments to be performed ought to be augmented with a realistic implementation strategy that includes contingencies in case of delay due to non-technical factors. That is, the plan should not only describe a succession of experiments, with each new experiment leveraging off of previous results (from experiment, theory and simulation), but should also identify the preferred path forward in case of delays that might be anticipated (evolving regulatory requirements) or not (*e.g.*, accidents).

Second, the plan is less strategic than it could be, in that it does not include (or refer to) a national plan for sustaining major facilities required for the experimental program. We elaborate on this issue in the following paragraphs.

7.1 Experimental Facilities

The facilities required for the experimental program range from small-scale (*e.g.*, diamond-anvil cells) to large and expensive: synchrotrons; DARHT, U1a and other hydrodynamic capabilities; Z and other pulsed-power systems; NIF, Omega and other lasers; gas-gun and other impact facilities. The large facilities are not only expensive to build or modify, but are also expensive to use.

There is a need for a plan that describes what facilities are required in the U.S., both on technical and programmatic grounds, and how these facilities - including their operation - will realistically be sustained (i.e., maintained with at least the critical level of funding and expertise). For example, the Stockpile Stewardship Program needs experimental access to certain conditions (P, T, strain rates, etc.). These are technical considerations that should help to prioritize the need for various facilities. At the same time, there are programmatic considerations that should also be taken into account. For example, is it essential for the US to have gas-gun facilities for shock-wave experiments, not only to collect data but also to attract and train students? If so, how many facilities, and where should they be located (academia, national laboratories, some combination?). What priorities should be associated with large facilities that are primarily for weapons-related experiments (e.g., DARHT, U1a), as distinct from facilities also useful for basic research (third and fourth-generation synchrotron radiation sources, Z and NIF)?

The current array of facilities is a consequence of historical initiatives, and not the result of national-level planning. It is therefore not optimized, perhaps not entirely rational, and likely not sustainable. Both the technical needs for the next decade's experiments (*e.g.*, 2007 DPE plan) and programmatic needs must be taken into account (maintaining both scientific and specialized capabilities; supporting collaborations between the labs and academia, both for maintaining excellence and for purposes of recruiting).

Our perception is that some of the facilities have excellent researchers funded at sub-critical levels, and other facilities are less-immediately useful than others. This means either that there can be enhanced efficiencies and cost savings, or that the rationales for some of the facilities have not been well articulated. In either case, sustainability is at risk. More often than not, people advocate for facilities at their own laboratories, rather than on the basis of what is needed with highest priority for stockpile stewardship and the national capability on which it depends.

Our concern is heightened by the expectation that budgets will remain tight - or become tighter - over coming years, suggesting that some tough decisions will have to be made about shutting down some facilities in order to make sure that other activities can be adequately sustained. Technical and programmatic prioritization is therefore essential in formulating a strategic, national plan for DPE-related experimental facilities. As such, we applaud the efforts of NNSA to drive the laboratories to prioritize their facilities plans to support weapons science programs. This complex-wide experimental facilities plan should include both near-term facilities needs as well as longer term (decadal) plans.

7.2   Maintaining Expertise

The success of stockpile stewardship depends on maintaining technical expertise; without the necessary expertise, no amount of funding or facilities can ensure the safety, security and reliability of the U.S. nuclear-weapon stockpile.

Two related, but distinct kinds of expertise must be maintained: i) scientific expertise, by which we mean a strong foundation in the fields of science, engineering and technology underlying the laboratories' missions, and ii) specialized expertise directed toward nuclear weapons. The latter includes deep understanding of topics such as nuclear-weapon design, properties of the relevant materials, how to measure those properties, and how to safely and securely handle those materials. Maintaining

this specialized expertise is a programmatic requirement for the laboratories, and for NNSA more generally. This is a difficult task because the topics are arcane and intellectually challenging, yet the information needs to be protected (these are not topics taught in universities, nor should they be). Fundamental, focused and integral experiments, along with simulation (by which we mean simulation of weapon configurations and processes), are necessary for maintaining specialized expertise.

Scientific expertise is also essential, because it provides the foundation on which the specialized knowledge can be developed. Scientific expertise can be maintained through unclassified research that can also provide the basis for collaborations with universities and others in the scientific community, including foreign colleagues. There are many advantages to such collaborations with the scientific community at large, ranging from keeping laboratory scientists working at the state of the art of their specialties to recruitment opportunities.

A question is balancing how much is enough for stewardship of the stockpile versus promoting scientists to pursue challenges and establish rewards for excellence for work in discovery and thereby furthering knowledge ultimately relevant to weapons performance. JASON suggests reformulating or reassessing the Science Campaign structure in order to enhance fundamental science while at the same time maintaining essential stewardship of nuclear weapons. Scientists need this as an incentive. This would entail an extended dialogue among those involved in the relevant Science Campaigns at the three laboratories and their counterparts at NNSA to identify the issues and formulate the proper balance.

7.3 Foundational Science in Stockpile Stewardship

JASON studies performed over the past decade on diverse aspects of stockpile stewardship have documented the fact that NNSA's programs have succeeded in maintaining the safety and effectiveness of the nation's nuclear weapons deterrent without the

need for new underground explosive nuclear testing. Based on legacy information, designs, and experience, and new tools and methods developed during the first 20 years of stockpile stewardship, future life extension programs are confidently expected to maintain for the foreseeable future the safety and effectiveness of the stockpile under US policy described in the 2010 NPR.

The 2011 JASON study is tasked to examine the experimental programs supporting stockpile stewardship. An emergent theme is the importance of what we term "foundational science" to the future of stockpile stewardship. Our present focus on foundational science should not imply that there is some technical problem in today's stockpile or in our long-standing confidence in today's science-based approach to stockpile stewardship. Rather, it is our sense that the successes gained by the first generation of post-cold-war stockpile stewards point to new opportunities to evolve stockpile stewardship to be more responsive to possible technical surprise and policy change, while facing up to plausible future technology and funding trends.

The nuclear weapons laboratories identify their experimental goals in terms of "fundamental", "focused", and "integral" experiments, described in detail in the present study report. Data are collected in these experiments to better specify relevant "sub-grid" physics processes employed in simulations of weapons behavior and performance. Theoretical advances in adapting known physics to the conditions encountered in nuclear explosions illuminate the validity limits of nuclear weapons models. Knowing and staying within the limits of validity of our knowledge of nuclear weapons physics is central to estimating performance margins and their associated uncertainties, the key metrics of stockpile stewardship.

New experimental tools, such as DARHT and NIF at the largest scales and others at smaller scales, were built in large part to serve stockpile stewardship and are now coming on line. These new facilities, coupled with the emphasis on fundamental and focused data emerging from experience with stewardship needs, constitute what we feel is an elevation of the role of experiments from validation of computer models to full

scientific partnership along with theory and simulation in what we call foundational science. The weapons community has a similar vision, which they term "predictive capability." Under either rubric, we see potential advantages for considering now the inclusion of such a thrust in stockpile stewardship under appropriate conditions.

The main argument for inclusion of a foundational science component in the stockpile stewardship program is to provide broader scientific knowledge in anticipation of changes of requirements that will affect the stockpile. Such changes could be: a) technical surprises that might be revealed in weapons surveillance or life-extension programs, or b) policy changes requiring departures of designs from well-tested legacy models. Should the world sometime agree to eliminate nuclear weapons stockpiles, this kind of foundational program would certainly be retained as a hedge against future threats.

We feel that the substantial scientific goals of a foundational science program will draw excellent technical people to the weapons program while also permitting them to build their scientific reputations in the larger, unclassified scientific community. There are good examples of this "dual-life" approach working well now at the weapons labs.

For a new foundational weapons science program to be accepted by the government, it must demonstrate that it can perform the present mission of stockpile stewardship while providing its benefits of future flexibility at minimal or no additional cost. The details of what should constitute a foundational science program for future stockpile stewardship needs, supported under NNSA, must be developed and prioritized by cognizant technical people working in stockpile stewardship in partnership with laboratory leadership and government officials.

7.4 Findings and Recommendations: Strategic Plan

7.4.1 Findings

1. Technical and programmatic prioritization is essential in formulating a strategic plan for experimental facilities for the hydrodynamic and nuclear experiments program. This complex-wide experimental facilities plan should include large scale facilities to smaller scale support laboratories and both near-term facilities needs as well as longer term (decadal) plans. This prioritization is an important opportunity to define future needs for Stockpile Stewardship as a whole.

2. Both scientific expertise, with a strong foundation in the fields of science, engineering and technology underlying the laboratories' missions, as well as specialized expertise directed toward nuclear weapons should be maintained. Reformulating or reassessing the Science Campaign structure may enhance fundamental science while at the same time maintaining essential stewardship of nuclear weapons. The three laboratories and NNSA should identify the issues and formulate the proper balance.

3. The substantial scientific goals of a foundational science program will draw excellent technical people to the weapons program while also permitting them to build their scientific reputations in the larger, unclassified scientific community. The details of what should constitute a foundational science program for future stockpile stewardship needs, supported under NNSA, must be developed and prioritized by cognizant technical people working in stockpile stewardship in partnership with laboratory leadership and government officials.

7.4.2 Recommendations

1. The laboratories, working with NNSA, should update the 2007 DPE program plan, and augment it by including 1) an implementation strategy and 2) a sustainable facilities plan (including future facilities, or evolution of existing fa-

cilities) that takes both technical and programmatic considerations into account in its prioritization.

2. The laboratories, again working with NNSA, should develop a coherent program that strengthens the foundational science in support of the weapons program. This can be clone by re-examining the campaign structure NNSA in the context of modern national security needs. A strengthened science base will enable the weapons program to adapt to new challenges that may arise in the future, whether due to technical surprise or policy changes.

References
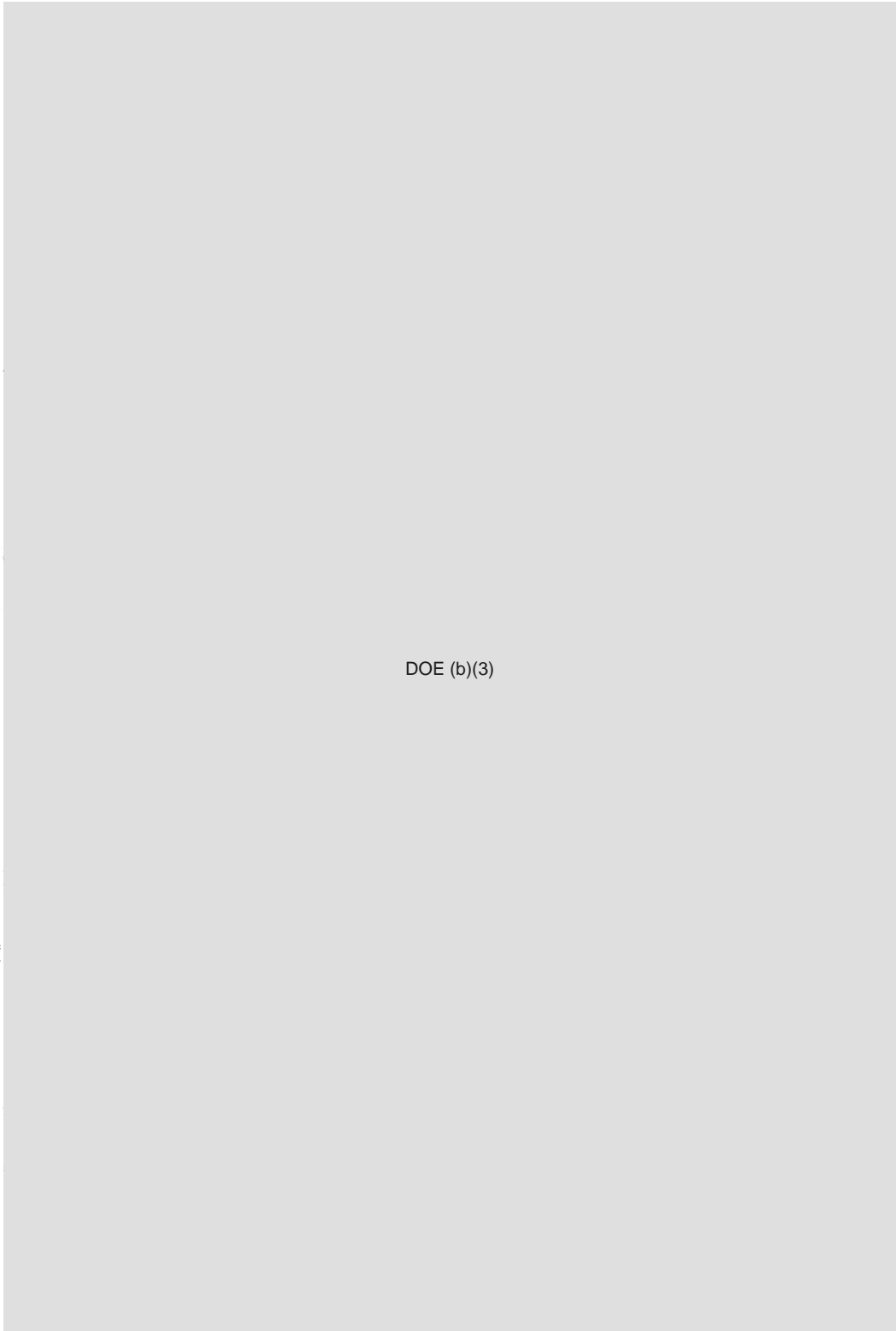
DOE (b)(3)

DOE b(3)

DOE b(3)
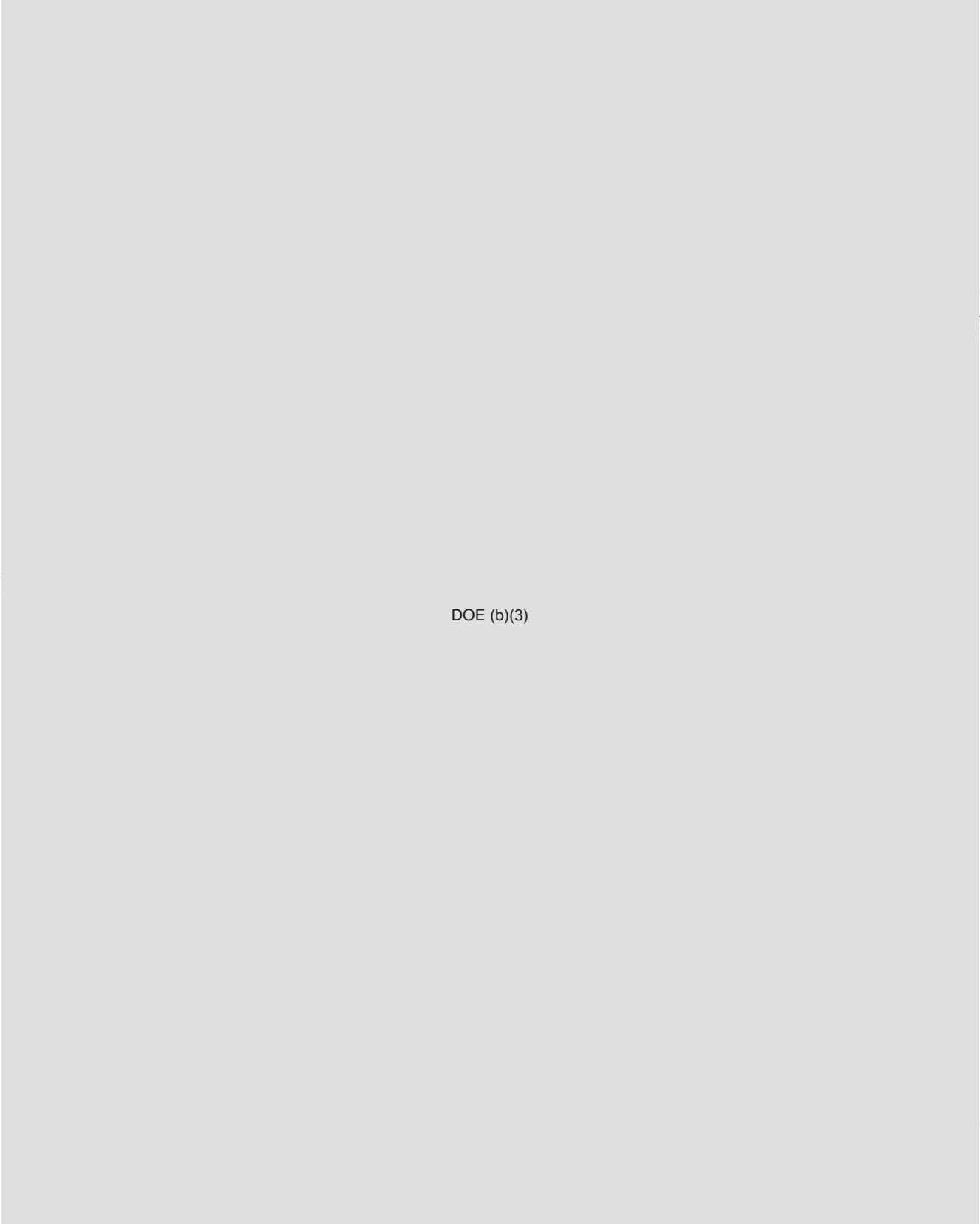
DOE (b)(3)

DOE (b)(3)

DOE (b)(3)

A UNCERTAINTY QUANTIFICATION

A.1 Image Quantification

A main purpose of this study is to help the laboratories make quantitative comparisons of the value of fundamental, focused, and integral (including scaled) experiments, in order to generate a balanced program of experiments and supporting simulations. We start from the premise that any experiment must have quantifiable value beyond what comes from the data from the specific experiment, allowing for comparison with other proposed experiments. We concentrate on the problems of image quantification (IQ) of radiographs in experiments such as core punches, discussing some of the methods that could be used for quantification, and on the difficulties of quantification that we encounter. We do not pretend to know the answers to the questions we raise, but do suggest some promising lines of investigation. Some good ideas from the laboratories will go a long way toward resolving difficult device physics problems.

Core punches and other experiments produce radiographic images that can be quantified in order to compare with simulated radiographs. Often, however, qualitative judgment ("eyeballing") is the basi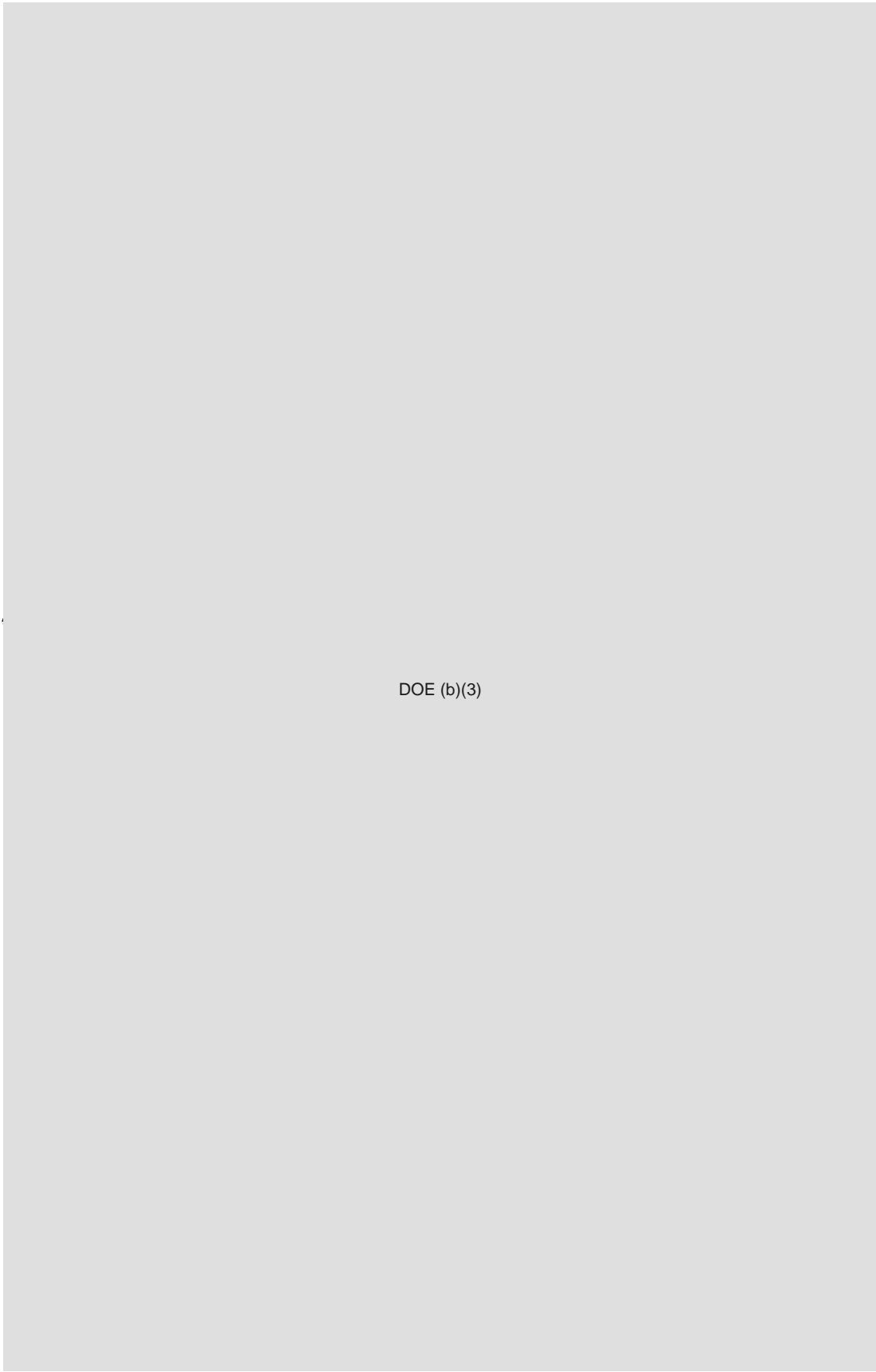s for comparison. Such image quantification (IQ) that is done typically compares surface to volume ratios of a gas cavity, areas inside contours, or makes polynomial expansions of contours and compares coefficients in the expansion, with only qualitative understanding of what differences in underlying physics models are responsible for the image differences. These are useful enough, but IQ would be vastly improved if there were ways to quantify the physics differences. Although flash radiographic images from facilities such as DARHT provide evaluations of implosions that go as far as possible for a non-nuclear experiment in mimicking a real device, these two-dimensional radiographs cannot furnish a complete set of three-dimensional initial conditions for boost (unless certain symmetries are hypothesized). But their data, much as assimilated data in weather forecasting, can give quantitative constraints on the simulations. Aside from its intrinsic value

as a constraint on simulations, physics-based radiographic IQ should be useful aids in understanding the values of, and the balance among, core punches and fundamental/focused experiments.

Other experiments, usually in the fundamental or focused category, produce nonimaging data that are much more readily quantifiable: equations of state (EOS), strength data, and the like. The procedures for quantifying non-image data are straightforward, and we will not comment on them. Our concern is how to do IQ that obeys several criteria:

1. IQ leads to a quantitative understanding of how close an experimental radiograph and a simulated radiograph are. "Close" does not necessarily mean that obvious image features, such as contours, are close to each other, but that the two images represent situations that are close in some broader measure of performance.

2. Such broader measures of performance will depend on a great deal of coupled physics, so the IQ methodology should be informed, as far as possible, by the physical processes leading to the image.

3. It is often the case that the physics of interest has some aleatory component, such that nearly-identical initial conditions and physics models may lead to imaged features in simulations that are quite different from one realization to the next and also different from a specific experimental realization. Yet such differences may mean very little to device performance. So IQ must be able to recognize and deal with these aleatory features.

A.2 Physics-Informed Image Quantification

There are many tools for image quantification (IQ). But IQ by itself is of limited value. One can quantify the contours and colors of a flower without knowing much about

the flower, either before or after the IQ. In Section A.3 we review a methodology already presented in the JASON RRW report [68], for helping to quantify how close to each other so-called "nearest neighbors" devices really are. This nearest-neighbor methodology can also be useful in deciding how close a simulated radiograph based on a device simulation is to an actual radiograph from, for example, DARHT, or how close two simulations based on different codes and physics models really are. An equally important issue is to quantify either the simulated or the actual radiograph in a way that is informed by the physics of the problem.

IQ for a primary implosion is hard, because many processes are aleatory and not reproducible from shot to shot. Even if the implosion physics and initial conditions are precisely captured in a simulation, the simulated radiograph may not have precisely (within knowable errors) the same features as, for example, the gas cavity found in a core punch. DOE (b)(3)

DOE (b)(3) It might be possible to understand purely empirically which descriptors really matter, but it would be much better to have a physics-based understanding of why one descriptor matters and another does not.

DOE (b)(3)
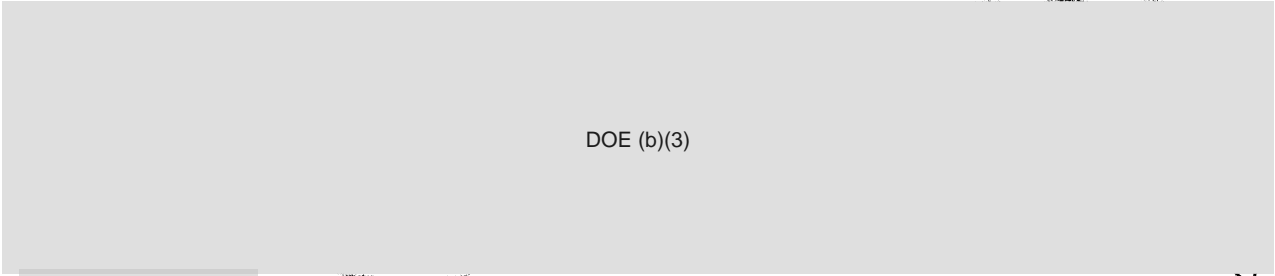
DOE (b)(3)

DOE (b)(3)   Sub-scale experiments using plutonium further reduce the attainable scaled resolution.

The IQ problem is not just to make quantitative comparisons of experimental radiographs with simulated radiographs, because unless such comparisons are informed by physics, aleatory image features will stand in the way. Physics-based comparison of multiple simulations is important, to find image metrics that are correlated to primary performance. Here are a couple of examples.

1. Some radiographic and PDV data from small-scale Pu coupon experiments are available on spall and ejecta at scales down to the μm level. Simulations at this scale can only be done for small coupons, so there is a good fit. DARHT core-punch radiographs could show some spall and ejecta data at spatial scales down to about 100 μm for comparison with full pit simulations at these scales. In either case it is meaningless to compare the mere quantification of images, which will be, as images, dominated by features (bubbles, spikes, blobs of ejecta) that are statistical in nature. These statistical features can be introduced as elements of the output vector space x and then quantitatively compared, using the afore-mentioned nearest-neighbor technology.

2. Another feature lending itself to a statistical rather than deterministic interpretation is the Hausdorff dimension (or possibly dimensions) that characterize a fractal gas cavity over a fairly wide range of spatial scales, assuming that the dynamical range of both experiment and simulation permits definition of the Hausdorff dimension. There are standard image-analysis techniques for finding a Hausdorff dimension, which (for a curvilinear contour) relates the number of

circles of a given size needed to cover the contour to the size of the circles.

In both of these cases the physics that should inform the IQ is the physics of Rayleigh-Taylor and Richtmeyer-Meshkov instabilities at the gas cavity/pit interface. Because of unavoidable variations in small pit surface irregularities, or the way spall has come off the pit, or many other small perturbations, such instabilities, simulated many times, may yield an ensemble of images of bubbles, spikes, and other phenomena no two of which much resemble each other or any specific radiograph. Yet there are metrics that change but little over the ensemble of images and that govern the outcome of the boost process. DOE (b)(3) DOE (b)(3) The physics problem is to discover these "extensive" variables and their influence on boost through multiple simulations; the IQ problem is to quantify these variables in radiographs.

A.3 Nearest-Neighbor Radiographs

In an earlier report [68], we discussed the so-called nearest-neighbor problem, which is to quantify the difference between two similar but not identical objects. We summarize it briefly here in the context of comparing a core punch radiograph and a simulation. For the sake of brevity, we simplify the problem to one of multi-variate Gaussians, but this is by no means essential. The end result is a metric, or cost function, that takes into account the uncertainties of the experimental data (the radiographic input), of the output of the simulation and its physics models, with a weighting that recognizes the sensitivities of various outputs to inputs. In principle, the nearest-neighbor metric can incorporate all known device physics. In practice, the physics-based IQ problem has to be reduced to a consideration of the most sensitive output variables.

The laboratories have IQ tools that might augment the nearest-neighbor algorithm. During the Summer Study we were briefed on a LANL effort for modeling

radiographs, called the Bayes Inference Engine (BIE) that is used to make simple forward models of various objects based on one or more 2D radiographic images; we have no information on corresponding efforts at other laboratories. One goal of the BIE is to infer physical information (3D density, for example) about the object with forward modeling, and to provide a quantitative framework for error analysis. Another, so far not yet fully realized, is as a tool for quantifying images in terms of useful geometric or physical features for comparison with other images. BIE-like algorithms may prove useful in analyzing this nearest-neighbor problem, but we are not arguing for use of the BIE to provide, via forward modeling, the experimental "radiograph" to be compared to a simulated one. Since the image or set of images is far from tomographically complete, only a limited amount of accuracy is possible in principle. The appropriate venue for forward modeling is the computer doing the simulation, which yields a simulated radiograph for comparison. BIE technology might prove useful in data assimilation, in which a computer simulation is governed not just by a zero-time set of initial conditions, but is updated from time to time with experimental radiographic information coming from, for example, multiple DARHT shots. We discuss data assimilation in a separate section.

There are uncertainties in extracting the radiograph from the radiographic data, involving noise, unknown offsets of experimental equipment and the like, and these uncertainties are readily quantified, leading for a single radiograph to a probability distribution function (PDF) $r(x)$ for the variables x describing the final radiograph. Here the dimension of the x-space is of order of the number of pixels in the radiograph. The operations taking the raw radiographic PDF $s(z)$ to $r(x)$ have the form

$$r(x) = \int (\mathrm{d}z) O(x|z) s(z) + \text{noise} \tag{23}$$

where $O(x|z)$ is a conditional PDF for an output radiograph described by x, given raw data described by z. We will not discuss the treatment of additive noise here, and so omit further reference to it. The question now is how to compare this radiograph *quantitatively* to a simulated radiograph resulting from computer codes.

A.4   Quantitative Comparison of Nearness

In the original context, formulas were given for comparing two sets of input (engineering and manufacturing) data and PDFs after processing by a single computer code. In the present context, there is processing for the experimental radiograph, as described in Equation (23), and processing for the computer simulation as described in Equation (24) below that will have very different quantitative properties. For simplicity we assume that all processes are Gaussian, but this is no real limitation; non-Gaussian processes must be integrated numerically while Gaussian processes lead to analytic forms that are useful for exposition.

Let x be a vector of dimension $dim(x)$ that describes the physical object and its modeled evolution out to a particular time. For short we call the vector x the *output*, and for comparison to the radiograph we restrict x to the same space as introduced in Section A.3. Let y, a vector of dimensions $dim(y)$, be a vector that comprises all the engineering and manufacturing data available for the initial description of the object, or the *input*. It will usually be true that $dim(x) > dim(y)$; for example, a two-dimensional radiograph has megabytes of information, greater than the engineering data. The data are described by a PDF $p(y)$, carrying the information about uncertainties in the engineering data. There is also a complicated PDF $P(x|y)$ that transforms the input into the output; if there were no errors and uncertainties in the code that produces output from input, there would be no probability distribution, but a deterministic transformation. Finally, let $q(x)$ be the probability distribution of the output, given by

$$q(x) = \int (\mathrm{d}y) P(x|y) p(y). \tag{24}$$

Normalization of the probability $q(x)$ requires that

$$\int (\mathrm{d}x) P(x|y) = 1. \tag{25}$$

Only for the sake of discussion, we use probability distributions $P(x|y), p(y)$ that

are generalized Gaussians:

$$P(x|y) = \mathcal{N} \exp[-\frac{1}{2}(x - f(y)) \cdot M \cdot (x - f(y))],$$

$$p(y) = \mathcal{N} \exp[-\frac{1}{2}(y - \bar{y}) \cdot N \cdot (y - \bar{y})]. \tag{26}$$

The dots indicate summation over the vectorial indices; $\mathcal{N}$ stands generically for unimportant normalization constants. The mean relation between input and output (response surface) is the set of equations $x = f(y)$. By using the conditional probability distribution $P(x|y)$ we broaden this response surface. First-order sensitivities K are given by the matrix of derivatives

$$K = \frac{\partial f}{\partial y}\Big|_{y=\bar{y}}. \tag{27}$$

If the matrix $M_{\alpha\beta}$ and the response surface depend generically on the input variables y_i a complete analysis is not possible. Reduction of the model to tractable Gaussians requires that the matrices M and N be constants and that the response surface is locally linear:

$$f(y) = \bar{x} + K \cdot (y - \bar{y}) \tag{28}$$

where $\bar{x}_\alpha = f_\alpha(y_i = \bar{y}_i)$. Without loss of generality we can translate x, y so that $\bar{x}, \bar{y} = 0$.

By integration, and by doing some not quite straightforward analysis, one computes

$$q(x) = \mathcal{N} \exp[-\frac{1}{2}x \cdot R \cdot x] \tag{29}$$

where, in matrix form,

$$R = M - MKL^{-1}K^T M$$

$$L = N + K^T MK \tag{30}$$

and the superscript T stands for transpose.

Finally, a metric (equivalent to a cost function) was proposed for comparing possible near neighbors, in terms of a dimensionless "distance" in device space between

two devices, labeled k and l, given by

$$\ell_{kl}^2 \equiv [\bar{x}^k - \bar{x}^l]\Sigma^{-1}[\bar{x}^k - \bar{x}^l] \tag{31}$$

where now we restore the previously-suppressed output mean values indicated by overbars, and

$$\Sigma = R^{-1} = M^{-1} + KN^{-1}K^T. \tag{32}$$

Note that Σ has contributions from model uncertainties and sensitivities as well as input uncertainties.

This comparison applies when only the input data means differ, but M, N, and K are the same. When they differ it is appropriate to use the Bhattacharyya distance as the metric:

$$\ell_{kl}^2 \equiv [\bar{x}^k - \bar{x}^l] \cdot [\frac{\Sigma_k + \Sigma_l}{2}]^{-1} \cdot [\bar{x}^k - \bar{x}^l] + \frac{1}{2}\left[\ln[\frac{\Sigma_k + \Sigma_l}{2}] - \frac{1}{2}\ln\det\Sigma_k\Sigma_l\right]. \tag{33}$$

Note that this is not the BIE metric (cost function), which is simply the mean-square differences of experimental and forward-modeled radiograph data. Nor is it a standard χ^2 metric that weights the mean-square difference with experimental variances; the cost function is based on weighting the uncertainties in the experiment and in the model. A weighting along similar lines should make it possible to de-emphasize the aleatory physics that, as we discussed earlier, might have little to do with integrated performance.

This Page Intentionally Left Blank

B BAYESIAN INFERENCE APPROACHES

B.1 Use of Bayes Theorem in Radiography

The main use made by the labs of Bayes rule, and the use that goes under the name of the Bayes Inference Engine (BIE), is, while correct, a bit misleading. In fact, while there are ways to use Bayes rule to improve knowledge of models of dynamical processes within the physical events occurring up to the making of a radiograph, the actual use appears to be for noise reduction in a formal, non-physical manner. The problem that seems to be set is this: given an image defined as a set of pixels y_a which is represented as a vector function of some parameters $f_a(\mathbf{p})$ vary the $\mathbf{p}$ to clean up the measured image which is taken as the function plus additive noise:

$$
\begin{aligned}
y_a &= f_a(\mathbf{p}) + \eta_a \\
\mathbf{y} &= \mathbf{f}(\mathbf{p}) + \eta.
\end{aligned}
\tag{34}
$$

The noise is usually taken to be Gaussian with zero mean and correlation function

$$
< \eta_a \eta_b >= R_{ab},
\tag{35}
$$

so the probability density function for η is

$$
P_M(\eta) \propto \exp -[\frac{1}{2} \sum_{ab} \eta_b R_{ba}^{-1} \eta_a].
\tag{36}
$$

Because the observations are taken to be the true signal $\mathbf{f}(\mathbf{p})$ plus noise, the conditional probability of the measurements given the state of the image (system) is

$$
P(\mathbf{f}(\mathbf{p})|\mathbf{y}) = P_M(\mathbf{y} - \mathbf{f}(\mathbf{p})).
\tag{37}
$$

Thus the question: how much do we know about the state of the system given the measurement, namely $P(\mathbf{p}|\mathbf{y})$ becomes

$$
P(\mathbf{p}|\mathbf{y}) = P(\mathbf{y}|\mathbf{p})P(\mathbf{p});
\tag{38}
$$

159

Bayes rule. This requires the *prior* $P(\mathbf{p})$ incorporating what we already know about the values of the parameters before the measurements.

The use of Bayes rule is usually restricted to looking for the mode of the distribution $P(\mathbf{p}|\mathbf{y})$, assuming it has a single maximum, by minimizing

$$-\log[P(\mathbf{p}|\mathbf{y})] = -\log P(\mathbf{y}|\mathbf{p}) - \log P(\mathbf{p})$$
$$= \frac{1}{2}\sum_{ab}(y - f_a(\mathbf{p}))_b R_{ba}^{-1}(y_a - f_a(\mathbf{p})))_a] \tag{39}$$
$$+ \frac{1}{2}(\mathbf{p} - \mathbf{p}_0)_b (C_p)_{ba}(\mathbf{p} - \mathbf{p}_0)_a, \tag{40}$$

assuming the noise is Gaussian and the prior knowledge of the parameters is distributed as a Gaussian about some set of parameters $\mathbf{p}_0$. Equivalently one might assume one knows nothing about the prior distribution of the parameters, in which case $P(\mathbf{p})$ is a constant uniform over the range of the parameters, and contributes a constant to the quantity to be minimized.

The image is now expressed in terms of same basis functions $\phi_j(\mathbf{x})$ across the plane $\mathbf{x}$ of the radiograph

$$\mathbf{f}(\mathbf{p}) = \mathbf{F}(\sum_k p_k \phi_k(\mathbf{x})), \tag{41}$$

and this is inserted into the minimization principle. All this is totally equivalent to a least squares minimization strategy of noise reduction. If the function $\mathbf{F}$ were linear, then the entire procedure is linear least squares. This may well result in an 'improved' radiograph, but as there is no physics whatsoever in the selection of the functions $\phi_k(\mathbf{x})$, there is no physical information added to the original measurements $y_a(\mathbf{x})$. In this case, we recommend that no 'improvement' be made to the original radiograph $\mathbf{y}(\mathbf{x})$, and the apparent enhanced sharpness or clarity of the image is totally a reflection of the choice of mapping $\mathbf{f}(\mathbf{p}) = \mathbf{F}(\sum_k p_k \phi_k(\mathbf{x}))$. There is, of course, significant information in the radiograph, and how to extract that is outlined below. Without formulae, the message is the following: use the dynamical model of the processes involved in the experiment to evolve the initial configuration of the 'pit' (made of Ta or whatever, and a whole or scaled structure) to the time at which

160

the radiograph is made. Use the known physics of the measurement apparatus to perform the transformation of the measured quantities in the sensors to an image equivalent to the raw radiograph, and compare, with whatever metrics one selects, those radiographs. Skip the so called BIE step which is an engineering noise reduction and adds no physical information to the problem. Indeed, if a designer or other person looks at the BIE-transformed image and claims insight into the underlying physical model created by the design process, then that is relying on the model of the image in $\mathbf{f}(\mathbf{p}) = \mathbf{F}(\sum_k p_k \phi_k(\mathbf{x}))$, and it sheds no new light on the design.

B.2   The Problem

We have a large model of a complex system with state variables $\mathbf{x}$ of dimension D and many fixed parameters $\mathbf{p}$. The measurements are snapshots at a fixed time, so we do not append a time index to the state variables or the parameters, which are constants in time anyway. We make a set of measurements $\mathbf{y}$ at some time which have dimension $L << D$. We wish to use the information in the measurements to improve the model. The measurements are noisy, the model has errors, and the state of the model at the time of the measurement is uncertain. Everything is stochastic, and the quantity of interest to us is the probability distribution for the state variables (fixed parameters now included in $\mathbf{x}$) conditional on the measurements: $P(\mathbf{x}|\mathbf{y})$.

The measurements are presumed to be connected to the state variables by a set of L observation functions $h_l(\mathbf{x})$; $l = 1, 2, ..., L$, and to determine how well the model does in predicting the measurements we want to compare the values y_l with the $h_l(\mathbf{x})$. The tool we have for doing this is $P(\mathbf{x}|\mathbf{y})$.

Suppose we knew the $P(\mathbf{x}|\mathbf{y})$ and we had measured $\mathbf{y}$; we want to evaluate the expected value of $\mathbf{h}(\mathbf{x})$ in this distribution. This is the quantity we can directly compare with the observations y_l. We have additional information actually because we can also estimate errors in the measurements or even the marginal distribution of

any of the $h_l(\mathbf{x})$. The expected value for $h_l(\mathbf{x})$ is

$$< \mathbf{h}(\mathbf{x}) >= \int d\mathbf{x}\, P(\mathbf{x}|\mathbf{y})\mathbf{h}(\mathbf{x}), \qquad (42)$$

and the RMS error in this estimated mean value is

$$RMS(\mathbf{h}(\mathbf{x}))^2 = \int d\mathbf{x}\, P(\mathbf{x}|\mathbf{y})(\mathbf{h}(x)- < \mathbf{h}(x) >)^2. \qquad (43)$$

We wish to have these moments, and maybe others, as well as maybe the marginal distributions of some of the $h_l(\mathbf{x})$. A marginal distribution $P_{h_l}(z)$ would be the expected value of $\delta(h_l(\mathbf{x}) - z)$.

B.2.1   Enter bayes

Using identities among conditional probabilities (Bayes' rule) we note

$$P(\mathbf{x}|\mathbf{y}) = \left\{ \frac{P(\mathbf{x},\mathbf{y})}{P(\mathbf{x})\,P(\mathbf{y})} \right\} P(\mathbf{x}), \qquad (44)$$

where we recognize the first term as the exponential of the mutual information between the measurements $\mathbf{y}$ and the model state $\mathbf{x}$:

$$\left\{ \frac{P(\mathbf{x},\mathbf{y})}{P(\mathbf{x})\,P(\mathbf{y})} \right\} = \exp MI(\mathbf{x},\mathbf{y})$$

$$MI(\mathbf{x},\mathbf{y}) = \log\left[\frac{P(\mathbf{x},\mathbf{y})}{P(\mathbf{x})\,P(\mathbf{y})} \right]. \qquad (45)$$

The expected value of any function of the model state $F(\mathbf{x})$ is then,

$$< F(\mathbf{x}) > = \int d\mathbf{x}\, P(\mathbf{x}|\mathbf{y})F(\mathbf{x})$$

$$= \int d\mathbf{x}\, e^{MI(\mathbf{X},\mathbf{Y})+\log[P(\mathbf{X})]} F(\mathbf{x})$$

$$= \int d\mathbf{x}\, e^{-A(\mathbf{X})} F(\mathbf{x}). \qquad (46)$$

The appearance of the mutual information between the data, considered as a transmitter of information, and the model, considered as a receiver of information is interesting. The maximum over the average of this quantity (using logarithms to base

2) in a conventional transmission channel defines the capacity of the channel in bits. Properties of this are extensively studied in communications and information theory. The mutual information, not averaged over an ensemble of transmissions and receptions,

$$MI(\mathbf{x}, \mathbf{y}) = \log_2 \left[\frac{P(\mathbf{x}, \mathbf{y})}{P(\mathbf{x}) \, P(\mathbf{y})} \right] \tag{47}$$

is something we wish to maximize (in a sense made precise in a moment) and tells us that our goal is transmitting a maximum amount of information from the data to the model. We know this intuitively anyway, but here it is formally. Indeed, this little formula also allows us to assess what measurements are more important than other measurements: choose to do measurements $\mathbf{y}^A$ over measurements $\mathbf{y}^B$ if

$$MI(\mathbf{x}, \mathbf{y}^A) > MI(\mathbf{x}, \mathbf{y}^B). \tag{48}$$

This is certainly model dependent and process dependent, so may be a good metric for determining what measurements to make. In the actual JASON study context, it may allow one to evaluate in a quantitative manner which set of measurements are more important for the actual goals of the program. We read this to say that the points in $\mathbf{x}$ in the integral are weighted by the distribution $e^{-A(\mathbf{X})}$, and we must find a set of points in D-dimensional space distributed in this manner. That will allow us to do the integral.

Suppose we assume that measurements $\mathbf{y}$ and their counterpart in the model $\mathbf{h}(\mathbf{x})$ are related by additive noise η with a distribution $Q(\eta)$. Tthen we have

$$\mathbf{y} = \mathbf{h}(\mathbf{x}) + \eta, \tag{49}$$

and $P(\mathbf{x}|\mathbf{y}) = Q(\mathbf{y} - \mathbf{h}(\mathbf{x}))$. The weight function in the integral is

$$A(\mathbf{x}) = -\log[Q(\mathbf{y} - \mathbf{h}(\mathbf{x}))] - \log[P(\mathbf{x})]. \tag{50}$$

If $Q(\eta)$ is Gaussian with correlation function $< \eta_l \, \eta_k >= R_{lk}$ and mean $< \eta_l >= 0$, then

$$\log[Q(\mathbf{y} - \mathbf{h}(x))] = -\frac{1}{2} \sum_{l,k=1}^{L} \eta_k R_{kl}^{-1} \eta_l + \text{constants}, \tag{51}$$

so $A(\mathbf{x}) = \frac{1}{2} \sum_{l,k=1}^{L} \eta_k R_{kl}^{-1} \eta_l + \text{constants} - \log[P(\mathbf{x})]$. The expected value of the function $F(\mathbf{x})$ is now given as

$$< F(\mathbf{x}) > = \frac{\int d\mathbf{x} \, e^{-A(\mathbf{X})} F(\mathbf{x})}{\int d\mathbf{x} \, e^{-A(\mathbf{X})}}. \tag{52}$$

The constants cancel out here. How are we to do this integral?

B.2.2   Saddle point

One way is the saddle point approximation which seeks a point $\mathbf{s}$ in D-dimensional space where

$$\frac{\partial A(\mathbf{x})}{\partial \mathbf{x}}\bigg|_{\mathbf{X}=\mathbf{S}} = 0, \tag{53}$$

and this is the usual variational formulation of the problem at hand. The series of approximations of which the saddle point is the first approximation is known as perturbation theory in statistical physics. One can systematically calculate corrections to the approximation. One of the deficiencies of the saddle point approximation is that a single answer $\mathbf{s}$ results, and there is no sense of the errors in that quantity. Here's a simple example of the deficit of the saddle point method which seeks only the point $\mathbf{s}$. Suppose the quantity x is one dimensional and distributed as

$$P(x) = e^{-A(x)},$$
$$A(x) = x^4 - 2ax^2; \; a > 0. \tag{54}$$

The saddle point

$$\frac{\partial A(x)}{\partial x}\bigg|_s = 0, \tag{55}$$

has three zeros: $s = 0, s = \pm\sqrt{a}$. Which one is appropriate? If one continues the expansion about the saddle point, there is a Gaussian integral to do near s, and two of the saddle points have positive curvature in $A(x)$, namely $s = \pm\sqrt{a}$. The saddle point $s = 0$ does not have an expansion about it as there is negative curvature there. Using an effective action, one can produce a closed formula for the generating function of the moments about the saddle points, but this requires a bit more work. More

directly we can ask for the moments about the saddle points by evaluating

$$
\begin{aligned}
< (x-s)^2 > &= < x^2 > + s^2, \\
< x^2 > &= \frac{1}{2}\frac{\partial}{\partial a}\log\left\{\int_{-\infty}^{+\infty} e^{-x^4+2ax^2}\right\}, \\
&= \frac{\int_{-\infty}^{+\infty} x^2\, e^{-x^4+2ax^2}}{\int_{-\infty}^{+\infty} e^{-x^4+2ax^2}}.
\end{aligned}
\tag{56}
$$

Just for completeness we note

$$
\int_{-\infty}^{+\infty} e^{-x^4+2ax^2} = \sqrt{\frac{a}{2}} e^{\frac{a^2}{2}} K_{1/4}\left(\frac{a^2}{2}\right),
\tag{57}
$$

where $K_\nu(z)$ is a modified Bessel function of order ν. This suggests that unless one knows with certainty that there is a single minimum of $A(\mathbf{x})$ one should not rely on the saddle point method, and, in any case, no error estimates are contained within this approach.

Now the ability to do the integral involved in Equation (56) is a special property of one dimensional integrals, so other methods must be pursued to go beyond the saddle point estimate of the mode of the distribution $P(\mathbf{x}|\mathbf{y})$.

B.2.3 Monte Carlo

Another way to do the integral approximately is to use Monte Carlo methods to select points in $\mathbf{x}$ space which are distributed as $e^{-A(\mathbf{X})}$ and then having selected NP such points $\mathbf{x}^j$; $j = 1, 2, ..., NP$ to estimate the weight function in the integral as

$$
e^{-A(\mathbf{X})} \approx \frac{1}{NP}\sum_{j=1}^{NP} \delta^D(\mathbf{x}^j - \mathbf{x}),
\tag{58}
$$

so

$$
< F(\mathbf{x}) > \approx \frac{1}{NP}\sum_{j=1}^{NP} F(\mathbf{x}^j).
\tag{59}
$$

Methods abound for selecting such points in a systematic manner.

B.3 Connection to Hydrodynamic Experiments

One connection is to radiographic images of an imploding object. As discussed in Section A, the radiograph is a set of measurements y_l where the index l is a set of points in the plane of physical (x, y, z) space from information on physical measurement devices of counts of photons or protons etc. associated with the device irradiating the object during its implosion. Suppose we have measurements on K instruments given by m_k; $k = , 1, 2, .., K$. Then the observations entering our conditional probability distribution are some function of the $\mathbf{m} = \{m_1, m_2, ..., m_K\}$:

$$y_l = F_l(\mathbf{m}), \tag{60}$$

which we presume known. Of course, this has many assumptions in it. Many parameters associated with the instruments used, and errors associated with noise in the instruments and imperfections of the instruments, and errors in the model of the instruments $F_l(\mathbf{m})$.

In a simulation of the processes in the implosion and the creation of the radiograph, we first must make a model involving numerous physical quantities such as the equation of state of the material in the imploding object, the stress strain relations for the material in various regimes of temperature and pressure, ... plus we must make a model of the way, given the physical state of the object, the probes (photons, protons, ..) of the radiograph scatter from different densities of material during the implosion. All of this should imitate the physical processes through which the object goes in the experiment from which the radiograph is constructed. The combination of all of these processes produces the simulation counterpart of the observations y_l; namely, the $h_l(\mathbf{x})$ derived from knowledge of the state of the imploded object at the time during the implosion at which the radiograph is constructed.

The quantities one wishes to compare are the radiograph y_l and the model equivalent of the radiograph $h_l(\mathbf{x})$. The latter, as just noted, is constructed from the model state $\mathbf{x}$ at the time during the implosion process that the radiograph is constructed.

Whatever operations take the instrumental data to the radiograph msut be performed on the instrumental output one evaluates from scattering of the probe radiation from the model state.

While one might want to 'sharpen up' the radiograph using some image processing techniques so that a prettier picture is presented, the information useful for assisting in the testing or improvement of the model is in the raw radiograph and is a comparison with the model equivalent of it. If one processes the radiograph, then one must perform precisely the same processing on the measurement function $h_l(\mathbf{x})$ before any comparison or data assimilation is performed. As an aside, the physical (x, y, z) space is not to be confused with the state variable space of the model of the processes which we call $\mathbf{x}$. Those variables are pressure, temperature, constituent density, ... that all depend on (x, y, z) which have been discretized and are part of the label a of the state variables : x_a; $a = 1, 2, ..., D$.

B.4 Using Models to Design Experiments: Use of Twin Experiments

There is another use of this machinery that could be of significant value in understanding how to utilize the information in an integrated experiment. The question to be addressed is this: what information in an integrated experiment can be used to inform the makers of model dynamics about the physics of the model? The procedure to use is outlined above for a single snapshot (radiograph), and this can be extended in a relatively straightforward manner to a sequence of snapshots. How, however, do we know how much can be learend by any selected set of measurements about the model itself? While one can give information theoretic formulas for this [?], the following is likely to be more useful. It is an expression of what geophysicists term a 'twin experiment'.

Choose a model for the collection of complex dynamics involved in an experi-

ment. The model has dynamical variables $\mathbf{s}(t)$ and parameters $\mathbf{p}$. Run that model from the time of initiation of the experiment through the sequence of measurements performed during the experiment. The parameters in the model: EOS statements, "strength" parameterizations, etc. are all in the model and fixed during this twin experiment. The measurements are expressible as a set of measurement functions $h(\mathbf{s}(T), \mathbf{p}')$ which are, generally non-invertible, functions of the state of the model system at the time T of the measurement and additional parameters $\mathbf{p}'$ in the measurement function. Operate on the state of the model $\mathbf{s}(T)$ arising from the evolution of the model from its state at the time of initiation of the experiment up to the time of measurement T. Using $\mathbf{s}(T)$ from the model, calculate $h(\mathbf{s}(T), \mathbf{p}')$ and compare that to the measurements to determine the states and parameters–known precisely in this twin experiment–of the model from the values of $h(\mathbf{s}(T), \mathbf{p}')$ alone.

This does *not* test the model, but it does tell one whether the selected set of measurement functions is able, or not able, to inform us about properties of this model. The method tests the procedures for extracting state and parameters of a model from the observations. This is a critical element in the design of experiments for use in answering the question: how can we improve the model or even test the model we have built using experiments. This allows the selection of experiments that address this key question.

It might be said this is too expensive in computing time, as the models have too many degrees of freedom and are too complex. Then one should simplify the model by reducing the degrees of freedom, use the simpler model to examine which experiments (measurement functions) allow the best estimation of the known parameters, and then systematically increase the resolution or complexity or number of degrees of freedom of the model until it does become too costly to do the required computations. Along the way one will illuminate, in a practical manner, what aspects of the model are in fact informed by this or that experiment (set of observation functions). These sorts of twin experiments can be utilized for scaled experiments, EOS experiments, etc., as well as for integrated experiments. Indeed, one should do this in detail for every

class of experiment *before* running the experiment and hoping the observations made in that, often expensive, enterprise are useful and informative about the physics of the processes as embodied in the model.

While we do not know *a priori* what this will tell about the various experiments proposed, this should be a selection procedure exercised before any experiments are designed or executed. For example, if integrated experiments resulting in one or a sequence of snapshots, via radiographs or other measurements, do not allow us, via the exercise of twin experiments, to learn items we wish to know about the underling model of the dynamical processes, they should be redesigned until they do, or simply not be performed.

This Page Intentionally Left Blank

C ACKNOWLEDGEMENTS

We acknowledge here the important contributions made to this study by the following briefers:

Briefer	Affiliation	Title
Robert Hanrahan	NNSA	Overview, Introduction and Background
Bruce Goodwin	LLNL	Stockpile Drivers
Mary Hockaday	LANL	Experimental Facilities, DYNEX
Robert Webster	LANL	Codes
Frank Graziani	LLNL	NBI/PCF
Dan Hooks	LANL	HE Deep Dive
Tariq Aslam	LANL	HE Deep Dive
Larry Fried	LLNL	He Deep Dive
Thomas Lorenz	LLNL	HE Deep Dive
Robert Cavallo	LLNL	HE Deep Dive
Paolo Rigg	LANL	EOS Deep Dive
John Boettger	LANL	EOS Deep Dive
Kenneth Eggert	LLNL	EOS Deep Dive
Loren Benedict	LLNL	EOS Deep Dive
Tom McAbee	LLNL	EOS Deep Dive
Dawn Flicker	SNL	EOS Deep Dive
Rusty Gray	LANL	Strength Deep Dive, Damage Deep Dive
Dean Preston	LANL	Strength Deep Dive
Bruce Remington	LLNL	Strength Deep Dive
Tom Arsenlis	LLNL	Strength Deep Dive
Robert Cavallo	LLNL	Strength Deep Dive
Davis Tonks	LANL	Damage Deep Dive

Briefer	Affiliation	Title
Nathan Barton	LLNL	Damage Deep Dive
Mukul Kumar	LLNL	Damage Deep Dive
Ray Tolar	LLNL	Damage Deep Dive, Integrated Experiments
William Buttler	LANL	Ejecta Deep Dive
Malcolm Andrews	LANL	Ejecta Deep Dive
Pat Egan	LLNL	Ejecta Deep Dive
Tom McAbee	LLNL	Ejecta Deep Dive
Don Roberts	LLNL	Radiographic Requirements, Integrated Experiments
Doug Fulton	LANL	Radiographic Options
George Caporaso	LLNL	Radiographic Options
Larry Schneider	SNL	Radiographic Options
Garry Maskaly	LANL	Integrated Experiments
George Tompkins	LANL	Integrated Experiments
David Holtkamp	LANL	Integrated Experiments
Barry Jacoby	LLNL	Integrated Experiments
Michael Burkett	LANL	Surety
Juliana Hsu	LLNL	Surety
Patrick Allen	LLNL	Surety

These individuals helped educate JASON on technical details and participated in discussions. We also wish to acknowledge the contributions of Juliana Hsu and Don Roberts from LLNL, who provided additional calculations as described in the report that were very helpful in formulating our conclusions. In addition, we thank Gilbert W. Collins (LLNL), Marcus Knudson (SNL), and Paolo Rigg (LANL) who joined us for discussions after the briefings. We are grateful for the contributions of these individuals. However, JASON is responsible for the findings and recommendations stated in this report.